THE UNIVERSITY OF NEW SOUTH WALES
THE SCHOOL OF SURVEYING

INTRODUCTION TO ELECTRONIC DISTANCE MEASUREMENT

J. M. Rüeger

INTRODUCTION TO ELECTRONIC DISTANCE MEASUREMENT

J.M.Rüeger

Second Edition

Fifth Impression
(with extended Tables)

January 1988

School of Surveying
The University of New South Wales
P.O. Box 1
KENSINGTON N.S.W. 2033
Australia

Published by

The School of Surveying
The University of New South Wales
Sydney, Australia. 2033

First Edition January, 1978
Second Edition March, 1980

Second Edition)
Second Impression) July, 1982
Third Impression June, 1984
Fourth Impression July, 1986
Fifth Impression January, 1988

National Library of Australia
Card Number and ISBN
0 85839 027 2

COUNTRY INTERLUDE

Surveyor: Good morning.

Jackeroo: G'day - hot ain't it!

Surveyor: Yes, it is a bit that way.

Jackeroo: Never lets up out here.

Surveyor: Do you think it will rain?

Jackeroo: No chance - say, when are you blokes going to start measuring?

Surveyor: We've been surveying for the past week.

Jackeroo: Yeah, I know, with the theodolite, but when are you gunna start measurin'?

Surveyor: Oh, we've been measuring all right, haven't you seen the box on top of the theodolite and the mirrors on the tripod in the distance?

Jackeroo: Yeah, I've been seen all that - funny looking mirrors, aren't they - but when are you going to get out that long wire and start measuring? All the surveyors I ever saw always seems to pull that wire around as though it was part of the scenery.

Surveyor: Oh, well, you see, we measure by light waves now; that's the idea of mirrors reflecting to the theodolite station.

Jackeroo: Garn!! You're kidding me.

Surveyor: No - that's the way we do it now - far more accurate as well.

Jackeroo: Struth. Do you mean to say the boss has had me dragging that ruddy old five chain bit of wire around for the last twenty years to measure crops when we could have been using a mirror!! Wait till I tell him a thing or two!!

True Story by Ted Hunter, N.S.W. Surveyors' Monthly Bulletin, February, 1980.

PREFACE TO THE SECOND EDITION

The second editions follows the format of the first edition and includes only minor amendments and extensions. The old Appendix E has been transferred as section 3.223 to the main text for easier reading. A new section 3.34 treats the determination of the coefficient of refraction from reciprocal zenith distance observations. Appendix F has been extended to include the derivation of the group refractive index in glass. The three new appendices E, G and H provide tables for the saturation vapour pressure, a standard atmosphere and design formulae for two types of EDM baselines. The tables 1 and 2 of Appendix D have been up-dated and now include a range of new instruments. A new table 4 provides information on the first velocity correction of a number of instruments. The bibliography also has been extended.

In addition, a number of typing errors have been eliminated. The author is grateful for all the information received in this respect. The contributions by Messrs. F. K. Brunner, C. S. Fraser, M. H. Lodewyk, S. W. Munsie, J. R. Pollard, R. J. Shoesmith, A. P. H. Werner and many students have been very helpful. The author is also indebted to Mr. K. I. Groenhout for the proof-reading and to Miss R. Banwell for the typing of the amendments to this monograph.

The author hopes that the second edition will continue to serve the interests of both surveyors and students and appreciates any further criticism and suggestion for improvement.

Sydney, March 1980 J. M. RÜEGER

PREFACE OF FIRST EDITION

The present monograph is designed to make the subject matter more readily available to students proceeding to the degree of Bachelor of Surveying at the University of New South Wales in absence of a suitable and reasonably priced textbook. It is an extended version of the author's lecture notes on the subject. The monograph may however also be useful to the surveying profession because of its comprehensive cover of all steps involved in using short range EDM instruments.

After a brief review of the history of EDM in Chapter 1, some physical laws and units on which EDM is based are repeated in Section 2.1. A broad view of various measurement principles and applications follows in Section 2.2 before the text concentrates on the discussion of instruments which employ the technique of phase difference measurement. The principles of electrooptical and microwave instruments are explained in Section 2.3. Section 2.4 deals then with the refractive index and its determination.

The Chapter 3 covers, in depth, velocity corrections and geometrical corrections of measured distances. Apart of the distance reduction to the spheroid, further considerations are given to the reduction to centre of distances and the computation of height differences from measured vertical angles and distances by EDM.

The electrooptical distance meters and their auxilliary equipment such as reflectors and batteries are treated in Chapter 4, in detail. The differences in modern short range instruments are pointed out and an introduction is given to instrumental errors and instrument calibration. The last chapter on microwave instruments reviews briefly the special problems encountered in microwave EDM.

The text uses only SI units, apart from the unit for pressure which is the millibar. Because millibar is generally accepted and used in meteorology and EDM it was felt that it should not be replaced by pascal or kPa at this stage. References in the text are indicated by square brackets [ ] and refer to the bibliography on the last pages of the monograph. The designation of parameters is usually repeated below final formulae in order to facilitate the use of the text as a compendium of formulae. The main symbols however are also set out in the list of symbols at the beginning of the text.

The author is gratefully indebted to Professor P.V. Angus-Leppan, Dr. F.K. Brunner, Messrs. C. Fraser, I. Groenhout and A.P.H. Werner for their valuable help in editing this text and for their detection of inconsistencies and suggestions for improvement. The writer would also like to thank Mrs. S. Kiriazis and Miss R. Banwell for typing the manuscript.

Sydney, January 1978. J.M. RÜEGER

TABLE OF CONTENTS

Page

LIST OF SYMBOLS

A = amplitude or maximum strength of electromagnetic signal

E'_W = saturation water vapour pressure at "wet bulb" temperature over water

E'_{ICE} = saturation waver vapour pressure at "wet bulb" temperature over ice

E_W = saturation water vapour pressure at "dry bulb" temperature over water

H_i = spheroidal height of "i"th station

ΔH = height difference = $H_2 - H_1$

H_M = mean height = $0.5 (H_1 + H_2)$

I = electric current

J = radiant intensity at distance d

J_o = radiant intensity at emitter

K = line scale factor on N.S.W. I.S.G. (section 3.41)

K = point scale factor on N.S.W. I.S.G. (section 3.42)

K' = first velocity correction

K'' = second velocity correction

K_1 = first arc-to-chord correction (d_1 to d_2)

K_2 = slope correction (d_2 to d_6)

K_3 = sea level correction (d_6 to d_3)

K_4 = second chord-to-arc correction (d_3 to d_4)

K_{23} = chord-to-chord correction (d_2 to d_3)

K_5 = slope correction (d_2 to d_5)

K_6 = sea level correction (d_5 to d_3)

L = fraction of unit length U

L = phase difference (section 2.3133)

N = refractivity

P_o = radiant power output

R = mean radius of curvature of spheroid along a line

R_M = mean radius of curvature of spheroid for a specific area (N.S.W. I.S.G. R_M = 6370 100 m)

S = grid distance on N.S.W. I.S.G. (section 3.42)

T = atmospheric transmittance

U = unit length of an EDM instrument

c = velocity of light in a medium

c = additive constant (section 4.6)

c_y = cyclic error correction (section 4.62)

c_g = group velocity of light in a medium

c_o = velocity of light in a vacuum

d = measured distance, including first velocity correction

d' = measured distance (displayed on instrument)

d_1 = wave path length (= $d' + K' + K''$)

d_2 = wave path chord

d_3 = spheroidal chord

d_4 = spheroidal distance

d_5 = horizontal distance at height of EDM instrument station (Appendix E)

d_6 = $d_2 + K_2$

d^* = distance between satellite stations

d_v = meteorological range, visibility range

d_{TH} = distance along zenith distance ray

d_{EDM} = wave path chord (d_2) (section 3.32)

e = partial water vapour pressure

e = eccentricity of satellite station (section 3.33)

e = eccentricity of EDM instrument (sections 4.133, 4.134)

f = frequency of signal

f_D = doppler frequency

h = relative humidity (sections 2.44 and 2.474)

h_{EDM} = height of trunnion axis of EDM instrument above survey mark

h_R = height of reflector above survey mark

h_{TH} = height of trunnion axis of theodolite above survey mark

h_T = height of target above survey mark

Δh = $h_{EDM} - h_{TH} + h_T - h_R$

k = coefficient of refraction

k_o = central scale factor (in section 3.4)

k_L = coefficient of refraction of light waves

k_M = coefficient of refraction of microwaves

n = refractive index of a medium

n_L = group refractive index of light waves for arbitrary atmospheric conditions

n_M = refractive index of microwaves for arbitrary atmospheric conditions

n_{REF} = reference refractive index of a specific EDM instrument

n_g = group refractive index of atmosphere for standard conditions

p = atmospheric pressure

s = chord distance (= d) (section 3.13)

r = radius of curvature of wave path

t = time (in section 2.1)

Δt = time lag of electromagnetic signal

Δt = time interval (in section 2.23)

$\Delta t'$ = flight time of a signal between transmitter and receiver

t = "dry bulb" temperature

t' = "wet bulb" temperature

v = speed

z_i = measured zenith distance at station P_i

z_{ij} = zenith distance at station P_i to P_j

z = attenuation or extinction coefficient (section 2.41)

Φ = phase angle of electromagnetic signal

$\Delta\Phi$ = phase lag of electromagnetic signal

$\Delta\Phi$ = measured phase difference (2.222)

α = coefficient of expansion of air (= 0.00367) (section 2.44)

α = azimuth of the measured line, clockwise through 360^o from true north (section 3.21)

α = vertical angle in section 3.311

α = horizontal angle (section 3.33) measured at centre station

α^* = horizontal angle measured at satellite station (section 3.33)

β = angle between the wave path normals through the terminals of a line

δ = refraction angle

$\delta( )$ = differential

ε_i = deviation of vertical at station P_i

ε = dielectric constant or permittivity (section 3.13)

ε_r = relative dielectric constant (section 3.13)

ζ_i = spheroidal zenith distance at station P_i

ν = angle (in section 3.311)

λ = wavelength

μ = magnetic permeability (section 3.13)

μ_r = relative magnetic permeability (section 3.13)

ν = radius of curvature of the spheroid in the prime vertical

ρ = radius of curvature of the spheroid in the meridian

σ = standard deviation (section 3.312)

σ = optical length (= d') (section 3.13)

ψ = angle (in section 3.332)

ψ = phase lag of contaminated signal (in section 4.521)

ω = angular velocity

1. History

Compared with the direct measurement of distances by tapes, band and chains, EDM has a short history. Its fast development is linked with the rapid progress in electronics during this century. The availability of relatively cheap instruments was only possible due to the rapid progress which has been made in solid state electronics since the early 1970s.

The development of the first light wave EDM instrument is connected with the name of the Swedish scientist E. Bergstrand. He designed the first Geodimeter (short form of GEOdetic DIstance METER) for the determination of the velocity of light in 1943. The commercial instrument Geodimeter NASM-2 became available in 1950, produced by a large Swedish manufacturer of chemicals, AGA. With the early Geodimeters, longer distances could only be measured at night. The latest long-range Geodimeters, models 600 and 8, are at present in wide use in geodetic surveying throughout the world.

The first EDM instrument using radiowaves was developed by T.L. Wadley at the National Institute of Telecommunications Research of South Africa in 1954. It became available under the name Tellurometer in 1957. Its range exceeded that of the Geodimeter and it was therefore in much wider use until lasers were introduced in EDM late in the 1960's.

The first prototypes of short range EDM instruments (incorporating luminescence diodes) appeared in the mid 1960's (Tellurometer MA 100 in 1965; Zeiss SM 11 in 1967). These instruments have been commercially released since the late 1960's (Wild/Sercel Distomat DI 10 in 1968; Tellurometer MA 100 in 1969; Zeiss SM 11 in 1970). Short range instruments with infrared (IR) light sources are now increasingly used for all types of surveys; long range instruments are used for the measurement of geodetic networks.

Two other groups also need be mentioned. The most precise EDM instrument to date, the Mekometer, was built by K.D. Froome and R.H. Bradsell in 1961 at the National Physical Laboratory, Teddington (U.K.) and became commercially available early in 1973. On short distances, accuracies of 0.2 mm can be achieved.

The first electronic tacheometer (sometimes termed "total station"), the Zeiss (Oberkochen) Reg Elta 14, became available in 1970 and featured electronic readout not only of distance but also of the vertical and horizontal circles. The second total station, the AGA Geodimeter 700 became available in 1971. Electronic tacheometers have a great future in large scale detail surveys, especially if combined with electronic booking and computerized data processing and plotting.

2. Fundamentals of Electronic Distance Measurement

2.1 Physical Laws (and Units) related to EDM

2.11 Definitions

The frequency f and the wave length λ of electromagnetic waves are related by the following fundamental equations:

$$\lambda = \frac{c}{f} \qquad (2.1) \qquad\qquad f = \frac{c}{\lambda} \qquad (2.2)$$

where c = velocity of electromagnetic waves in a medium, usually referred to as the *velocity of light* in the medium.
f = frequency of singal
λ = wave length in the medium

The mode and velocity of propagation of an electromagnetic wave depend to a certain extent on the frequency of the signal and on the nature of the earth's atmosphere. The distance between two stations can be computed, if the travelling time of the radiation is measured:

$$c\,\Delta t' = d \qquad (2.3)$$

d = distance between the two points
$\Delta t'$ = time taken by the signal to travel from first to second station ("flight" time)
c = velocity of light in the medium

It is assumed in equations (2.1) to (2.3), that the velocity of light in a medium(normally air) is known. This velocity can be calculated if the refractive index of the medium (viz. air) and the velocity of light in a vacuum is known.

$$c = \frac{c_o}{n} \qquad (2.4)$$

n = refractive index of a medium
c_o = velocity of light in a vacuum
c = velocity of light in a medium

The velocity of light in a vacuum is a physical constant which has to be determined by experiment. The determination of c_o remains a permanent challenge to physicists and even has led to the development of EDM instruments, as discussed earlier. More information about this natural constant is given in section 2.13. The refractive index of a medium can be derived from formulae given in section 2.4. It is very difficult to accurately assess the refractive index along the wave path, and consequently the accuracy of EDM is often limited by the accuracy to which the integral refractive index is known.

Electromagnetic radiation can be described by the following formulae:

$$y = A \sin(\omega t) \qquad (2.5a)$$

$$= A \sin \Phi \qquad (2.5b)$$

where A = amplitude or maximum strength
ω = angular velocity (angular frequency, angular rate of alternation)
f = frequency of signal
t = time
Φ = phase angle

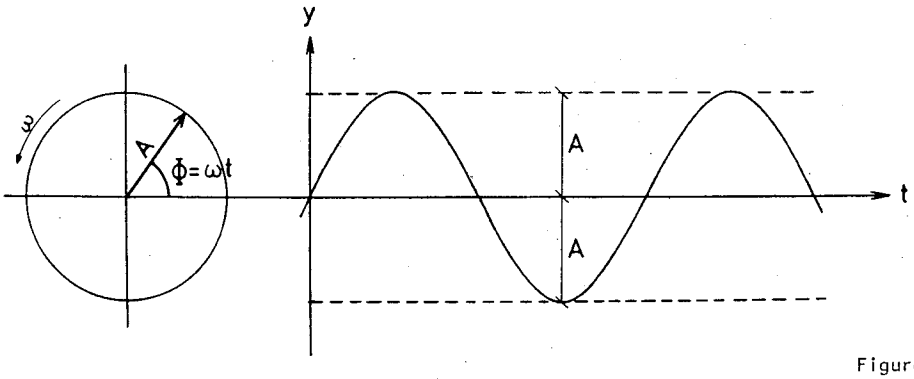

Figure 1a.

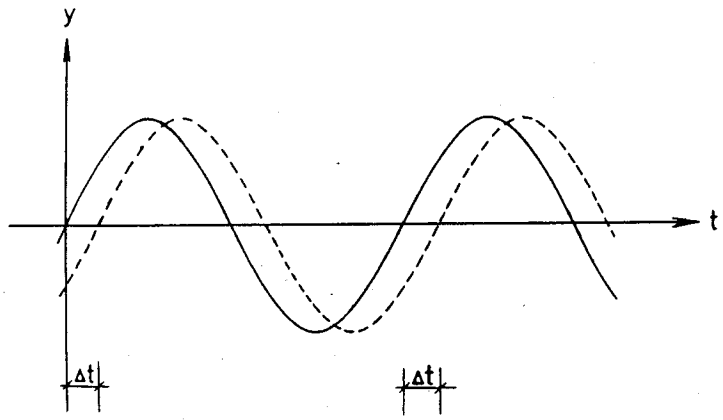

Figure 1b.

and where $\Phi = \omega t$ (2.6a)

$$\omega = 2\pi f \quad (2.6b)$$

The parameters are further explained in figure 1a.

A signal with a phase lag of $\Delta\Phi$ can be expressed as:

$$y = A \sin(\Phi + \Delta\Phi) \quad (2.7a)$$

$$y = A \sin \omega(t + \Delta t) \quad (2.7b)$$

where Δt = time lag
$\Delta\Phi$ = phase lag

The effect of a time lag is depicted in figure 1b.

The phase lag may be written as a function of the time lag:

$$\Delta\Phi = \Delta t\, \omega \quad (2.8a)$$

$$\Delta t = \frac{\Delta\Phi}{\omega} \quad (2.8b)$$

2.12 Frequency Spectrum

The bands of the frequency spectrum are listed below and also depicted in figure 2, where those used for EDM are hatched.

Radiation	Wave Length λ	Frequency f
X-rays	1.6×10^{-11} - 6.6×10^{-8} m	1.9×10^{19} - 4.5×10^{15}Hz
Ultra-violet	1.4×10^{-8} - 3.6×10^{-7} m	2.2×10^{16} - 8.3×10^{14}Hz
Visible light	3.6×10^{-7} - 7.8×10^{-7} m	8.3×10^{14} - 3.8×10^{14}Hz
Infrared	7.8×10^{-7} - 3.4×10^{-4} m	3.8×10^{14} - 8.8×10^{11}Hz
Radiowaves:		
Extra high EHF	1×10^{-3} - 1×10^{-2} m	3×10^{10} - 3×10^{11} Hz
Super high SHF	1×10^{-2} - 1×10^{-1} m	3×10^{9} - 3×10^{10} Hz
Ultra high UHF	1×10^{-1} - 1 m	3×10^{8} - 3×10^{9} Hz
(Television)		
Very high VHF	1 - 10 m	3×10^{7} - 3×10^{8} Hz
(Television, FM Broadcasting)		
High HF	10 - 100 m	3×10^{6} - 3×10^{7} Hz
(Short waves)		
Medium MF	10^{2} - 10^{3} m	3×10^{5} - 3×10^{6} Hz
(AM Broadcasting)		
Low LF	10^{3} - 10^{4} m	3×10^{4} - 3×10^{5} Hz
(Long waves)		
Very low VLF	10^{4} - 10^{5} m	3×10^{3} - 3×10^{4} Hz
Extra low ELF	10^{5} - 10^{6} m	3×10^{2} - 3×10^{3} Hz

Radiowaves belonging to the SHF and UHF bands and parts of the EHF and VHF bands are traditionally called *microwaves*. They may be divided into:

	Wavelength λ	Frequency f
V Band	5.3 mm - 6.5 mm	46 - 56 GHz
Q Band	6.5 mm - 8.3 mm	36 - 46 GHz
K Band	8.3 mm - 27.5 mm	10.9 - 36 GHz
X Band	27.5 mm - 57.7 mm	5.2 - 10.9 GHz
S Band	57.7 mm - 0.194 m	1.55 - 5.2 GHz
L Band	0.194 m - 0.769 m	0.39 - 1.55 GHz
P Band	0.769 m - 1.333 m	0.225- 0.390 GHz

Microwaves are mainly used for telecommunication purposes and Radar (*RA*dio *D*etection *A*nd *R*anging) systems. For example, the Australian telephone network is partly based on microwave links.

The infrared part of the spectrum is also divided further:

	Wavelength
Near infrared NIR	0.76 µm - 3.0 µm
Middle infrared MIR	3.0 µm - 6.0 µm
Far infrared FIR	6.0 µm -15.0 µm
Extreme infrared XIR	15.0 µm - 1 mm

NIR radiation has propagation characteristics which are close to those of visible light and this facilitates its use both in optical telecommunication systems (glass fibres) and EDM.

Electrooptical EDM instruments use mainly NIR radiation of about 900 nm wavelength or red LASER (*L*ight *A*mplification by *S*timulated *E*mission of *R*adiation) light of 633 nm wavelength. Microwave EDM instruments use mainly wavelengths of 3 cm and are therefore classified within

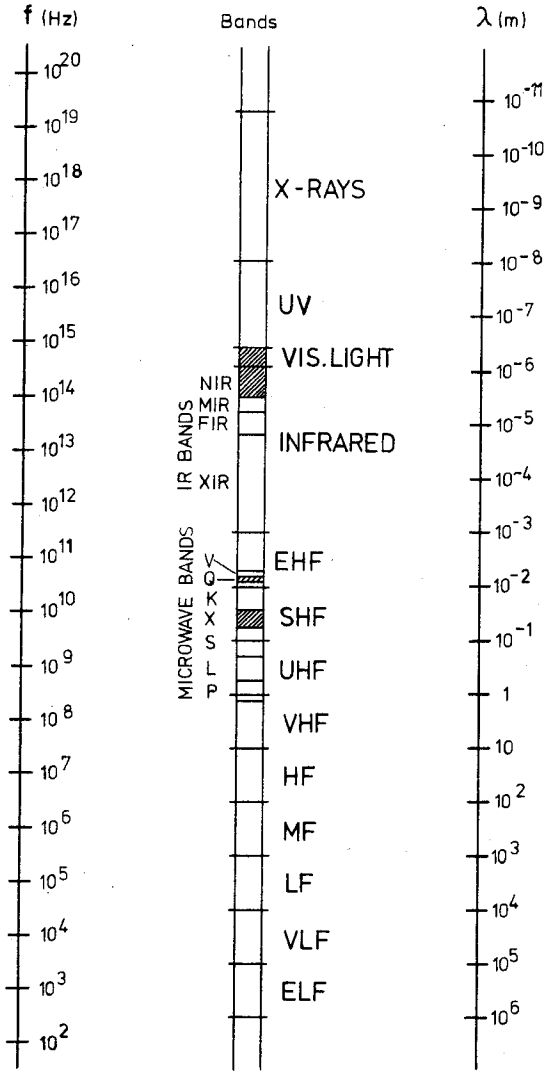

Figure 2.

the X band and the SHF band. Navigation systems make use of a larger range of radiowaves. For example, the DECCA system operates in the LF band and TORAN and DECCA HI-FIX operate in the HF band.

2.13 Velocity of Light in a Vacuum, c_o

Over the last 300 years different techniques have been used by astronomers and physicists to determine c_o. The precision of determination has improved during the last twenty years from ± 1 km/s to ± 1 m/s. Some of the instruments and techniques of this development has been applied by EDM instrument manufacturers. Experiments by Essen and Froome in 1951 led to a formula for the calculation of the refractive index of microwaves [27]. Some determination methods used a "reverse EDM process", namely to derive the unknown velocity of light from a distance which was measured with precise invar wires or by interferometry.

In 1957 the XIIth General Assembly of the International Scientific Radio Union recommend the value

$$c_o = 299\,792.5 \qquad \pm 0.4 \text{ km s}^{-1}$$

This value was accepted later by the International Union for Geodesy and Geophysics (IUGG). It is used for the scale definition of all distance meters.

At the XVIth General Assembly of the IUGG in 1975, the following revised value for c_o was recommended [2]:

$$c_o = 299\ 792\ 458 \qquad \pm 1.2\ m\ s^{-1}$$

The standard deviation of c_o quoted above amounts only to 0.004 ppm and is mainly due to the uncertainty in the definition of the metre. In EDM c_o can therefore be considered as an error free value, because the accuracy of EDM is rarely better than one part per million (1 ppm). The change between the 1957 and the 1975 value of c_o is 42 $m.s^{-1}$ or 0.14 ppm; it may usually be ignored but not for precise, long range EDM with an accuracy greater than 0.1 ppm.

2.14 Units and their Definitions

It is useful to review the definitions of two important units upon which electronic distance measurement is based. The derived frequency unit and one meteorological units are also mentioned, the latter, because it is not a standard SI unit.

2.141 Second of Time, s

The second was defined by the XIIIth General Conference for Measures and Weights in 1967 as follows:

"The second is the duration of 9 192 631 770 periods of the radiation corresponding to the transition between the two hyperfine levels of the ground state of the Caesium - 133 atom".

Derived units are:

One millisecond = 1 ms = 1×10^{-3} s
One microsecond = 1 µs = 1×10^{-6} s
One nanosecond = 1 ns = 1×10^{-9} s

This atomic standard of the second can be reproduced to an accuracy of 1 in 10^{-11} according to the National Standards Laboratory [3]. The time standard is maintained by atomic clocks (Ceasium standards).

2.142 Metre

The metre was defined by the XIth General Conference for Measures and Weights in 1960 with the following terms:

"The metre is the length equal to 1 650 763.73 wave lengths in vacuo of the radiation corresponding to the transition between the levels $2p_{10}$ and $5d_5$ of the krypton-86 atom."

Derived units are:

One kilometre = 1 km = 1×10^{3} m
One millimetre = 1 mm = 1×10^{-3} m
One micrometre = 1 µm = 1×10^{-6} m
One nanometre = 1 nm = 1×10^{-9} m

The metre can be reproduced with an accuracy of 1 in 10^{-8}, according to [3]. A more accurate definition of the metre may become available in future.

2.143 Other Units in EDM

Frequency units are not basic units but are based entirely on the definition of time. The name of the frequency unit is taken from the name of the German physicist, Heinrich Hertz (1857-1894), who discovered the existence of electromagnetic waves.

One Hertz = 1 Hz = 1 cicle per second = s^{-1}
One Kilo Hertz = 1 KHz = 1×10^3 Hz
One Mega Hertz = 1 MHz = 1×10^6 Hz
One Giga Hertz = 1 GHz = 1×10^9 Hz

In contrast to the derived SI unit for *pressure*, the pascal, the unit of pressure generally used by meteorologists, by international agreement, is the millibar (mb). All formulae in this text involving pressure will be based on millibars. The following relations apply:

$$\text{One millibar} = 1 \text{ mb} = 1 \times 10^{-3} \text{ bar} = 10^2 \text{ Pa} = 10^2 \text{ Nm}^{-2}$$

where N (Newton) is the SI unit for force.

The conversion between mm or inches of mercury(Hg) and mb is as follows:

$$1 \text{ mb} = 0.75006 \text{ mm Hg} = 0.029530 \text{ inch Hg}$$

Example: 1013.246 mb = 760 mm Hg = 29.9213 inch Hg = 101.3246 kPa

2.2 Principles and Applications of EDM

There are many ways to measure distances by electronic means. Four basic principles will be presented although only one will be discussed in greater depth.

2.21 Pulse Method

2.211 Principle of the Pulse Method

A short, intensive signal is transmitted by an instrument. It travels to a target point and back and thus covers twice the distance d. Measuring the so-called flight-time between transmission and reception of the same pulse, the distance may be calculated as

$$2d = c\,\Delta t'$$

$$= c(t_R - t_E) \qquad (2.9)$$

d = distance between instrument and target
c = velocity of light in the medium
$\Delta t'$ = flight time of pulse
t_E = time of departure of pulse, timed by gate G_E
t_R = time or arrival of returning pulse, timed by gate G_R

Figure 3 depicts such a instrument. G_E and G_R are gates, where the passage of a pulse is monitored and its time recorded.

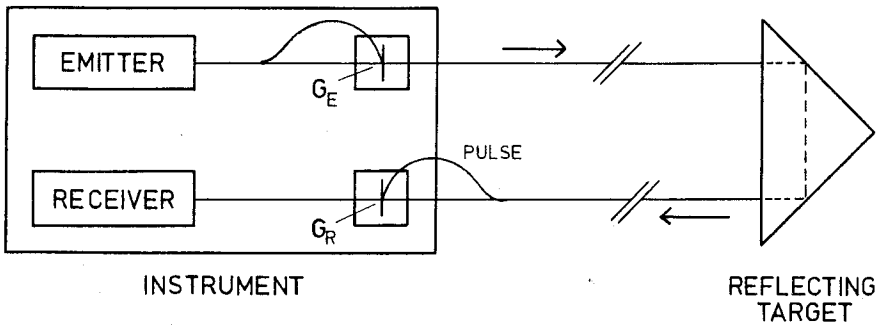

Figure 3.

Depending on the nature (light or radio wave) and power of the pulse and on the distance to be measured, suitable natural or artificial features of landscape (or air space) or special retroreflectors may be used as reflecting agents in terrestrial applications. High powered laser systems are used in military laser ranging, thus allowing for the use of the first type of reflecting surfaces. Civil users prefer well defined, special targets to increase range and precision.

It can be seen from equation (2.9), that the accuracy of the distance is dependent on the accuracy of the flight time measurement. An accuracy in the recording of time of 0.1 ns is equivalent to an accuracy of 15 mm.

2.212 Applications of the Pulse Method

The pulse method is widely used at present in geodesy, navigation and in military applications. Powerful pulsed laser systems are employed in geodesy for extremely long distance measurement. These systems require retroreflectors as targets. Military laser rangers provide medium distances by "shooting" at natural or man-made features visible in the topography. Light wave applications are:

(1) Lunar Laser Ranging
(2) Satellite Laser Ranging and Tracking
(3) Pulsed Laser Rangers
(4) Airborne Laser Terrain Profiler

One lunar laser ranging station is presently operated by the Division of National Mapping (NATMAP) near Canberra. A pulsed two-stage-ruby-laser emits pulses of 3 Joules energy and 25 ns length, or of a power of 0.1 to 0.2 GW. About 10^{19} photons per pulse are emitted, one of which may be expected to be received after reflection. The flight time to the moon and back amounts to about 2.6 seconds. A telescope with a 1500 mm (diameter) mirror is used. The laser beam divergence is such that the footprint on the moon has a diameter of about 4 km. Reflectors set up by the lunar missions of Apollo 11, 14, 15 and Lunakhod are used as targets. The accuracy of one distance measurement is between 1.0 m and 0.1 m. Major problems with lunar laser ranging are encountered in the pointing of the heavy telescope (4 tons) and in the detection of the laser return photons which are often obscured in the large background noise of other photons (e.g. moon light).

Other applications of the pulse method, using radiowaves, for navigational purposes are:

(5) RADAR (*RA*dio *D*etection *A*nd *R*anging)
(6) LORAN (*LO*ng *RA*nge *N*avigation for Aircraft)
(7) SHORAN (*SH*ort *RA*nge *N*avigation for Aircraft)
(8) HIRAN (*HI*gh Precision Sho*RAN*)

Radiowaves are also used in two other geodetic applications:

(9) Satellite Radar Altimeter
(10) Airborne Radar Profiler

The Satellite Radar Altimeter measures continuously the distance between the satellite and the sea surface. A first instrument was used in the Skylab mission in 1973, a second one in the GEOS-C satellite from 1975 on. Satellite altimeters are used for ocean geoid determinations and for detailed determinations of the sea surface topography. The accuracy of altimeter data is better than 1 m.

2.22 Phase Difference Method

The phase difference method is defined here as the method of measuring phase differences of continuous waves for distance measurement.

2.221 Phase Difference between Transmitted and Received Signal

All common EDM instruments used in surveying are based on this principle, regardless of whether they use light waves, infrared waves or microwaves as carrier waves. The measuring signal, which is modulated on the carrier wave in the emitter, travels to the reflector (in the case of an optical carrier wave) and back to the EDM instrument, where it is picked up by the receiver, see figure 4.

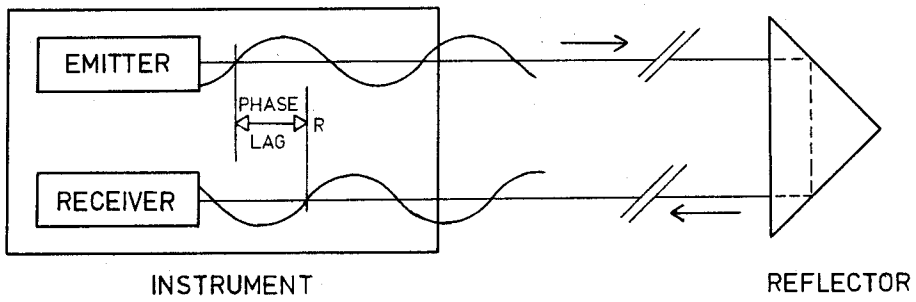

Figure 4.

In the receiver, the phases of the outgoing and the incoming signals are compared and the phase lag $\Delta\Phi$ is measured.

Outgoing signal $y_E = A \sin(\omega t)$ (2.5a)

$= A \sin \Phi$ (2.5b)

Incoming signal $y_R = A \sin \omega(t + \Delta t)$ (2.7a)

$= A \sin (\Phi + \Delta\Phi)$ (2.7b)

Because a continuous signal is used, the values of y_E and y_R will change with time. But the phase lag $\Delta\Phi$ (as well as the time lag Δt) will remain constant. The instrument can therefore measure a constant phase lag despite the fact that the amplitudes of both signals vary continuously. According to equation (2.9) the distance could be computed as follows:

$$d = \frac{c}{2} \Delta t' \qquad (2.10)$$

Unfortunately, $\Delta t'$ cannot be obtained through phase comparison. Phase comparison provides only a time lag Δt. A time equivalent to the number of full cycles elapsed during the flight of a specific signal has to be added to Δt to obtain the total flight time $\Delta t'$.

$$\Delta t' = mt^* + \Delta t \tag{2.11}$$

where $\Delta t'$ = flight time of a specific signal
m = integral number of full wavelengths over the measuring path
t^* = elapsed time for one full cycle of the modulation signal
Δt = time lag in phase measurement

In (2.11), all variables except m and $\Delta t'$ are known. The time lag Δt can be derived from (2.7a) as a function of the measured phase lag $\Delta\Phi$. Substituting ω and f from equations (2.7b) and (2.2) leads finally to

$$\Delta t = \frac{\Delta\Phi\ \lambda}{2\pi\ c} \tag{2.12}$$

where λ is the modulation wavelength.

The time interval of one full cycle of the modulation wavelength (t^*), can be obtained by substituting 2π for $\Delta\Phi$ in equation (2.12). This leads to:

$$t^* = \frac{\lambda}{c} \tag{2.13}$$

Equation (2.10) can now be written in a new form, considering also (2.11), (2.12) and (2.13)

$$\begin{aligned} d &= \frac{c}{2}\,(mt^* + \Delta t) \\ &= \frac{c}{2}\,(m\frac{\lambda}{c} + \frac{\Delta\Phi}{2\pi}\frac{\lambda}{c}) \\ &= m\frac{\lambda}{2} + \frac{\Delta\Phi}{2\pi}\frac{\lambda}{2} \end{aligned} \tag{2.14}$$

With the exception of m all variables of equation (2.14) are known.

Usually, the term $\frac{\lambda}{2}$ is replaced by U which is called the unit length of an EDM instrument. The unit length U is the scale, on which the EDM instrument measures a distance.

$$U = \frac{\lambda}{2} \tag{2.15a}$$

The second term of (2.14) is also replaced by a new term L indicating the fraction of U.

$$L = \frac{\lambda}{2}\frac{\Delta\Phi}{2\pi} = \frac{\Delta\Phi}{2\pi}\,U \tag{2.15b}$$

where L = fraction of unit length U to be determined by phase measurement,
$\Delta\Phi$ = (measured) phase lag (in radians)
U = unit length of distance meter

The fundamental equation (2.14) now reads as follows:

$$d = m\,U + L \tag{2.16}$$

m is an integral number of unit lengths and is still unknown. The ambiguity of equation (2.16) is solved, not by the determination of m but by the introduction of more than one unit length in an EDM instrument. The procedure may be best explained through some examples. The most important unit length of an instrument is always the smallest, which coincides with the highest frequency. This so-called "main" unit length is used for the

fine measurement of distances. The precision of an instrument depends on the choice of this main unit length, because of the limited resolution of the phase measurement.

2.2211 First Example: The HP 3800B

The Hewlett-Packard Distance Meter HP 3800B uses a total of four unit lengths ranging from 10 m to 10 km. The basic principle of operation is explained in the table below.

Step i	Switch Position	Reading $\frac{\Delta\Phi_i}{2\pi}$	Unit Length U_i	Fraction $L_i = \frac{\Delta\Phi_i}{2\pi} U_i$
1a	◎	0.825	10 m	8.25 m
1b	o	0.8250	10 m	8.250 m
2	O	0.382	100 m	38.2 m
3	○	0.433	1000 m	433.0 m
4	○	0.244	10000 m	2440.0 m
Displayed distance d = 2438.250 m				

The underlined figures are transferred mechanically to the distance readout of the instrument. The main unit length of the instrument is 10 metres.

2.2212 Second Example: The Kern DM 500

The Kern Short Range Distance Meter DM 500 uses only two unit lengths of 10 m and 1000 m; the main unit length of the instrument is 10 m.

Step i	Reading $\frac{\Delta\Phi_i}{2\pi}$	Unit Length U_i	Fraction $L_i = \frac{\Delta\Phi_i}{2\pi} U_i$
1	0.8253	10 m	8.253 m
2	0.4384	1000 m	438.4 m
Displayed distance d = 438.253 m			

The underlined figures are on display. The phase measurement is done automatically by digital means. Step one of the procedure is called "fine" measurement, step two "coarse" measurement. For distances longer than one kilometre, 1000 m would have to be added to the readout of the instrument.

2.2213 Third Example: The AGA Geodimeter Model 6A

Older AGA Geodimeter models do not use a set of unit lengths which are related by factors of ten, hundred, thousand etc. They employ unit lengths which are close together. The coarse measurement of distance is derived by computation from differences of three fine measurements with slightly different unit lengths.

The computation method described below is used not only with the model 6A, but also with the models 4, 6 and 8, which use the same four basic frequencies. (The Geodimeter models 6B and 6BL use other frequencies, and a different readout system, which leads to more convenient computations.)

The Geodimeter 6A employs four different unit lengths but needs only three to measure distances up to two kilometres. The fourth is rarely used, because multiples of two kilometres can be easier obtained from other sources, such as maps. The fourth unit

length will therefore not be discussed here.

The three units lengths are as follows:

U_1 = 5.000 000 m
U_2 = 4.987 532 m
U_3 = 4.761 905 m

A large portion of the Geodimeter literature ([5], [6], [7]) quotes unit lengths which are exactly half of the above values because the phase measurement operates only in a range equivalent to half of the unit lengths.

Fine measurements are executed with all three unit lengths. The distance can therefore be computed three times:

$$d = m_1 U_1 + L_1 \qquad (2.17a)$$

$$d = m_2 U_2 + L_2 \qquad (2.17b)$$

$$d = m_3 U_3 + L_3 \qquad (2.17c)$$

where m_1, m_2, m_3 are unknown integers and L_1, L_2, L_3 are the measured fractions of the unit lengths U_1, U_2, U_3 respectively. The unit lengths are related as follows

$$400\ U_1 = 401\ U_2 = 2000 \text{ m} \qquad (2.18a)$$

$$20\ U_1 = 21\ U_3 = 100 \text{ m} \qquad (2.18b)$$

The result of the equations (2.18a) and (2.18b) is that the differences $A = (L_2 - L_1)$ and $B = (L_3 - L_1)$ display a linear rise from zero to five with an increase in distance. Equal values of $A = (L_2 - L_1)$ occur with a period of 2000 metre and equal values of $B = (L_3 - L_1)$ with a period of 100 metre. Based on the values A and B, which are derived from measurements, it is possible to determine the unknown integers m_1, m_2 and m_3 of equations (2.17a), (2.17b) and (2.17c) respectively and thus to calculate the unknown distance d three times.

The necessary computations are fully described in appendix C. A numerical example is also given in the same appendix.

2.222 Phase Difference between two Received Signals

Another form of distance measurement by phase measurement is adopted in navigation systems such as TORAN and DECCA which work in the so-called hyperbolic mode.

Two radio transmitters M and S transmit continuous unmodulated signals of equal frequency. The signals are received at a station R of unknown position. See figure 5.

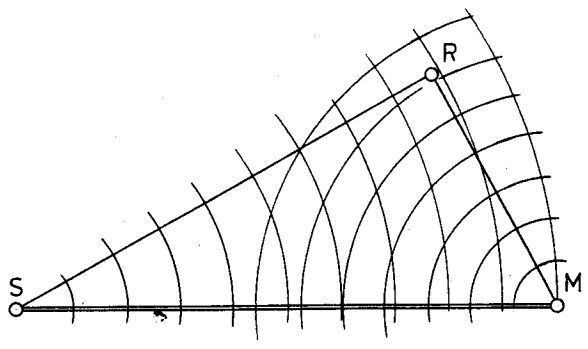

Figure 5.

If Φ_M and Φ_S are the phase angles at any instant of the two radiated signals, their phase difference at station R will be

$$\Delta\Phi = (\Phi_M + \frac{\omega}{c}\overline{MR}) - (\Phi_S + \frac{\omega}{c}\overline{SR})$$

$$= (\Phi_M - \Phi_S) + \frac{2\pi}{\lambda}(\overline{MR} - \overline{SR}) \qquad (2.23)$$

where $\Delta\Phi$ = measured phase difference at station R.
Φ_M, Φ_S = phase angles of the M and S transmitters respectively.
f = frequency of the M and S transmitters.
c = velocity of light in air.
$\overline{MR}$ = distance between transmitter M and receiver R.
$\overline{SR}$ = distance between transmitter S and receiver R.

The phase angles Φ_M and Φ_S are kept in a constant relation. Both transmitters are phase locked, which produces a constant $(\Phi_M - \Phi_S)$. The second term in equation (2.23) is variable and depends on the difference of path lengths from the two transmitters. Lines of equal path difference generate a set of hyperbolae with S and M as foci. A position fix by means of one hyperbola intersecting another requires a second base S_2M. This is provided by a third transmitter. In figure 6, M represents the "master" transmitter and S_1 and S_2 represent "slave" transmitters.

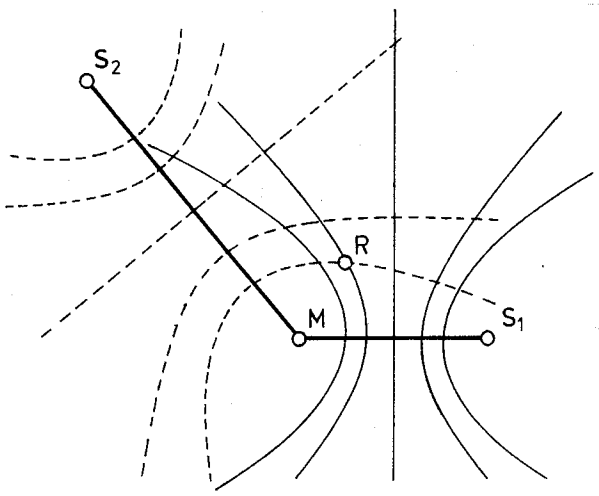

Figure 6.

See references [6] and [7] for more information about navigation systems.

2.23 Doppler Methods

The variation in the pitch of a tone, heard whilst the source of the tone is moved relative to the observer, was first studied by the Austrian physicist Christian Doppler (1803-1853) and later named after him. The *Doppler-effect* is not only observed with acoustic waves but also with all electromagnetic waves. It may be explained with the aid of a terrestrial example; its application in satellite geodesy will be discussed later. Figure 7 depicts a mobile instrument which consists of a microwave transmitter and receiver. The instrument moves at speed v toward a reflecting surface. The transmitted signal is reflected at this surface and picked up by the receiver.

The emitted frequency is expressed as

$$f_T = \frac{c}{\lambda} \qquad (2.24)$$

where c = velocity of light in a medium
λ = wavelength of emitted radiation

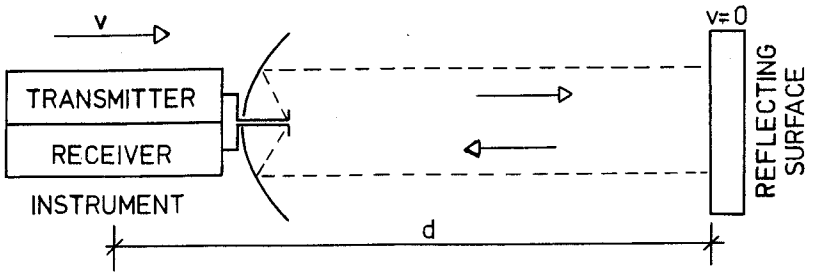

Figure 7.

The following frequency arrives at the reflecting surface:

$$f_S = \frac{c + v}{\lambda} \tag{2.25}$$

where v = speed of instrument relative to reflecting surface.

Back at the receiver R the frequency f_R is received.

$$f_R = \frac{c + 2v}{\lambda} \tag{2.26}$$

Mixing of both frequencies f_T and f_R in the instrument, produces, by interference, the Doppler difference frequency f_D

$$\begin{aligned} f_D &= f_R - f_T \\ &= \frac{c + 2v}{\lambda} - \frac{c}{\lambda} \\ &= \frac{2v}{\lambda} \end{aligned} \tag{2.27}$$

The procedure for measuring the Doppler frequency depends on the type of waves used. The Doppler frequency f_D may be obtained by either:

(1) Counting the beats per second in the case of sound waves.
(2) Counting the bright (or dark) fringes of an optical interference pattern in the case of light waves.
(3) Counting the cycles of the Doppler signal ("Doppler counts") per second in the case of radio waves.

Equation (2.27) may be written as:

$$v = \tfrac{1}{2} f_D \lambda \tag{2.28}$$

The distance travelled by the instrument between time t_1 and time t_2 is

$$d_{12} = \int_{t_1}^{t_2} \tfrac{1}{2} f_D \lambda \, dt \tag{2.29}$$

The Doppler method is used at present for position fixing. In geodesy it involves signals from satellites and Doppler Receivers. See figure 8. The latest Doppler receiver consists of three portable parts: an antenna which is set up and centred over the survey mark, the receiver unit with tape recorder, and the battery or power supply.

Five or six U.S. navigation satellites are permanently in orbit around the earth thus providing a world wide navigation system. Setting up a *Doppler Receiver* at a station and recording a number of successive satellite passes allows the computation of the coordinates of the ground station. The doppler receiver measures the distance differences

$$\begin{aligned} \Delta d_1 &= d_1 - d_2 \\ \Delta d_2 &= d_2 - d_3 \\ \Delta d_3 &= d_3 - d_4 \\ &\cdots\cdots \end{aligned}$$

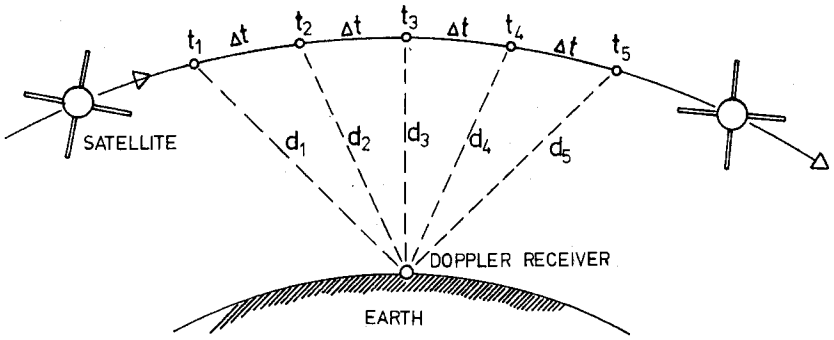

Figure 8.

using Doppler counts of the Doppler frequency f_D from interference between the received satellite broadcast frequency and internal reference frequency.

$$\Delta d_i = \int_{t_i}^{t_{i+1}} f_D \, \lambda \, dt$$

$$= \lambda \, [\text{doppler counts}]_{t_i}^{t_{i+1}} \qquad (2.30)$$

The satellite orbit is known and the position of the ground station can therefore be obtained by intersecting hyperboloids of revolution. Hyperboloids are the loci in space of equal distance differences with respect to two points. Each time interval Δt (figure 8) produces one pair of hyperboloids of revolution with focal points corresponding to the satellite positions at the beginning and the end of the time interval. The position of the Doppler receiver can be obtained in a geocentric coordinate system, with accuracies of better than 1 m in each of the three coordinates x, y and z [8].

2.24 Interferometry

The principle of optical interference is used in interferometers for metrology, for high precision distance measurements over short distances and also in the definition of the metre.

The basic principle of an interferometer is depicted in figure 9. A light source LS such as a laser or a Krypton lamp produces a light beam which is directed towards a beam splitter BS. This allows one portion of the beam to pass to the moving reflector MR and deflects another portion to the fixed reflector FR. The beams, returned by the reflectors, pass again through the beam splitter BS and produce an interference pattern there. The interference pattern is recorded by the photo detector PD and Doppler counts are recorded by the digital counter C.

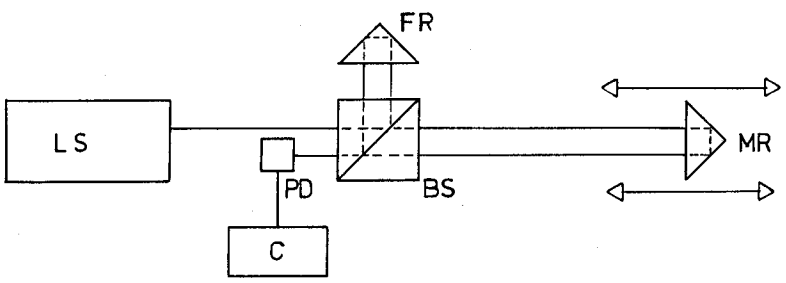

Figure 9.

The two waves superimposed in the beam splitter are of equal frequency and amplitude (coherent waves) because they are generated by the same light source. They have however, a constant phase difference because of the difference in path lengths. They may be described according to (2.5a) and (2.7a) :

$$y_1 = A \sin (wt)$$

$$y_2 = A \sin (wt + \Delta\Phi)$$

The superimposed signal is of the form

$$y = y_1 + y_2 = (2A \cos (\frac{\Delta\Phi}{2})) \sin (\omega t + \frac{\Delta\Phi}{2}) \qquad (2.31)$$

y reaches a maximum for a phase lag of $\Delta\Phi = 0$ (constructive interference) and minimum for $\Delta\Phi = \pi$(destructive interference). During a displacement of the movable reflector MR, the photo detector counts the number of bright fringes in the interference pattern of the beam splitter.

The distance between the beginning and the end positions of the reflector is derived from

$$2d = (\text{number of bright fringes}) \times \lambda \qquad (2.32a)$$

where λ = wave length of light source.

Or in the final form:

$$d = (\text{number of bright fringes}) \times \frac{\lambda}{2} \qquad (2.32b)$$

The high resolution of interferometers is based on the direct use of the wave length of light waves for measurement. Some EDM instruments use light waves as carrier, but a modulated signal is used for the measurement. Considering a laser interferometer with a HeNe-laser light source, the wave length is $\lambda = 632.8$ nm thus leading to a least count of about 0.3 µm. The overall accuracy of such systems however, is limited to about 0.1 ppm by the uncertainty of the refractive index. Common laser interferometers have a maximum range of about 80 m and are mainly used indoors. They are not only utilized for precise length measurements but generally also in metrology for measurement of straightness, squareness, parallelism, flatness and angle. For example, the Hewlett-Packard HP5526A laser measurement system is used for such measurements.

2.3 Basic Working Principles of Electronic Distance Meters

EDM instruments are classified according to the type of carrier wave employed. Instruments using light or IR waves are classified as *electrooptical instruments*. Instruments based on radio waves are generally called *microwave instruments*. Because of the different structure of these two types of instruments, they will be discussed separately.

2.31 Electrooptical Instruments

2.311 Principle and Components

The basic working principle of an electrooptical distance meter is explained with reference to the type of instrument which uses an analogue phase measuring system. Such instruments display the functions of the different components more clearly. Figure 10 depicts the major parts and the flow of information.

The *LIGHT-SOURCE* produces the so-called carrier wave. The wave is described by the carrier wavelength λ_{CARR}. The following light sources are presently in use (in order of importance):

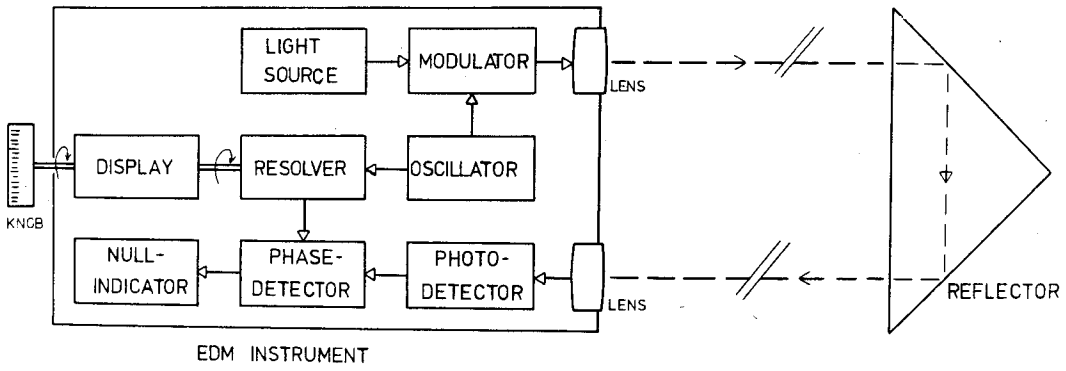

Figure 10.

(1) GaAs Infrared Emitting Diode (Luminescence Diode) and GaAs Diode Laser .
$0.800 < \lambda_{CARR} < 0.950$ µm

Gallium Arsenide diodes have a bandwidth of about 30 nm and are therefore almost monochromatic. The emission of photons at the p-n junction of the diode is produced by an applied drive current (see figure 13 in section 2.3121). The degree of coherence of the radiation depends on the type of diode. The radiant power output could be as high as 40 mW but is usually much lower. It depends largely on the drive current applied, the modulation frequency and the ambient temperature. The effective source size is about 0.5 mm. Gallium Arsenide diodes are used in most short-range and medium-range EDM instruments.

(2) HeNe-Laser $\lambda_{CARR} = 0.6328$ µm

The radiant power output of these "red" gas lasers varies between 1 mW and 10 mW. Lasers produce a coherent and monochromatic light of high power density and small divergence. Lasers are used mainly in long range EDM instruments. Distances up to 80 km may be measured, visibility permitting.

(3) Tungsten Lamp. $\lambda_{CARR} = 0.550$ µm

Tungsten lamps of 3 to 20W were built into the older Geodimeter instruments. The Geodimeter 6A uses a 3W lamp.

(4) Xenon Flash Tube. $\lambda_{CARR} = 0.480$ µm

High pressure Xenon flashtubes are used only in the Kern Mekometer ME 3000. Flashes of 1.0 µs duration and 0.04 Joule energy are produced at a repetition rate of 100 Hz.

(5) Mercury Lamp $\lambda_{CARR} = 0.549$ µm

High pressure mercury lamps (100W) were used in earlier Geodimeter models to increase the range. Small electrical generators were necessary to produce sufficient current for this equipment.

The *MODULATOR* varies the amplitude by intensity modulation of the carrier wave at a modulation frequency produced by an oscillator. The light beam will therefore alternate between bright and dark sequences. The modulation wavelength λ_{MOD} is always much longer than the carrier wavelength, λ_{CARR}, or in other words, the modulation frequency is much lower than the carrier frequency. Different modulation techniques are discussed in section 2.312.

The *TRANSMITTER LENS SYSTEM*, which may have a fixed or adjustable focus, produces a beam divergence of about 5 minutes of arc for short range instruments and 20 seconds of arc for long range laser instruments such as the Geodimeter model 8. Narrow beams produce

strong return signals but because of the pointing precision demanded, they may take pointing to distant reflectors a very tedious operation.

The *REFLECTOR* consists of a glass prism in a housing. All incident rays are reflected in such a way that the reflected rays are parallel to the incoming ones. The rays are therefore returned to the EDM instrument without the necessity of very accurate orientation of the reflector. Details of reflectors are described in section 4.3.

The *RECEIVER LENS SYSTEM* may again be of the fixed or adjustable focus type. It focuses the return signal onto the photo detector.

The *PHOTO DETECTOR* transforms the light beam's intensity variations into variations of current. Two devices are commonly used for this purpose:

(1) In the range of semiconductors such as Si-(Silicon)-photo-diodes or Si-avalanche-photo-diodes (APD), Silicon-photo-diodes are preferred to Germanium-photo-diodes because of their higher response at wavelength λ = 900 nm. Si-avalanche-photo-diodes are preferred to Si-photo-diodes because of their better signal-to-noise ratio, and are therefore used in most short-range EDM instruments.

(2) Photomultipliers (photo tubes): Light falls onto the cathode which, being coated with a photo-electric substance, emits electrons according to the light's energy. Between anode and cathode, the number of electrons is multiplied by an array of dynodes . Amplification factors up to 10^8 are possible. Such devices are used mainly in long range EDM instruments. See references [4] and [6].

The *OSCILLATOR* produces the modulation frequency and consists of an oscillator circuit which is locked to the resonant vibration frequency of a quartz crystal. To obtain a unit length of 10 m, the modulation frequency needs to be approximately 15 MHz. The resulting frequency is a function of the shape and size of the quartz crystal employed. Changes in ambient temperature and ageing of the quartz yield changes in the frequencies of oscillators. Differing systems are employed on EDM instruments to minimize temperature effects:

(1) Oven-controlled oscillators are accurate to ±1 ppm or better. They need a warm-up time of at least fifteen minutes.

(2) Temperature-compensated oscillators need no warm up time and are accurate to ±1 ppm in the range 0° to $+50^{\circ}$C and ±3 ppm in the range -20° to $+50^{\circ}$C.

(3) Non-compensated oscillators are accurate to about 5 to 15 ppm (-25° to $+50^{\circ}$C) and require no warm-up time.

Ageing may change the oscillator frequency by up to 5 ppm per year.

The *RESOLVER* shifts the phase of the reference signal. In figure 10, a rotation of the phase shift knob simultaneously changes the readout and the resolver angle, and thus the phase of the reference signal.

The *PHASE DETECTOR* provides the phase comparison between the return and the reference signal. The result of this phase detection is displayed on the *NULL INDICATOR*. The null indicator reads zero when both signals are exactly in phase. This is achieved by turning the resolver as explained above. More information on phase measurement is given in section 2.313.

The *DISPLAY* is directly coupled with the resolver. It indicates the position of the resolver and is therefore a readout of the measured phase difference. Both display and resolver position can be altered by turning the PHASE SHIFT KNOB.

2.312 Methods of Modulation and Demodulation of Light or Near Infrared Waves

2.3121 Direct Modulation

With direct modulation, electrical current is directly transformed into radiation. This can be done easily with luminescense or light-emitting diodes (as for example GaAs infrared emitting diodes). Here the radiated power and the intensity of radiation are functions of the injection current. A modulated injection current will produce an equally modulated radiation. The basic principle of this process is depicted in figure 11.

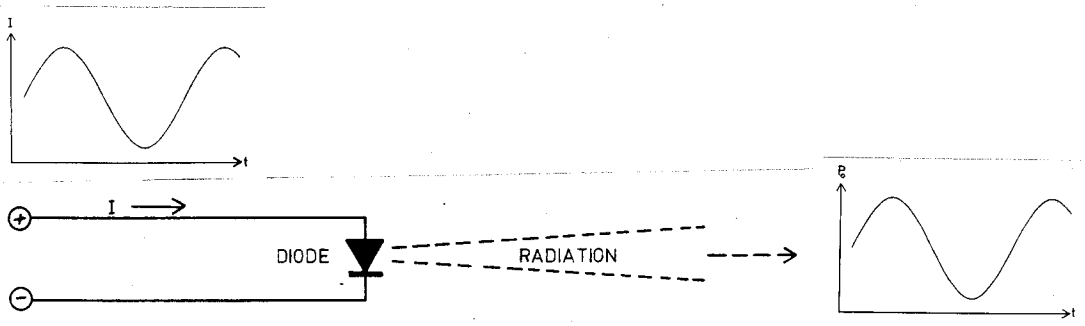

Figure 11. I = electric current, P_o = radiant power output, t = time.

The direct conversion of a modulated current into a modulated radiation is based on the transfer characteristics of such diodes. In figure 12, a typical radiant power output P_o is given as a function of the drive (or injection) dc-current I. For example in a typical diode, an amplitude modulation of the dc drive current between 10 and 30 mA leads to an amplitude modulated power output P_o between 0.4 and 1.2 mW (RCA 40736R).

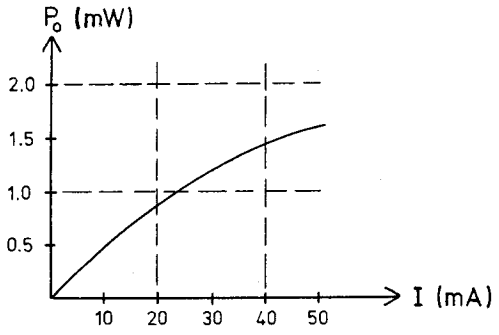

Figure 12.

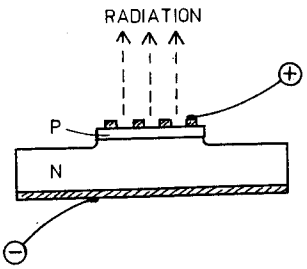

Figure 13.

Figure 13 depicts a cross section through a surface emitting gallium arsenide diode. P stands for p-type semiconductor (acceptor) and N stands for n-type semiconductor (donor). GaAs diodes are pn-junction diodes where the radiation is produced at the junction of both materials. GaAs diodes have some properties which affect the operation of EDM instruments. The so-called phase inhomogeneities in the emitted radiation cone describes the fact that the radiation intensities produced at different points of the pn-junction are not equal at any one same time, thus causing a variation in the phase of the modulation signal on the diode surface. The effect is caused by the different path lengths travelled by the current within the pn-material of high refractive index. Further properties are the decrease of radiant power P_o with an increase of ambient temperature and with ageing of the diode.

2.3122 Direct Demodulation

Photo-diodes have the property of transforming radiation into electrical current: the higher the radiation power, the higher the current flow through the diode. The mechanism of photo diodes will not be explained in depth, because they display basically the reverse

effect of emitting diodes. EDM instruments use mainly Silicon Photo-Diodes or Si-Avalanche (Multiplication) Photo-Diodes (APD). The latter produce a much higher amplification. Photodiodes have similar properties and deficiencies to luminescence diodes.

2.3123 Indirect Modulation

Indirect modulation may be achieved by passing a continuous light beam through two polaroid filters of perpendicular polarization planes. Between the two filters the plane of the polarized light is rotated by a special device in phase with a modulation signal. This results in an amplitude modulated light beam emerging from the second filter. The principle is explained in figure 14. Two devices for the rotation of the polarization plane are commonly used in conjunction with EDM instruments.

Kerr Cell

The Kerr cell is a glass tube filled with nitrobenzene and containing two built-in parallel plates, which form the two electrodes of a condenser. A potential difference across these plates causes a rotation of the plane of polarisation of light passing between them. This electrooptical *Kerr-effect* makes it possible by rotating the incident polarization plane of light, to modulate the intensity of the emerging light beam.

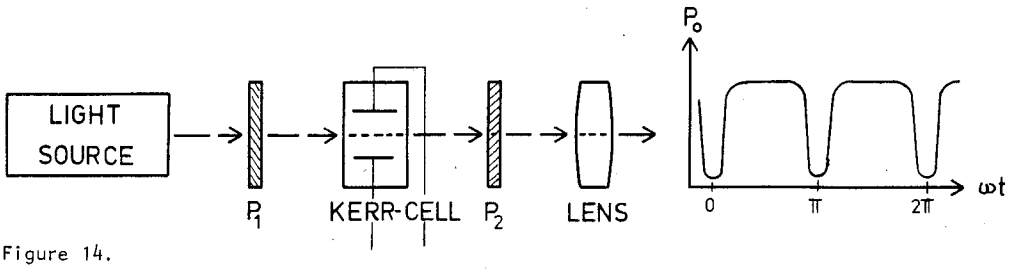

Figure 14.

In figure 14, P_1 and P_2 indicate polaroid filters with polarization planes set perpendicular. The Kerr cell's electrodes make an angle of 45° with the polarization planes of P_1 and P_2.

In order to produce the light modulation shown, the modulation frequency is superimposed on the high bias voltage applied to the Kerr cell electrodes. See reference [4] for more details of Kerr cells. Kerr cells can be found in the Geodimeter models 6, 6A, 6B, 6BL, 700/710, 600 and also in all earlier Geodimeter instruments.

KDP Crystals

The potassium di-hydrogen phosphate crystals KDP (K from the chemical symbol for Potassium) exhibit another electrooptical effect, which is called *Pockel's effect*. The plane of a polarized light beam is rotated by the KDP crystal in proportion to the voltage applied to the crystal. After passing a second polaroid filter, the light beam is amplitude modulated. Such crystals are incorporated in the Geodimeter model 8 and the Mekometer.

2.3124 Indirect Demodulation

Indirect demodulation is mostly combined with the subsequent phase measurement. Two devices of this kind are used in present day instruments.

Photomultiplier

The conversion of light into electric current by means of photomultipliers, has already been mentioned in 2.311. The photomultiplier can be operated with a modulated voltage, the modulation being equal to that of the outgoing light wave. The photomultiplier will then produce a maximum current output when the transmitted and the received measuring signals are in phase. It will produce a minimum current if both signals have a phase difference of 180^{o}. The Geodimeter models 6, 6A, 6B, 600, 8 and 700/710 are equipped with photomultipliers.

KDP Crystal

KDP crystals can not only be used for modulation but also for demodulation purposes. The same amplitude-modulated voltage applied to the transmitter crystal is applied to the receiver crystal. A maximum light output after the second crystal and its polaroid filter results if there is no phase difference between transmitted and received signal. For a phase difference of 180^{o} the light output would be zero. Such a system is employed in the Mekometer where the light output is detected by a photomultiplier.

2.313 Methods of Phase Measurement

2.3131 Optical-Mechanical Phase Measurement

The principle of optical-mechanical phase measurement is depicted in figure 15. The return signal travels through an internal light path the length of which can be varied by one full unit length. The phase difference can be measured easily and directly in terms of length, by recording that displacement of the moving prisms which is required to null the null-indicator. Such a manual system is used in the Mekometer; there, it has been found to be unaffected by cyclic errors (see section 4.52).

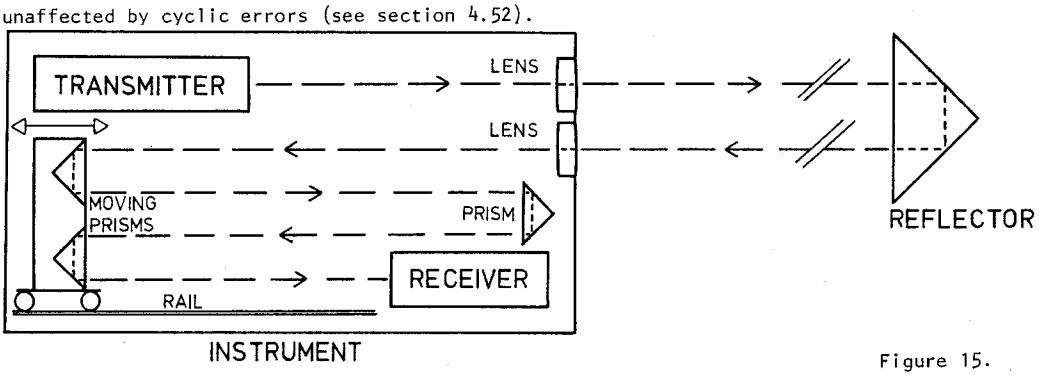

Figure 15.

2.3132 Electric Analogue Phase Measurement

The principle of the analogue phase measurement involves the delay of a reference signal of the same characteristics as the transmitted signal until a zero phase lag with the return signal is obtained. Electrical delay lines are mostly designed as *resolvers*, which are very similar to an electric motor. The phase angle therefore becomes a physical quantity based on the revolution of the resolver. All instruments equipped with resolvers (eg. Geodimeters, Wild DI 10, Tellurometer MA 100) may be subject to systematic errors within the phase measurement interval. These so-called cyclic errors are sometimes termed the non-linearity of the phase measurement. The wave length of such cyclic errors is normally equal to half of the unit length ($\frac{\lambda \text{ MOD}}{4}$).

The HP3800B has another system of analogue phase measurement; the phase angle is transformed into a direct current. In this system some systematic errors may also occur but these will not be of a sinusoidal nature.

The testing of analogue phase measurement systems is usually carried out in conjunction with the examination of cyclic errors. See section 4.62.

2.3133 Electric Digital Phase Measurement

The digital phase measurement is based on the comparison of two low-frequency sinusoidal signals of equal frequency. One signal is the reference (or transmitted) signal, the other the return signal. Both signals are triggered into square waves and operate a gate. The gate is opened when the reference signal begins a new cycle, and closed when the return signal does the same. During the time of the open gate, pulses from a high frequency oscillator are accumulated in a counter. See figure 16 for the corresponding block diagram.

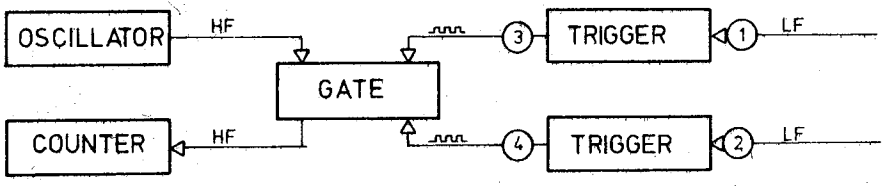

Figure 16.

The phase difference between the two signals can be deduced in two different ways. A first possibility is depicted in figure 17, which also illustrates the whole measurement: (1) depicts the reference (transmitted) signal, (2) the return signal, (3) the triggered reference signal, (4) the triggered return signal. (5) shows the phase counts "i" between the opening of the gate (GO) and the closure of the gate (GC). In (6), a full wavelength is counted ("j" counts). The phase difference L can be computed according to figure 17 as:

$$L = \frac{i}{j} \times U \qquad (2.33)$$

where U is the unit length which corresponds to the frequency of reference and return signals.

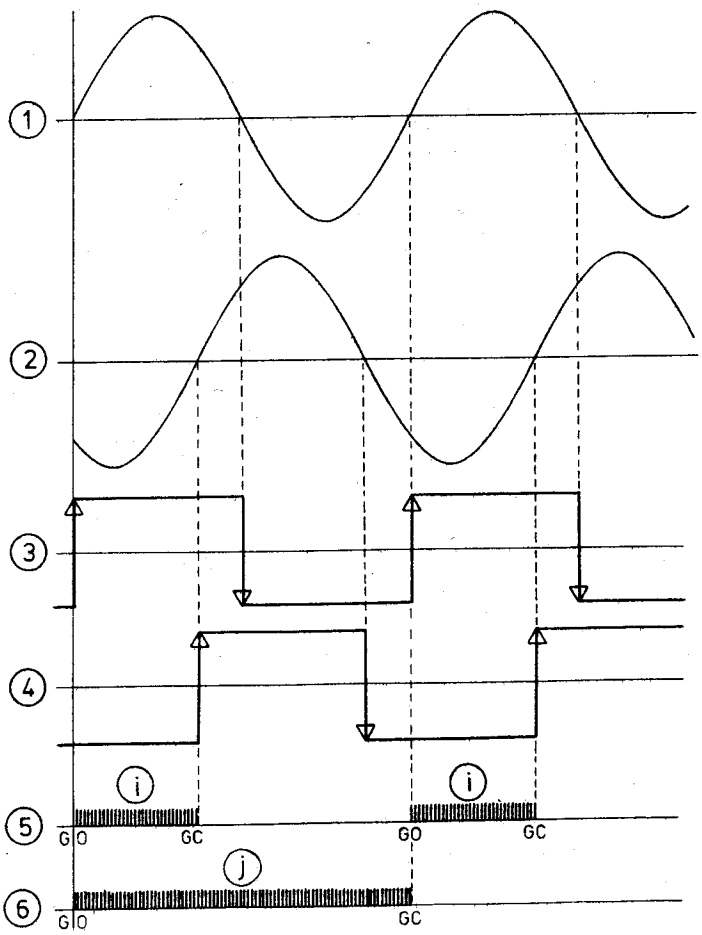

Figure 17.

This procedure does not need a constant ratio between the oscillator's high frequency and the low frequency of the return and reference signals.

Another solution can be achieved, if the high frequency pulses are in a fixed ratio to the low frequencies of the measurement signals. This can be easily achieved, if both frequencies are derived from the same master oscillator in the transmitter. In the HP3805, for example, the return and reference signals have a low frequency of 3745 Hz whilst the high frequency pulses are at 14 987 103 Hz. There are therefore, during one full low frequency cycle, exactly 4000 pulses of the high frequency. The number of "j" need not be measured this time but is obtained by calculation as 4000. This leads to the following formula for the phase difference L:

$$L = \frac{i\, f_{LOW}}{f_{HIGH}}\, U \qquad (2.34)$$

where U is again the corresponding unit length of the distance meter.

Example: HP 3805A $\quad L = \frac{i}{4000}\, U$

where U is either 2000 m (coarse measurement) or 10 m (fine measurement).

2.32 Microwave Instruments

A general outline of a microwave instrument using an analogue phase measuring system will now be given. Figure 18 depicts the basic design of the Tellurometer, the first microwave instrument which became available in 1957. In figure 18, the two functions of microwave instruments are clearly distinguished, namely the "Master" and the "Remote" mode. However both modes are usually incorporated in the instrument at each terminal of a line, so that the distance can be measured in 'forward' and 'reverse' directions.

The presence of a parabolic or horn radio antenna and the absence of optical parts are the most obvious differences from an electrooptical EDM instrument. In addition, microwave instruments not only make use of amplitude modulation (AM) but also of frequency modulation (FM) and they provide a built-in phone link between the two stations.

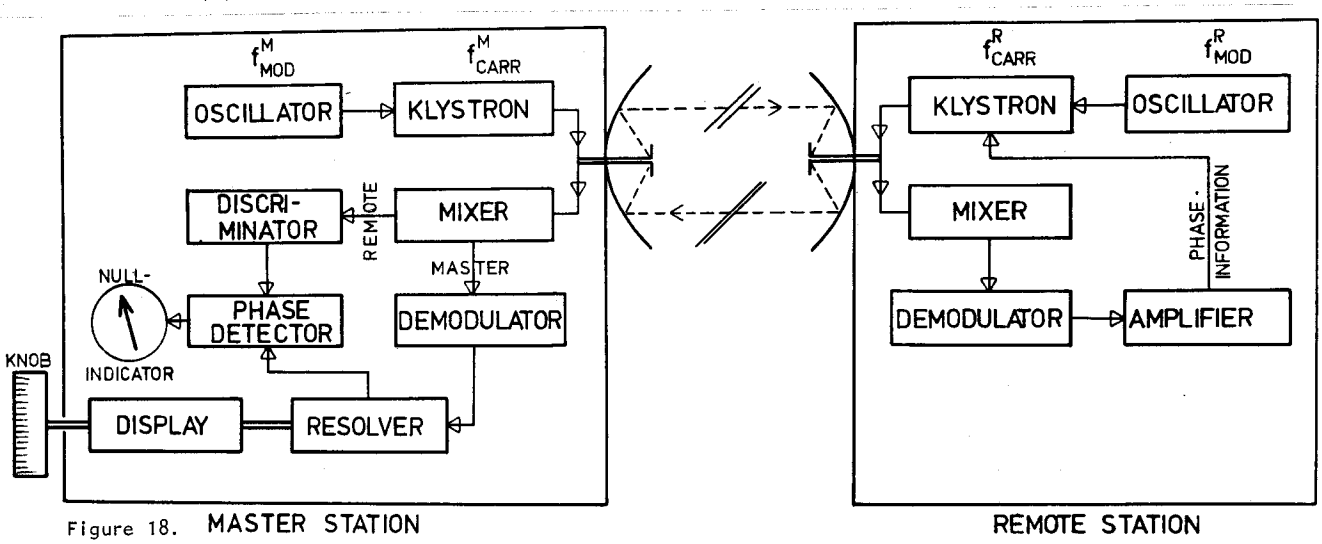

Figure 18.

The *OSCILLATOR* has the same function as that in electrooptical instruments. (See section 2.313). It can be switched through different quartz crystals to produce several modulation frequencies. Because microwave instruments are long range instruments, oscillator frequencies have to be temperature controlled, normally by provision of an oven.

The *KLYSTRON* or cavity resonator is an electronic tube producing a microwave. It is operated in such a way that the emerging microwave is frequency modulated by an oscillator frequency. See [4] for details.

The *ANTENNA* can be of parabolic shape (about 300 mm diameter) and has two small dipoles at its focus. These are perpendicular to each other set at 45^{o} to the vertical. Transmitted and received signals are polarized in two planes perpendicular to each other.

The *MIXER* mixes transmitted signal and the signal received at the antenna.

DEMODULATORS demodulate amplitude modulated (AM) signals into alternating currents (AC).

DISCRIMINATORS demodulate frequency modulated (FM) signals into alternating currents.

The functions of the resolver, phase detector, null indicator and the display have already been discussed.

Distance measurement with a microwave instrument is described as follows: Master and remote stations transmit a frequency modulated signal. The modulation frequencies are slightly different for the two stations. The transmitted and the received signals are mixed at both stations and the phase difference of both signals determined. Because phase information must be available at the master station for the phase measurement, the phase information of the remote station is transmitted back to the master instrument by an additional frequency modulation of the remote carrier wave. After demodulation by the discriminator, the remote phase information is used as a reference signal in the analogue phase measurement. The master phase difference information is demodulated by the demodulator and then used as "return" signal for the phase measurement. The latter has been described in 2.311.

2.4 Propagation of Electromagnetic Waves through the Atmosphere

2.41 Atmospheric Transmittance

The transmittance of the atmosphere is usually described by the quotient incident radiant power divided by transmitted radiant power. It is a measure of the attenuation and extinction of wave propagation. The transmittance is a function of numerous variables: wavelength, distance, temperature, barometric pressure, gaseous mixture, rain, snow, dust, aerosols, bacteria and, in more detail, the size of particles of all these constituents. The limitations of atmospheric transmittance are given by the scattering and absorption of the emitted radiation. Scattering by air molecules (Rayleigh Scattering) and scattering by larger aerosol particles (Mie scattering) can be distinguished. Absorption in several spectral regions in mainly caused by water vapour, carbon dioxide and ozone. Figure 19 depicts the transmittance of atmosphere as a function of wavelength for a part of the visible and near-infrared (NIR) spectrum under specific conditions [9]. The Figure shows that only a limited part of the NIR spectrum is suitable for EDM.

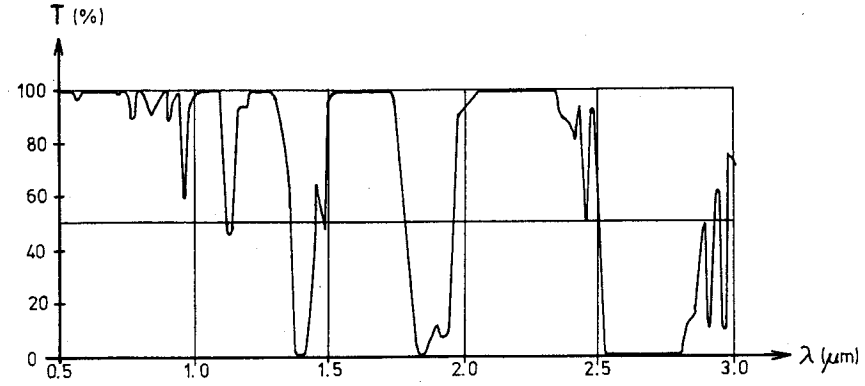

Figure 19. T = TRANSMITTANCE

Attenuation of radiation through the atmosphere is the intensity reduction of wave propagation through scattering and absorption (attenuation (in %) = 100 minus transmittance (in %)) and may be expressed by "Bouguer's" rule

$$J = \frac{J_o}{d^2} e^{-zd} \qquad (2.35)$$

where J = radiant intensity at some distance d from the emitter
J_o = radiant intensity at emitter
d = distance
z = attenuation coefficient or extinction coefficient

The first factor of equation (2.35) accounts for the purely geometrical propagation. The second, exponential, factor accounts for the transmittance of the atmosphere. The attenuation coefficient is a function of several variables already mentioned at the beginning of this section.

If the "visibility range" or the "meteorological range" is known, the attenuation coefficient can be derived as

$$z_v = \frac{3.912}{d_v} \qquad (2.36)$$

where z_v is the *attenuation coefficient* for the visible spectrum ($\lambda_{EFF} = 0.555$ µm) and d_v is the *meteorological range* in kilometres. The "meteorological range" is defined as the range over which one can just distinguish a large, black target such as a pine forest from the horizon.

In EDM, the transmittance of the atmosphere affects the range of instruments and the strength of the return signal. [84]

2.42 Refractive Index

The refractive index n of a medium is defined as

$$n = \frac{c_o}{c} \qquad (2.37)$$

where c_o = velocity of light in a vacuum
c = velocity of light in a medium.

The refractive index of air is a function of:

(1) the gaseous composition of the atmosphere, which is very nearly a constant;
(2) the amount of water vapour pressure in the atmosphere;
(3) the temperature of the gaseous mixture;
(4) the pressure of the gaseous mixture; and
(5) the frequency of the radiated signal.

The variation of the refractive index with frequency constitutes the phenomenom of *dispersion*.

2.43 Group Refractive Index of Light

In electrooptical EDM, the refractive index is dependent on the wavelength of the visible or infrared radiation, i.e. a well defined frequency and its associated frequency band which is formed by several frequencies. The different frequencies would have the same propagation velocity in a vacuum, but not in air, as interference between the different frequencies occurs. The signal resulting from the sum of all frequencies will have the so-called group velocity which is always smaller than the wave velocities of its individual frequencies:

$$c_g = c - \frac{dc}{d\lambda} \lambda \qquad (2.38)$$

where c_g and c are the group velocity and individual wave velocity respectively.

Calling n_g the group refractive index, the following equation may be written:

$$c_o = c_g n_g \tag{2.39}$$

and after substituting (2.39) and (2.4) in (2.38) and re-arranging:

$$n_g = n - \frac{dn}{d\lambda} \lambda \tag{2.40}$$

where λ is the wavelength in a vacuum.

The group refractive index may be calculated according to Barrell and Sears [32] :

$$(n_g - 1) \times 10^6 = 287.604 + 3\left(\frac{1.6288}{\lambda^2}\right) + 5\left(\frac{0.0136}{\lambda^4}\right) \tag{2.41}$$

where λ is expressed in μm (micrometres).

This formula is valid for visible light in dry air at 0^oC, 1013.25 mb (760 mm Hg) and 0.03 per cent CO_2. λ is the "effective" wavelength in a vacuum. Equation (2.41) describes the group refractive index with an accuracy of ±0.1 ppm or better.

Formula (2.41) was derived from experiments and was adopted by XIIth General Assembly of IUGG in Helsinki, 1960 together with another formula by B. Edlen [33]. Both formulae agree within 0.1 ppm for $\lambda = 0.56$ µm as well as for $\lambda = 0.90$ µm.

First Example: The Hewlett-Packard Distance Meter HP 3800B has a Ga-As luminescence diode emitting radiation of wavelength $\lambda = 910$ nm. Under standard conditions of 0^oC, 1013.25 mb, dry air (e = 0) and 0.03 per cent CO_2 in the air, the group refractive index reads:

$$(n_g - 1)10^6 = 287.604 + \frac{4.8864}{\lambda^2} + \frac{0.0680}{\lambda^4} \tag{2.42}$$

and for $\lambda = 0.910$ µm,

$$(n_g - 1)10^6 = 293.604$$

$$n_g = 1.000\ 293\ 6$$

It is common practice to accept equation (2.41) as valid for NIR carrier waves with wavelengths close to the visible range.

Second Example: The AGA Geodimeter 6A uses a simple Tungsten lamp with an effective wavelength of $\lambda_{EFF} = 550$ nm.

The same standard atmospheric conditions apply as for example 1 and the group refractive index may be written as

$$(n_g - 1)10^6 = 287.604 + 16.1534 + 0.7431$$

$$(n_g - 1)10^6 = 304.5005$$

$$n_g = 1.000\ 304\ 5$$

Error Analysis

Differentiating formula (2.41) with respect to λ demonstrates that an error $d\lambda$ in λ of 5 nm causes an error dn_g of 0.3 ppm. The carrier wavelength must therefore be known quite accurately.

2.44 Refractive Index of Light

For the purpose of computing the refractive index for actual atmospheric conditions, Barrell and Sears [32] have given the following formula, which reads, with millibar as the pressure unit:

$$n_L = 1 + \frac{n_g - 1}{1+\alpha t} \cdot \frac{p}{1013.25} - \frac{4.1 \times 10^{-8}}{1+\alpha t} e \qquad (2.43)$$

where n_L = group refractive index valid for atmospheric conditions described by t, p, e.
t = "dry bulb" temperature of air (^oC)
p = atmospheric pressure (mb)
α = coefficient of expansion of air (= 0.003 67 per ^oC)
e = partial water vapour pressure (mb)

Kohlrausch has given another form of equation (2.43) which reads, after substituting $(273.15)^{-1}$ for α:

$$(n_L - 1) = (n_g - 1) \frac{273.16\ p}{(273.16 + t)1013.25} - \frac{11.20 \times 10^{-6}}{(273.16 + t)} e \qquad (2.44)$$

This formula was adopted by the XIIth General Assembly of IUGG in 1960 in Helsinki. Equation (2.44) is valid within the temperature range -40^oC - $+50^oC$ and the pressure range 533 mb - 1067 mb and has a maximum error of 0.2 ppm.

Error Analysis

The effects of errors in the variables p, t, and e on the derived quantity n_L may be analysed by their partial differentials. For a temperature of 15^oC, a pressure of 1007 mb, a partial water vapour pressure of 13 mb and a group refractive index n_g of 1.000 304 5 differentiation of equation (2.44) yields:

$$dn_L \times 10^6 = -1.00\ dt + 0.28\ dp - 0.04\ de \qquad (2.45)$$

where dn_L = differential of the (group) refractive index of light
dt = differential of temperature t (^oC)
dp = differential of pressure p (mb)
de = differential of partial water vapour pressure e (mb)

The significance of equation (2.45) can be summarized as follows:

(1) An error in t of 1^oC affects refractive index and distance by 1 ppm.
(2) An error in p of 1.0 mb affects refractive index and distance by 0.3 ppm.
(3) An error in e of 1 mb affects the refractive index by 0.04 ppm and e therefore need not be known very accurately.

Temperature is critical for the determination of the refractive index. Temperature may be measured very accurately at both terminals of a line and the refractive index calculated for both terminals and the mean taken. Even so, the mean value of the refractive index generally does not represent the prevailing integral value over the wave path to better than 1 ppm. The accuracy of electrooptical distance measurement is therefore normally limited to 1 ppm of the measured distance although a better accuracy (> 0.1 ppm) can be obtained using special techniques. See section 2.48 for more details.

Humidity

Very often, the effect of the partial water vapour pressure e is disregarded in formulae provided by manufacturers. Ignoring the following term of equation (2.44)

$$- \frac{11.20 \times 10^{-6}}{(273.16 + t)} e$$

causes the following errors of the refractive index and, subsequently, of distance.

Temperature t	Errors in refractive index	
	h = 50 percent	h = 100 percent
0° C	0.1 ppm	0.2 ppm
10°	0.2 ppm	0.5 ppm
20°	0.4 ppm	0.9 ppm
30°	0.8 ppm	1.6 ppm
40°	1.4 ppm	2.8 ppm
50°	2.3 ppm	4.6 ppm

The relative humidity h is related to e. Its definition will be given later in section 2.474.

In summertime, the refractive index could be in error by 1.3 ppm in the Sydney area (30°C, 80 per cent relative humidity), if the partial water vapour pressure is not taken into account.

Users of reduction formulae or diagrams designed by instrument manufacturers should be aware of this fact. It is recommended that humidity be considered for more precise work and over longer distances.

2.45 Refractive Index of Microwaves

The XIIth General Assembly of IUGG , 1960, in Helsinki, adopted the formula by Essen and Froome [27] for the determination of the refractive index of microwaves. The equation is the result of experiments carried out at the National Physical Laboratory (Teddington, U.K.) in 1951 with the aid of cavity resonators.

$$(n_M - 1)10^6 = \frac{77.64}{(273.16 + t)}(p - e) + \frac{64.68}{(273.16 + t)}\left(1 + \frac{5748}{(273.16 + t)}\right) e \qquad (2.46)$$

where n_M = refractive index for microwaves
t = "dry bulb" temperature of air ($^{\circ}$C)
p = pressure of air (mb)
e = partial water vapour pressure (mb)

The accuracy of equation (2.46) is ±0.1 ppm under normal conditions and better than ±1 ppm under extreme conditions. The above equation is valid for carrier wavelengths between $\lambda = 0.03$ and $\lambda = 1.00$ m.

Error Propagation

The total differential of equation (2.46) allows the effects of errors in p, t and e on n_M to be assessed. The coefficients of the total differentials are computed for $t = 10^{\circ}$C, $p = 1013.25$ mb and $e = 13$ mb.

$$dn_M \times 10^6 = -1.4\ dt + 0.3\ dp + 4.6\ de \qquad (2.47)$$

dn_M = differential of refractive index of microwaves n_M
dt = differential of temperature t ($^{\circ}$C)
dp = differential of pressure p (mb)
de = differential of partial water vapour pressure e (mb)

Equation (2.47) leads to the following statements:

(1) An error of 1°C in t causes an error of 1.4 ppm in n_M and therefore in distance.
(2) An error of 1 mb in the atmospheric pressure p causes an error of 0.3 ppm in n_M or distance.
(3) An error of 1 mb in the partial water vapour pressure e causes an error 4.6 ppm in n_M or distance.

From these values it becomes obvious that the critical parameter in the case of refractive index of microwaves is the partial water vapour pressure. This is the main reason why microwave measurements are likely to be of lower accuracy than the corresponding measurements using light or "near-infrared". An accuracy better than ±3 ppm in n_M cannot easily be achieved, even if e is measured very precisely at both instrument stations.

Unlike measurements with light wave carriers, microwave EDM requires the partial water vapour pressure e to be measured under all circumstances, if the full precision is required. The measurement of e will be discussed later.

2.46 Coefficient of Refraction

It is known from the theory of trigonometric levelling, that the refractive index of air not only affects the velocity of light but also the geometry of its path. When a wave path passes through regions of differing refractive index n, the wave path will depart slightly from a straight line. The effect will be different for light waves and microwaves because of their different refractive indices.

If R is the mean radius of curvature of the spheroid along a line and r the radius of curvature of the wave path, the coefficient of refraction is defined as:

$$k = \frac{\text{curvature of ray path}}{\text{curvature of spheroid}} = \frac{\frac{1}{r}}{\frac{1}{R}} = \frac{R}{r} \qquad (2.48)$$

The curvature of the wave path itself is defined as

$$\frac{1}{r} = -\sin z \, \frac{1}{n}\left(\frac{dn}{dh}\right) \qquad (2.49)$$

where (dn/dh) is the vertical gradient of the refractive index of air, and z is the angle between the direction of the gradient of the refractive index and the tangent to the wave path. The change of n with height h is caused by the vertical density gradient of air.

The following mean values are generally adopted:

$$\text{Light waves:} \quad k_L = 0.13 \qquad r_L = 8R \qquad (2.49a)$$

$$\text{Micro waves:} \quad k_M = 0.25 \qquad r_M = 4R \qquad (2.49b)$$

These values may vary considerably under differing atmospheric conditions, for example during the night, at sunrise or at sunset. Some examples may illustrate the range of values. Höpcke [10] has reported the following range of refraction coefficients for the layer of air between 40 m and 100 m above ground.

$$k_M = +0.25 \text{ to } +0.50, \qquad k_L = +0.13 \text{ to } +0.30$$

Larger variations were reported for the layer between 2 m and 13 m:

$$k_M = -1.2 \text{ (early morning) to } +3.5 \text{(early evening)}$$

$$k_L = -0.5 \text{ (noon) to } +2.5 \text{(early morning).}$$

Brunner [11] has reported refraction coefficients k_L in the range of -2.3 to +1.5 for light paths 1.5 m over ground on clear days. The coefficients of refraction for rays in 3 m height above ground were found to be between -1.0 and +1.0 on clear days.

The mean values given in equations (2.49a) and (2.49b) should therefore be used with caution. Special attention should be given to assumed coefficients of refraction if they

are not only used for distance reductions but also for the computation of height differences. See section 3.31 for more details.

2.47 Measurement of Atmospheric Parameters

The extent and precision required in measurement of atmospheric parameters depends largely on the EDM instrument type, its internal accuracy, the distance accuracy required and the length to be measured. Temperature measurement for short range instruments with an internal accuracy of ±5 mm requires a simple mercury thermometer for distances of about 1000 metres; an aneroid will suffice for the measurement of pressure. For shorter distances of a few 100 metres length, a good estimate based on experience or daily weather information may be sufficient. An error of 10°C in temperature, for example, would cause an error in a 100 metre distance of only 1 mm, which can be neglected in relation to the instrument's internal accuracy of ±5 mm. Thermometers and barometers used for these purposes would not require precise calibration. However regular comparison of the instruments with calibrated instruments or standards should be made.

Medium and long distance measurements with microwave instruments and long distance measurements with laser instruments require precise determination of the atmospheric temperature, pressure and humidity at least at the terminals of the EDM line. Details of accurate meteorological measurements follow in the next sections. More refined methods of refractive index determination are discussed in sections 2.48 and 3.13.

2.471 Measurement of Atmospheric Pressure

It has been demonstrated in section 2.44 and 2.45 that an error of 1 mb affects distances by only 0.3 ppm. A good quality aneroid with an accuracy better than 1 mb is therefore generally sufficient. It should be checked against a reference mercury barometer before and after field trips. Aneroids may need corrections for temperature, scale errors and zero errors. The National Measurement Laboratory in Sydney tests aneroids (and mercury barometers) for a relatively small fee. The standard test includes the determination of the hysteresis effect and corrections at a number of points over the full range of the instrument. Tests on temperature compensation are done on request [12].

Aneroids should be handled with great care and should always be set up level and in the shade. They should be allowed time to settle before reading.

2.472 Measurement of Atmospheric Temperature

Atmospheric temperature is generally determined, together with humidity, using an aspiration psychrometer. This instrument will be discussed in 2.473 in more depth. The temperature should be measured with an instrument which provides an accuracy of ±0.2°C. Such instruments are:

(1) Mercury-in-glass thermometers
(2) Platinum resistance thermometers
(3) Electronic thermistor thermometers

The advantage of equipment (2) and (3) is that the actual measuring device (probe, sensor) is separated from the display unit, and from the thermal effects of the observer. The probe can be put on a mast, enabling a continuous, electronic recording of data. Temperatures should be measured in the shade, exposed to wind and well above the ground. The distance to any object, including the ground or people, should be more than 1.5 m. At low temperatures, mercury thermometers should be shielded from the heat radiation of the human body by a transparent plastic plate. During distance measurement, temperature readings should be taken at a rate of at least one reading per minute for a minimum period of five minutes, to account for the fluctuations of meteorological parameters. Electronic devices have a much

faster response to temperature changes than mercury thermometers. More observations should therefore be taken to provide a reliable mean value if no automatic recording device is used. Thermometers should be calibrated from time to time, at least for the zero error. Graduation errors need to be checked at least once. The National Measurement Laboratory of CSIRO in Sydney provides a thermometer testing service [12].

2.473 Measurement of Humidity

Two types of procedures and instruments are used to measure atmospheric humidity:

(1) HYGROMETER

The hair hygrometer was originally based on the change in length of human hair as a function of relative humidity. The present day hygrometers may also use other materials for the same purpose. Hair hygrometers provide the relative humidity directly in per cent. The accuracy is about 3% which is not accurate enough for EDM purposes. Hygrometers have a very slow response to humidity changes and thus provide a mean value over a period of time.

(2) ASPIRATION PSYCHROMETER

Designed by R. Assmann, the aspiration psychrometer consists basically of two thermometers, one of which is covered with a cotton wick which must be kept wet with distilled water. The "dry bulb" and "wet bulb" thermometers are enclosed in tubes to protect them from radiation. An air current of 2 to 3 ms^{-1} is used to aspirate the thermometer bulbs. The psychrometer provides readings of the dry bulb and the wet bulb temperature from which the partial water vapour pressure is derived.

Several types of *aspiration psychrometers* are commercially available:

(1) Mercury-inGlass psychrometer

Originally designed by Assmann, these comprise a dry bulb and wet bulb thermometer and a small spring driven fan and are accurate to $0.2^{o}C$.

(2) Electric Psychrometer

These are compact instruments with two built-in mercury-in-glass thermometers, accurate to $0.1^{o}C$, and a battery driven fan. The bulbs are read through a glass window thus providing improved shielding.

(3) Thermistor Psychrometer

The mercury thermometers are replaced by thermistors, which allow temperature readings at a distance from the probes. The fan is again operated electrically. An accuracy of about $0.2^{o}C$ can be achieved.

(4) Platinum Resistance Psychrometer

The thermistors can be replaced by platinum resistance thermometers. The accuracy is about $0.1^{o}C$. This form of psychrometer is not yet commercially available.

In addition to the operating instructions for simple thermometers, given in section 2.472, further care is required in using (mercury) psychrometers. After wetting the wet bulb wick, repeated readings must be taken to confirm that the wet bulb has reached its equilibrium.

An increase in wet bulb temperatures may indicate that the wick has run dry. The wick must be clean and in contact with the thermometer. No water should bridge the gap between wick and shield. The observer should avoid breathing on the air intake, especially at low temperatures, and should stand clear of the instrument. More advice may be found in [13] , page 54. Some of the problems are eliminated, if thermistor and platinum resistance instruments are used.

A psychrometer should be calibrated periodically and needs some maintenance with regard to the polished shields and thermometers and the replacement of the wick. The internal air velocity also must be checked and should be 2 - 3 ms^{-1} to ensure proper functioning. A test service is provided by the National Measurements Laboratory of CSIRO in Sydney [12].

2.474 Computation of the Partial Water Vapour Pressure

The partial water vapour pressure e, which is required for the determination of the refractive index (see section 2.44 and 2.45), can be derived from dry bulb and wet bulb readings of an aspiration psychrometer. The psychrometric equation by A. Sprung is ([17], p.228):

$$e = E'_W - 0.000\,662\ p\ (t - t') \qquad (2.50a)$$

where E'_W = saturation water vapour pressure for temperature t' (wet bulb temperature) in mb over water.
t = dry bulb temperature (^oC)
t' = wet bulb temperature (^oC)
p = atmospheric pressure (mb)
e = partial water vapour pressure (mb)

This formula is accurate to ±1% and valid for $t > 0^oC$ and $t' > 0^oC$. In case of a frozen wet bulb wick, the following equation must be used:

$$e = E'_{ICE} - 0.000\,583\ p\ (t - t') \qquad (2.50b)$$

where E'_{ICE} is the saturation water vapour pressure over ice at the temperature t' (wet bulb temperature) in millibars.

The saturation water vapour pressure over water and over ice can be obtained from tables in Appendix E [14] and [15]. Alternatively the saturation water vapour pressure may be calculated according to the equation by Magnus-Tetens ([17] , p 228)

$$E'_W = 10^{\left(\frac{7.5\ t'}{237.3 + t'} + 0.7858\right)} \qquad (2.51a)$$

$$E'_{ICE} = 10^{\left(\frac{9.5\ t'}{265.5 + t'} + 0.7858\right)} \qquad (2.52a)$$

or its revised form by Murray [22]:

$$E'_W = 6.1078 \exp\left(\frac{17.269\ t'}{237.30 + t'}\right) \qquad (2.51b)$$

$$E'_{ICE} = 6.1078 \exp\left(\frac{21.875\ t'}{265.50 + t'}\right) \qquad (2.52b)$$

where E'_W and E'_{ICE} are the saturation water vapour pressures (in mb) over water and ice, and t' is the wet bulb temperature (^oC). The equations (2.51 and 2.52) are valid for the temperature range -70^oC to $+50^oC$. (2.51) is accurate to 0.1 mb between 0^oC and 40^oC.

Example

$t = 21.3^{\circ}C \qquad t' = 17.9^{\circ}C \qquad p = 1010.6$ mb

$$E'_W = 10^{(\frac{7.5 \times 17.9}{237.3+17.9} + 0.7857)} = 20.50 \text{ mb} \qquad \text{(from equation (2.51))}$$

$$e = 20.50 - 0.000\,662\,(1010.6)(21.3-17.9)$$

$$= 20.50 - 2.28 = 18.22 \text{ mb}$$

Effect of the Precision of t, t' on n_M

If the refractive index n_M of microwaves is computed from a value of the partial water vapour pressure obtained by psychrometer observations of t and t', it can be shown that an error of $0.22^{\circ}C$ in the dry bulb temperature t or an error of $0.14^{\circ}C$ in the wet bulb temperature t' causes an error of 1 ppm in n_M. Psychrometer observations must therefore be carried out with the highest possible care. On long distances, the accuracy of a distance is limited mainly by the accuracy of the psychrometric data.

Partial Water Vapour Pressure from Relative Humidity

The partial water vapour pressure e may also be derived from a known value of the relative humidity h. The latter may be available from hygrometer readings or daily weather information. However since the accuracy of h from these sources is limited, partial water vapour pressures derived from h should only be used in EDM in special cases. Short range microwave EDM may be one such case. The partial water vapour pressure e is computed from

$$e = \frac{E\,h}{100} \qquad (2.53)$$

where e = partial water vapour pressure (mb)
E = saturation water vapour pressure (mb) at temperature t (dry bulb temperature)
h = relative humidity in per cent.

The values for E may be taken from tables ([14], [15]) or computed from equations (2.51) or (2.52). Replace E' by E and t' by t. Tables for E are also given in Appendix E.

2.48 Determination of the Refractive Index

On short distances, p, t and t' are measured at the instrument station only. On longer distances, p, t and t' are measured at both ends of the EDM line. The refractive indices, or the first velocity corrections, are computed separately for both endpoints of a line and the mean refractive index, or the mean first velocity correction, is then used to correct the measured distances. The practical approach to such computations is given in section 3.1 on velocity corrections.
The refractive index evaluated from temperature, pressure and humidity readings, taken at end points only, does not necessarily represent the integral value over the path length. For example it is a common experience to find light wave instruments giving longer distances than microwave instruments during simultaneous measurements. The difference amounts usually to 2-3 ppm.

The precision of the technique of end point measurements can be increased, if the atmosphere can be interpreted by means of a 'model' and if the profile of the line is known. According to Brunner & Fraser [16], the atmosphere is found to be homogeneous between 10.00 and 15.00 hrs on clear days. A model for EDM reduction which describes this situation is given in [16]. It requires additional observations of wind speed and eventually net radiation, heat flux into the ground and evaporation. Earlier approaches to solve the problem are described in [17], pages 236 - 262.

There has been the suggestion to utilize reciprocal zenith distance measurements simultaneously with EDM observations, or alternatively one measured zenith distance together with the given height difference for a more accurate determination of the refractive index. These methods are described in [17], pages 265-268 and in [18], [19].

A further technique is the continuous recording of pressure, temperature and humidity along the wave path. This method of airborne meteorological profiles requires an appropriately equipped plane or helicopter. It is applied, for example, during the distance measurements in the control network which monitors the movements of the San Andreas Fault in Canifornia. Accuracies in scale of ±0.2 ppm have been reported [20].

Another method is the use of microwave refractometers. This was taken up by the designers of the Precision Distance Meter "Mekometer". The Mekometer reduces all measurements automatically for the first velocity correction according to the ambient refractive index. The assumption is made that the refractive index at the instrument is representative of the whole wave path.

Another possibility is to make use of the differing refractive indices of different wave lengths (dispersion). Simultaneous distance measurements, using two or three different carrier waves, allow the determination of the differential refractive index between the different carriers and lead to a greatly reduced dependency on accurate determinations of atmospheric parameters. Accuracies of 0.15 ppm (and better) were obtained using a special instrument incorporating three wavelengths λ_{RED} = 632.8 nm (HeNe-Laser), λ_{BLUE} = 441.6 nm (HeCd-Laser) and $\lambda_{MICROWAVE}$ = 32 mm [21] [85].

3. Corrections to Measured Data

3.1 Velocity Corrections

3.11 First Velocity Correction

The basic formula for the computation of d was introduced in sections 2.11 and 2.211. Equation (2.9) may be written, after substitution of equation (2.4) for c, to describe the distance value d' actually displayed on a distance meter:

$$d' = \frac{c_o}{n_{REF}} \frac{\Delta t'}{2} \tag{3.1}$$

where d' is the distance displayed on the EDM instrument, c_o is the velocity of light in a vacuum, $\Delta t'$ is the measured "flight" time of the signal to the reflector and back and n_{REF} the reference refractive index of the instrument.

The instrument constant n_{REF} is defined by the following equations:

$$n_{REF} = \frac{c_o}{\lambda_{MOD} f_{MOD}} \tag{3.2a}$$

$$= \frac{c_o}{2 U f_{MOD}} \tag{3.2b}$$

where λ_{MOD} is the constant modulation wavelength of the fine measurement for which the instrument is designed, f_{MOD} is the constant modulation frequency of the fine measurement and U is the exact half of λ_{MOD}, called the unit length of the instrument. It may be seen from appendix D (tables 1 and 2) that 10 m is the most common unit length at present.

The reference refractive index n_{REF} of an instrument is fixed by the manufacturer by adopting a suitable unit length and by adjusting the main oscillator to such a modulation frequency f_{MOD} that the then fixed value n_{REF} corresponds more or less to an average refractive index encountered under field conditions.

The length of the wave path d is

$$d = \frac{c_o}{n} \frac{\Delta t'}{2} \tag{3.3}$$

where n is the actual refractive index which ideally is the mean value over the distance.

Subtracting d' (3.1) from d (3.3) leads to the *first velocity correction* K':

$$K' = d - d' = c_o \frac{\Delta t'}{2} \left(\frac{1}{n} - \frac{1}{n_{REF}}\right)$$

$$= c_o \frac{\Delta t'}{2} \left(\frac{n_{REF} - n}{n \times n_{REF}}\right)$$

$$= \frac{c_o \Delta t'}{2 n_{REF}} \left(\frac{n_{REF} - n}{n}\right) \tag{3.4}$$

The denominator in (3.4) may be set equal to one, to sufficient accuracy. After substitution of (3.1), the first velocity correction K' thus may be written with sufficient accuracy as

$$K' = d'(n_{REF} - n) \tag{3.5}$$

and the corrected distance d as

$$d = d' + d' (n_{REF} - n) \tag{3.6}$$

$$= d' + K' \tag{3.7}$$

Formulae for the first velocity correction are derived by the manufacturers for each specific type of EDM instrument. Two examples may illustrate the derivation of such formulae.

3.111 First Velocity Correction for the EDM Instrument Hewlett Packard HP 3800B

For the distance meter HP 3800B the following parameters are given:

$$c_o = 299\ 792\ 500\ ms^{-1}$$

$$f_{MOD} = 14\ 985\ 454\ Hz$$

$$U = 10\ m\ exactly = \frac{\lambda_{MOD}}{2}$$

The modulation frequency f_{MOD} and the unit length U refer to the fine measurement and were laid down by the manufacturer.

The reference refractive index n_{REF} is the only unknown in equation (3.2b) and may be computed as follows:

$$n_{REF} = \frac{c_o}{\lambda_{MOD}\ f_{MOD}} = \frac{299\ 792\ 500\ ms^{-1}}{20 \times 14\ 985\ 454\ ms^{-1}} = 1.000\ 2783 \qquad (3.8)$$

Using equation (3.5) leads to:

$$K' = d'(n_{REF} - n)$$

$$= d'(1.000\ 2783 - n)$$

$$= d'\{\ 1 + (1.000\ 2783 - 1) - (1 + (n-1))\ \}$$

Equation (2.44) in section 2.44 gives the following value for $(n_L - 1)$:

$$(n_L - 1) = (n_g - 1)\ \frac{273.16\ p}{(273.16 + t)1013.25} - \frac{11.20\ e\ 10^{-6}}{(273.16 + t)}$$

Substitution of this equation yields:

$$K' = d'\ \{278.3 \times 10^{-6} - (n_g - 1)\ \frac{273.16\ p}{(273.16 + t)1013.25} + \frac{11.20\ e}{(273.16+t)} \times 10^{-6}\ \}$$

The group refractive index for a carrier wavelength of $\lambda_{CARR} = 910$ nm (as in HP 3800B) is according to the formula of Barrell and Sears [32] and the first example in section 2.43:

$$n_g = 1.000\ 2936$$

Therefore $$(n_g - 1) = 293.6 \times 10^{-6}$$

and $$K' = d' \times 10^{-6}\ \{278.3 - 293.6\ \frac{273.16\ p}{(273.16+t)1013.25} + \frac{11.20\ e}{(273.16+t)}\ \}$$

Finally, for the HP 3800B:

$$K' = d' \times 10^{-6}\ \{278.3 - \frac{79.148\ p}{(273.16+t)} + \frac{11.20\ e}{(273.16+t)}\ \} \qquad (3.9)$$

where K' = first velocity correction
d' = measured distance displayed on EDM instrument
t = dry bulb temperature (^oC)
p = atmospheric pressure (mb)
e = partial water vapour pressure (mb) (computed from dry and wet bulb readings on a psychrometer)

Example:

Measured distance	d'	= 1528.790 m
Temperature	t	= $31.2^{o}C$
Pressure	p	= 1006.85 mb
Partial water vapour pressure	e	= 20.9 mb

$$K' = 1528.790 \times 10^{-6} \{ 278.3 - 261.84 + 0.77 \}$$

$$= + 0.026 \text{ m}$$

$$d = d' + K'$$

$$= 1528.816 \text{ m}$$

Note

The Hewlett-Packard derivation replaces the third term of equation (3.9) by a constant value of +0.4 and obtains

$$K' = \{278.7 - \frac{79.148\ p}{(273.16+t)}\} 10^{-6} \times d' \qquad (3.10)$$

The constant term 0.4 is equivalent to relative humidities of 82% at $10^{o}C$; 44% at $20^{o}C$; and 25% at $30^{o}C$.

3.112 First Velocity Correction for the SIEMENS-ALBIS Microwave Instrument SIAL MD60

The SIAL MD60 is a microwave instrument with a range of up to 150 km. It is a push-button type instrument with digital read out. Its stated accuracy is ±(10 mm + 3 ppm). The following data are given:

$$c_o = 299\ 792\ 500 \text{ ms}^{-1}$$

$$f_{MOD} = 149\ 848\ 300 \text{ Hz}$$

$$\lambda_{MOD} = 2 \text{ m exactly}$$

$$U = 1 \text{ m exactly}$$

The modulation frequency f_{MOD}, the modulation wave length λ_{MOD} and the unit length U refer to the fine measurement of the distance. Using equation (3.2a) the reference refractive index of the SIAL MD60 may be computed as follows:

$$n_{REF} = \frac{c_o}{\lambda_{MOD}\ f_{MOD}} = \frac{299\ 792\ 500 \text{ ms}^{-1}}{2 \times 149\ 848\ 300 \text{ ms}^{-1}} = 1.000\ 3200 \qquad (3.11)$$

Should the refractive index of the ambient atmosphere coincide with n_{REF}, then the displayed readout would be the correct distance.

The first velocity correction K' is obtained according to equation (3.5) as:

$$K' = (n_{REF} - n)d'$$

$$= ((n_{REF} - 1) - (n - 1)\ )\ d'$$

Substituting equation (2.46) (see section 2.45) for (n-1) gives -

$$K' = \{320 \times 10^{-6} - \frac{(77.64)\ 10^{-6}}{(273.16+t)} (p-e) - \frac{(64.68)\ 10^{-6}}{(273.16+t)} (1 + \frac{5748}{(273.16+t)})\ e\}\ d'$$

So that for the SIAL MD60:

$$K' = \{320.0 - \frac{77.64\ (p-e)}{(273.16+t)} - (1 + \frac{5748}{(273.16+t)})\ \frac{64.68\ e}{(273.16+t)}\}\ 10^{-6} \times d' \qquad (3.12)$$

where p = air pressure (mb)
t = temperature (^{o}C)
e = partial water vapour pressure (mb)
d' = measured distance (reading on display of instrument)

3.113 Correction Charts

Most manufacturers provide a correction chart which can be used *either* to set an environmental correction dial so that the first velocity correction is incorporated in the result *or* to determine the first velocity correction to be added manually. Users should always be aware of the assumptions on which such "environmental" correction charts are based.

Appendix A depicts the correction chart of the Hewlett-Packard Distance Meter HP 3800B (and also HP 3805A). It is based on formula (3.10). The scale for elevations is based on a standard atmosphere and can be used if the atmospheric pressure is not measured. The accuracy of such a procedure is limited because deviations of up to 30 mb from the standard pressure may occur from time to time. This is equivalent to scale errors of 10 ppm.

Appendix B shows a correction nomogram of the AGA Geodimeter Model 6A. The nomogram is based on the following formula [5]:

$$K' = d' \times 10^{-6} \{309.2 - 82.102\ \frac{p}{(273.2+t)}\} \qquad (3.13)$$

where p has to be taken in mb and t in ^{o}C. An average correction for humidity of -0.6 (corresponding to the third term in equation (3.9)) is included. Formula (3.11) can be developed in a similar way to that used in sections 3.111 and 3.112, based on f_{MOD} = 29 970 000 Hz, λ_{MOD} = 10 m, U = 5.0 m and n_g = 1.000 304 5 (see section 2.43).

3.12 Second Velocity Correction

As mentioned earlier, pressure and psychrometer observations are taken normally only at instrument and reflector stations or, for microwave instruments, at the master and remote stations. The first velocity corrections are computed for both terminals of a line. The mean of both values is subsequently used to correct the distance. However an error is introduced if the mean first velocity correction of both stations is used without a further small correction, called the second velocity correction.

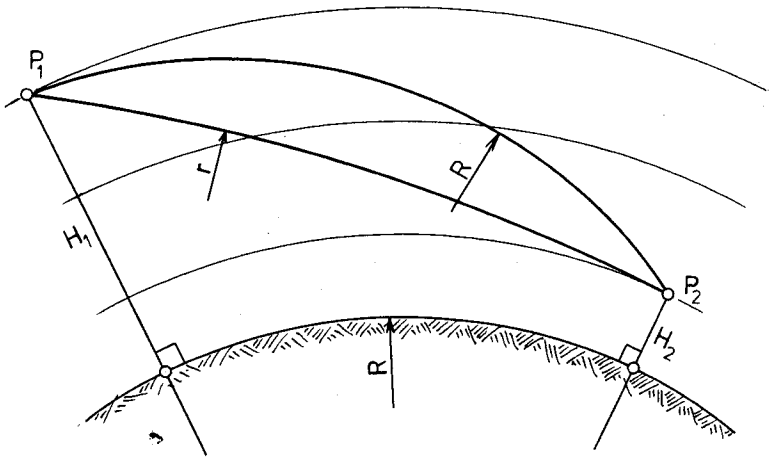

Figure 20.

In figure 20, the mean radius of curvature of the spheroid along the line is denoted by R and the radius of the wave path by r. The mean refractive index $n = \frac{1}{2}(n_1 + n_2)$ would be correct for the upper curve with a radius R but not for the actual wave path below it having radius r, assuming a spherically layered atmosphere on a sphere. For the actual wave path, the correct refractive index would be, assuming linear vertical gradients of temperature and pressure [10], [28]:

$$n = \frac{n_1 + n_2}{2} + \Delta n \qquad (3.14)$$

where $$\Delta n = (k-k^2)\frac{d'^2}{12R^2}$$

The second velocity correction may be written as

$$K'' = - d' \Delta n$$

or

$$K'' = - (k-k^2)\frac{d'^3}{12R^2} \qquad (3.15)$$

where K'' = second velocity correction
k = coefficient of refraction (see section 2.46)
d' = measured distance, displayed on instrument
R = mean radius of curvature of the spheroid along the line

The second velocity correction K'' is more important for microwaves than for light waves and more important on long distances than on short distances. For example, K'' would become -50 mm for a distance d' of 50 km, measured by a microwave instrument ($k_M = 0.25$).

The wave path length d_1 is obtained as

$$d_1 = d' + K' + K''$$

where d' = measured distance, displayed on instrument
K' = first velocity correction according to section 3.11
K'' = second velocity correction

3.13 Refined Methods

Using basic theorems of geometrical optics a formula can be developed which gives the direct relation between the measured optical path and the straight line between two stations. This formula replaces not only the first and second velocity correction, but also the first arc-to-chord correction, which is discussed in section 3.2. A few basic theorems are listed here. A comprehensive treatise of the principles of optics and electromagnetic waves is given in [23]. The development of appropriate EDM reduction formulae has been demonstrated in [16] and [24].

The refractive index n, defined in section 2.11, is the *absolute* refractive index (the index of refraction from a vacuum to a medium). A first definition of n was given by equation (2.4) in section 2.11. Another relationship between the velocity of electromagnetic waves in a vacuum and in a medium may be derived from Maxwell's equations:

$$c = \frac{c_o}{\sqrt{\varepsilon_r \mu_r}} = \frac{1}{\sqrt{\varepsilon \mu}} \qquad (3.17)$$

where ε is the *dielectric constant* (or permittivity) and μ is known as the *magnetic permeability*. The values of ε_r and μ_r are close to unity and are termed the relative dielectric constant and the relative magnetic permeability. They are defined as:

$$\mu = \mu_o \, \mu_r \tag{3.17a}$$

$$\varepsilon = \varepsilon_o \, \varepsilon_r \tag{3.17b}$$

where μ_o = magnetic permeability in a vacuum
= 1.256×10^{-6} $VsA^{-1}m^{-1}$
and ε_o = dielectric constant in a vacuum
= 0.08859×10^{-10} $AsV^{-1}m^{-1}$

μ is generally constant for all non-magnetic mediums. ε is dependent on the medium and the frequency of the radiation (Effect of *Dispersion*). Equations (2.4) and (3.17) lead to a second definition of the refractive index:

$$n = c_o \sqrt{\varepsilon \, \mu} = \sqrt{\mu_r \, \varepsilon_r} \tag{3.18}$$

The principle of FERMAT (Principle of shortest optical path or principle of least time) states that the optical length σ of an actual ray between any two points P_1 and P_2 is shorter than the optical length of any other curve through the same two points. In mathematical form:

$$\sigma = \int_{P_1}^{P_2} d\sigma = \int_{P_1}^{P_2} n \, ds = c \int_{P_1}^{P_2} dt \tag{3.19}$$

ds is an incremental chord element: $ds^2 = dx^2 + dy^2 + dz^2$. Since EDM is based on the measurement of time, the optical length σ can be considered as the direct readout distance d'.

The basic equation of geometrical optics can be derived from Maxwell's equations assuming very small wavelengths ($\lambda \to 0$).

$$(\text{grad } \sigma)^2 = \left(\frac{\partial \sigma}{\partial x}\right)^2 + \left(\frac{\partial \sigma}{\partial y}\right)^2 + \left(\frac{\partial \sigma}{\partial z}\right)^2 = n^2 \, (x, y, z) \tag{3.20}$$

The first order partial differential equation of the optical length σ is also known as the *eikonal equation* and describes the effect of vertical and horizontal refraction for EDM. The solution of the eikonal equation corresponds to the conformal projection of the geodesic and was developed by Moritz [25]. In the form of Brunner and Angus-Leppan [24], the solution for EDM reduction reads:

$$\Delta s = \sigma - s = 10^{-6} \int_o^s N dx - \tfrac{1}{2} 10^{-12} \int_o^s \left[\left(\int_o^x \frac{dN}{dy} \xi \, d\xi \right)^2 + \left(\int_o^x \frac{dN}{dz} \xi \, d\xi \right)^2 \right] \frac{dx}{x^2} \tag{3.21}$$

where σ is the optical length, s is the wave path chord, N is the *refractivity* ($N = (n-1) \times 10^6$) and ξ is an integration variable along x.

The origin of the cartesian coordinate system x, y, z is defined at one endpoint of the line. The x-axis is colinear with the chord. The z-axis is perpendicular to the x-axis and on a vertical plane through the origin. The y-axis is in a horizontal plane through the origin. All integrations are carried out along the x axis. Equation (3.21) is mathematically accurate to 2×10^{-11} s assuming that the laws of geometrical optics are valid for describing the wave propagation. However, the practical accuracy of Δs will largely depend on the accuracy of the refractivity N and its gradients. The gradients can be derived from a combination of measurements of atmospheric parameters (see 2.47) and atmospheric models. Atmospheric models are usually only valid for certain specific conditions of the atmosphere. Such a model has been presented in [16].

Refined methods of reducing an optical length (or measured distance) σ to its chord length s will not be considered further in this text, because their application requires both field observations of additional atmospheric parameters and extensive computations. However, for high precision and long range EDM the application of such refined methods should be considered. [24] [75] [76] [77] [80] [81] [82] [83] [86] [87]

With respect to the following, the correction $\Delta s = \sigma - s$ shall be approximated in the traditional way by the sum of the first and the second velocity correction and the first arc-to-chord correction.

3.2 Geometrical Corrections

After applying the two velocity corrections to the actual observation the length of the wave path d_1 is obtained. This length then has to be reduced to the equivalent spheroidal distance on a geodetic reference surface, for example the Australian Geodetic Datum. Selected methods of reduction to the spheroid will now be reviewed, prior to a discussion of additional corrections and computations.

There are basically two different methods of reduction. The first method uses known or measured heights, the second measured zenith distances. The first method is employed in conjunction with medium to long range distance measurements. The second method is used for short ranges where the heights of target stations are usually not available.

3.21 Reduction to the Spheroid, using Station Heights

The reduction problem is illustrated in figure 21; d_1 stands for the wave path length, d_2 for the wave path chord, d_3 for the spheroidal chord and d_4 for the spheroidal distance. The spheroidal distance corresponds to the length of a normal section and differs only slightly from the length of the geodesic. The difference is less than 20 mm for a distance of 3000 km and may therefore be ignored [13]. The radius of curvature of the wave path is denoted by r and the mean radius of curvature of the spheroid along the line by R. H_1 and H_2 are the spheroidal heights of stations P_1 and P_2, measured along the normal to the spheroid. The spheroidal height is the sum of the orthometric (geoidal) height and the corresponding height of the geoid above the spheroid (geoid-spheroid separation). γ is the angle between the normals to a sphere of radius R through P_1 and P_2, and β is the angle between the tangents to the wave path through P_1 and P_2 and also the angle between the wave path normals through P_1 and P_2.

The value R is computed from

$$R = \frac{\nu\rho}{\nu \cos^2 \alpha + \rho \sin^2 \alpha} \qquad (3.22)$$

where ν = radius of curvature of the spheroid in the prime vertical
ρ = radius of curvature of the spheroid in the meridian
α = azimuth of the measured line, clockwise through 360^o from the north.

The spheroid between the terminals of a line is always replaced by a sphere of radius R for the reduction of distances. This leads to an intersection of the spheroidal normals which were originally skew. Sometimes, a mean radius R_M is adopted for a certain area to avoid repeated computations of R. The New South Wales Integrated Survey Grid refers for example to a mean radius of R_M = 6 370 100 m ([29] , p.18) causing errors of less than 1 ppm in reduced distances for N.S.W. latitudes.

Spheroidal heights are often replaced by orthometric (geoidal) heights because the former are usually not readily available. Orthometric heights, for example heights based on the Australian Height Datum (A.H.D.), may be obtained from spirit and trigonometric levelling. The use of orthometric instead of spheroidal heights for the reduction of distances may lead to small errors in the spheroidal distance depending on the height of the geoid above the spheroid at the two terminals of a line [26]. Two cases may be distinguished:

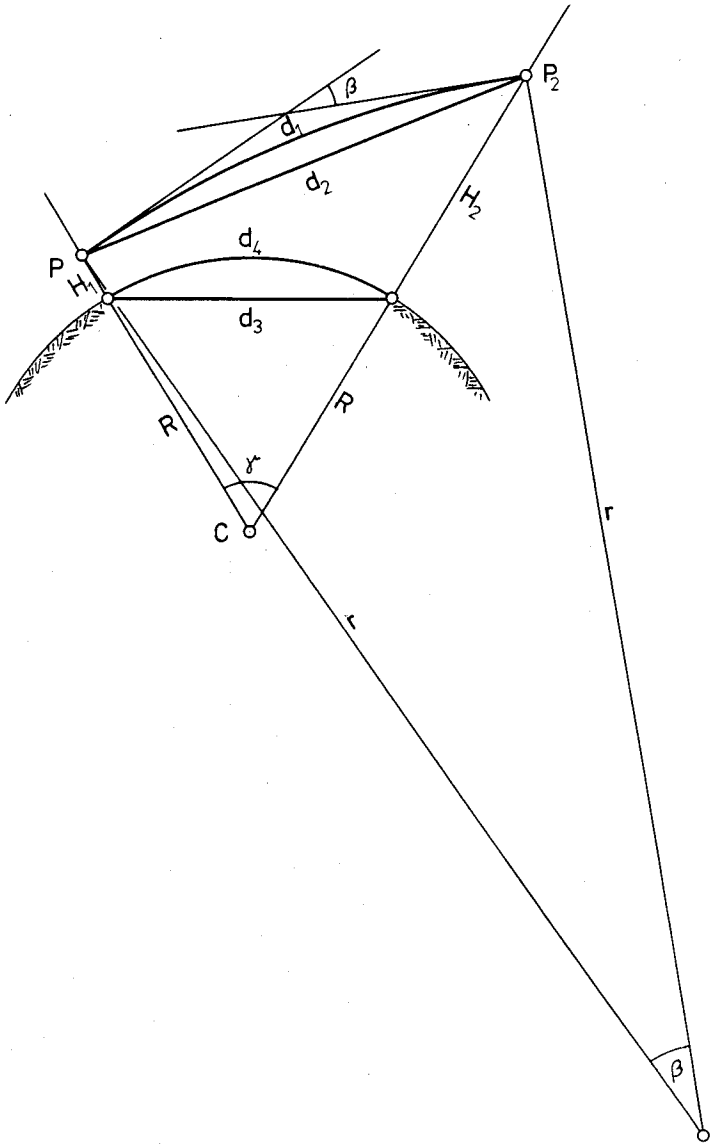

Figure 21

(1) Equal heights of geoid above spheroid at the terminals of a line introduce errors of 1 ppm per 6 m geoid-spheroid separation.

(2) Unequal heights of geoid above spheroid at the terminals produces an additional error which may be estimated using the first term of equation (3.41) in section 3.213. For extreme cases in alpine areas, errors of up to 0.15 m for 2.5 km lines have been reported. [34]

Spheroidal heights should be used in high order geodetic surveys. However, the difference between spheroidal and orthometric heights is usually ignored in low order and short range surveys, because the effect on EDM reduction becomes negligible.

Two calculation methods are now presented. The first executes the reduction in several steps. The second gives a closed solution.

3.211 First Method (In Steps)

3.2111 First Arc-to-Chord Correction K_1 (d_1 to d_2)

d_1 stands for the measured distance along a wave path with radius of curvature r and already includes the first and second velocity correction explained in section 3.1.

Thus:

$$d_2 = 2r \sin \frac{\beta}{2} = 2r \sin \frac{d_1}{2r} \tag{3.23}$$

Developing $\sin \frac{d_1}{2r}$ by its series expansion:

$$d_2 = d_1 - \frac{d_1^3}{24r^2} + \frac{d_1^5}{1920r^4} - \ldots$$

The third term amounts to 1 mm for d = 1000 km and r = 4R, and hence may be safely neglected.

Therefore

$$d_2 = d_1 - \frac{d_1^3}{24r^2} \tag{3.24}$$

Substituting equation (2.48)

$$r = \frac{R}{k}$$

in equation (3.24) leads to

$$d_2 = d_1 + K_1 \tag{3.25a}$$

and

$$K_1 = - \frac{d_1^3}{24r^2} = -k^2 \frac{d_1^3}{24R^2} \tag{3.25b}$$

3.2112 Chord-to-Chord Correction K_{23} (d_2 to d_3)

Applying the cosine rule to the triangle P_1P_2C (figure 21) yields:

$$d_2^2 = (R + H_1)^2 + (R + H_2)^2 - 2(R + H_1)(R + H_2) \cos \gamma \tag{3.26}$$

Cos γ can now be expressed by known values. The basic relationship

$$\cos \gamma = 1 - 2 \sin^2 \frac{\gamma}{2}$$

may be used, and by substituting $\sin \frac{\gamma}{2} = \frac{d_3}{2R}$ (see figure 21), the following equation is obtained:

$$\cos \gamma = 1 - \frac{d_3^2}{2R^2} \tag{3.27}$$

Also, substituting (3.27) in (3.26) leads to:

$$d_2^2 = R^2 + 2RH_1 + H_1^2 + R^2 + 2RH_2 + H_2^2 - 2R^2 - 2RH_1 - 2RH_2 - 2H_2H_1 + \frac{d_3^2}{R^2}(R+H_1)(R+H_2)$$

$$= (H_2 - H_1)^2 + d_3^2 \, (R+H_1)(R+H_2) \frac{1}{R^2}$$

Solving for d_3 yields:

$$d_3 = + \sqrt{\frac{d_2^2 - (H_2 - H_1)^2}{(1+\frac{H_1}{R})(1+\frac{H_2}{R})}} \tag{3.28}$$

where d_2 = wave path chord
d_3 = spheroidal chord
H_1, H_2 = spheroidal heights

Equation (3.28) is a rigorous formula for a spherical reference surface of radius R.

The chord-to-chord correction is sometimes split into two separate corrections, namely

(1) the *slope correction* K_2 (d_2 to d_6) and
(2) the *sea level correction* K_3 (d_6 to d_3) leading to:

$$d_6 = d_2 + K_2 \tag{3.29a}$$

$$d_3 = d_2 + K_2 + K_3 \tag{3.29b}$$

Both corrections may be derived from the rigorous equation (3.28), which may be written as follows:

$$d_3 = d_2 \left[1 - \left(\frac{H_2 - H_1}{d_2}\right)^2\right]^{\frac{1}{2}} \left[1 + \left(\frac{H_1 + H_2}{R} + \frac{H_1 H_2}{R^2}\right)\right]^{-\frac{1}{2}} \tag{3.30a}$$

Substituting $\Delta H = H_2 - H_1$ and $H_M = 1/2(H_1 + H_2)$ and expanding the terms in the second brackets leads to:

$$d_3 = d_2 \left[1 - \left(\frac{\Delta H}{d_2}\right)^2\right]^{\frac{1}{2}} \left[1 - \frac{H_M}{R} - \frac{H_1 H_2}{2R^2} + \frac{3}{2}\frac{(H_M)^2}{R^2} + \frac{3}{2}\frac{H_M H_1 H_2}{R^3} + \frac{3}{8}\frac{(H_1 H_2)^2}{4R^4} - \ldots\right] \tag{3.31a}$$

The magnitude of the terms in the second bracket may be estimated by substituting maximum values (applicable in Australia) for $H_1 = H_2 = H_M = 2.5$ km and assuming $R = 6370.1$ km:

$$\frac{H_M}{R} = 4 \cdot 10^{-4}, \quad \frac{H_1 H_2}{2R^2} = 8 \cdot 10^{-8}, \quad \frac{3H_M^2}{2R^2} = 2.4 \cdot 10^{-7}, \quad \ldots$$

Also, all terms with R^2, R^3 etc. in the denominator may be safely disregarded. The maximum error resulting from this omission of terms will not exceed 0.2 ppm for heights below 2500 m.

Equation (3.31a) may therefore be written in a reduced form

$$d_3 = d_2 \left[1 - \left(\frac{\Delta H}{d_2}\right)^2\right]^{\frac{1}{2}} \left(1 - \frac{H_M}{R}\right) \tag{3.31b}$$

Multiplication of the first two factors in equation (3.31b) leads to a "horizontal" distance d_6 computed in a right angled triangle. The correction which has to be applied to the "slope" distance to get the "horizontal" distance d_6 is traditionally called the slope correction. Considering the first two factors of equation (3.31) and equation (3.29b) the *slope correction* K_2 (d_2 to d_6) may now be defined as

$$K_2 = d_2 \left(1 - \left(\frac{\Delta H}{d_2}\right)^2\right)^{\frac{1}{2}} - d_2 \tag{3.32a}$$

$$= (d_2^2 - \Delta H^2)^{\frac{1}{2}} - d_2 \tag{3.32b}$$

or, using a series expansion of the square root term in equation (3.32a), as

$$K_2 = -\frac{\Delta H^2}{2d_2} - \frac{\Delta H^4}{8d_2^3} - \frac{\Delta H^6}{16d_2^5} - \ldots \tag{3.32c}$$

Considering equations (3.29b), (3.31b) and (3.32a), the so-called *sea level correction* K_3 (d_6 to d_3) yields:

$$K_3 = -\frac{H_M}{R}(d_2^2 - \Delta H^2)^{\frac{1}{2}} \tag{3.33a}$$

or with regard to equation (3.32b):

$$K_3 = -\frac{H_M}{R}(d_2 + K_2) \qquad (3.33b)$$
$$= -\frac{H_M}{R} d_6$$

Substitution of K_2 in equation (3.33b) by equation (3.32c) leads to a third equation for K_3:

$$K_3 = -\frac{H_M}{R} d_2 + \frac{H_M \Delta H^2}{2 d_2 R} + \frac{H_M \Delta H^4}{8 d_2^3 R} + \frac{H_M \Delta H^6}{16 d_2^5 R} + \ldots \qquad (3.33c)$$

The first term is the conventional value for the sea level correction which is not only used in EDM but also in reductions of horizontal distances to sea level and vice-versa. The first term of equation (3.33c) is not always sufficient for reducing EDM slope distances accurately to the spheroid because the slope correction K_2 does not lead to the chord at mean height H_M, which would be the true horizontal distance. The terms of higher order in equation (3.33c) may be estimated by inserting extreme values of ΔH = 1 km, d_2=1.5 km and H_M = 1.5 km. The second term then becomes 78 mm, the third 9 mm and the fourth 2 mm. The use of the first term of (3.33c) alone is therefore insufficient. It is advisable to use the rigorous formulae (3.33a) or (3.33b) for the sea level correction, in conjunction with slope corrections according to equations (3.32a) and (3.32b).

3.2113 Second Chord-to-Arc Correction K_4 (d_3 to d_4)

From figure 21 follows:

$$d_4 = R\gamma = 2R\left(\frac{\gamma}{2}\right) = 2R \arcsin\left(\frac{d_3}{2R}\right) \qquad (3.34)$$

Replacing arc sin by its series

$$d_4 = d_3 + \frac{d_3^3}{24R^2} + \frac{3 d_3^5}{640 R^4} + \ldots \qquad (3.35)$$

The third term in (3.35) amounts to only 1 mm for a distance d_3 of 200 km. It may be safely neglected.

$$d_4 = d_3 + K_4 \qquad (3.36a)$$

where $$K_4 = +\frac{d_3^3}{24R^2}$$

3.2114 Combined Correction for K'', K_1, K_4

A combined correction for the second velocity correction K'', for the first arc-to-chord correction K_1 and the second chord-to-arc correction K_4 was derived by Saastamoinen [28]:

$$K'' + K_1 + K_4 = -(k-k^2)\frac{d'^3}{12R^2} - k^2\frac{d_1^3}{24R^2} + \frac{d_3^3}{24R^2} \qquad (3.37)$$

Assuming $d' = d_1$ and $d_3 = d_1$:

$$K'' + K_1 + K_4 = \frac{d_1^3}{24R^2}(-2k + 2k^2 - k^2 + 1)$$
$$= \frac{d_1^3}{24R^2}(k^2 - 2k + 1)$$
$$= (1-k)^2\frac{d_1^3}{24R^2} \qquad (3.38)$$

3.212 Second (one step) Method

The reduction of the wave path length d_1 to the spheroidal distance d_4 can be done in one step, if several formulae of the last section (3.211) are combined. Considering the equation

$$d_4 = 2R \arcsin \left(\frac{d_3}{2R}\right) \tag{3.34}$$

and substituting equation (3.28) for d_3 leads to:

$$d_4 = 2R \arcsin \sqrt{\frac{d_2^2 - (H_2 - H_1)^2}{4(R+H_1)(R+H_2)}} \tag{3.39}$$

Substituting d_2 from equation (3.23) and considering equation (2.48) yields after some simple computations,

$$d_4 = 2R \arcsin \sqrt{\frac{R^2 \sin^2\left(\frac{d_1 k}{2R}\right) - \frac{k^2}{4}(H_2 - H_1)^2}{k^2(R+H_1)(R+H_2)}} \tag{3.40}$$

The The above formula is rigorous and reduces d_1 to d_4 without any approximations.

R = mean radius of curvature of the spheroid (along the line)
d_1 = wave path length
d_4 = spheroidal distance
H_1, H_2 = spheroidal heights of stations P_1, P_2
k = coefficient of refraction, defined by equation (2.48).

Note on the Use of Pocket Calculators

Before equation (3.40) is used in conjunction with pocket calculators the accuracy of the pocket calculator's trigonometric functions for small angles must be known. If the number of accurate significant digits is smaller than the number required, both trigonometric functions in equation (3.40) should be replaced by series expansions.

3.213 Analysis of Errors

To test the effect of errors of parameters in equation (3.40) on the spheroidal distance d_4, the total differential of equation (3.40) is taken ([17] p. 587):

$$\delta(d_4) = -\frac{\Delta H}{d_1}\,\delta(\Delta H) - \frac{d_1}{R}\,\delta(H_M) + \frac{d_1 H_M}{R^2}\,\delta(R) \tag{3.41}$$

where $\Delta H = H_2 - H_1$
$H_M = \frac{1}{2}(H_1 + H_2)$

and where $\delta(d_4)$, $\delta(\Delta H)$, $\delta(H_M)$ and $\delta(R)$ are the partial differentials of the variables d_4, ΔH, H_M and R respectively.

If an error δd_4 in d_4 should not exceed a certain limit, the maximum allowable errors in each of ΔH, H_M and R can be calculated from the total differential (3.41).

Example

Given: $d_1 = 1000$ m and $\Delta H = 400$ m

How accurately must ΔH be known, to cause errors smaller than 1 mm in the spheroidal distance d_4 ?

With $\delta(d_4) = 1$ mm:

$$\delta(\Delta H) = -\frac{d}{\Delta H}\,\delta(d_4) = \frac{1000\ m}{400\ m} \cdot 1\ mm$$

$$\delta(\Delta H) = -2.5\ mm$$

It follows that the use of given height differences for the reduction of relatively short distances may cause considerable errors in the reduced distances, if the height differences are not known with the necessary precision. Short distances are therefore usually reduced with the aid of measured zenith distances.

3.22 Reduction to the Spheroid, using Measured Zenith Distances

3.221 Introduction

The problem is depicted in figure 22, where

z_1, z_2 = measured zenith distances at stations P_1 and P_2 respectively

δ = refraction angle, assumed equal at P_1 and P_2

ε_1, ε_2 = deviation of vertical at points P_1 and P_2 in azimuth α_{12} of the line

ζ_1, ζ_2 = spheroidal zenith distance at P_1, P_2 respectively

r = radius of curvature of wave path

β = angle between wave path normal through P_1 and P_2

R = radius of curvature of the spheroid along the line

H_1, H_2 = spheroidal heights

d_1 = wave path length

d_2 = wave path chord

d_4 = spheroidal distance

ΔH = spheroidal height difference = $H_2 - H_1$

γ = angle between the spheroid normals through P_1 and P_2.

A rigorous reduction of the wave path length d_1 to the spheroidal distance d_4 is only possible if the spheroidal heights and the deviations of the vertical ξ are available. For practical purposes, the spheroidal zenith distances ζ usually are replaced by the measured zenith distances z, the spheroidal heights by the orthometric (geoidal) heights and R by the mean radius of spheroid for a specific area R_M. For example R is replaced by $R_M = 6\,370\,100$ m in the N.S.W. I.S.G. (see reference [29], p. 18). The impact of such approximations is described in section 3.21 and in reference [26]. The height difference ΔH may be computed from either spheroidal ζ or measured zenith distances z. In the former case, *spheroidal height differences* are obtained, in the latter case, *orthometric height differences*.

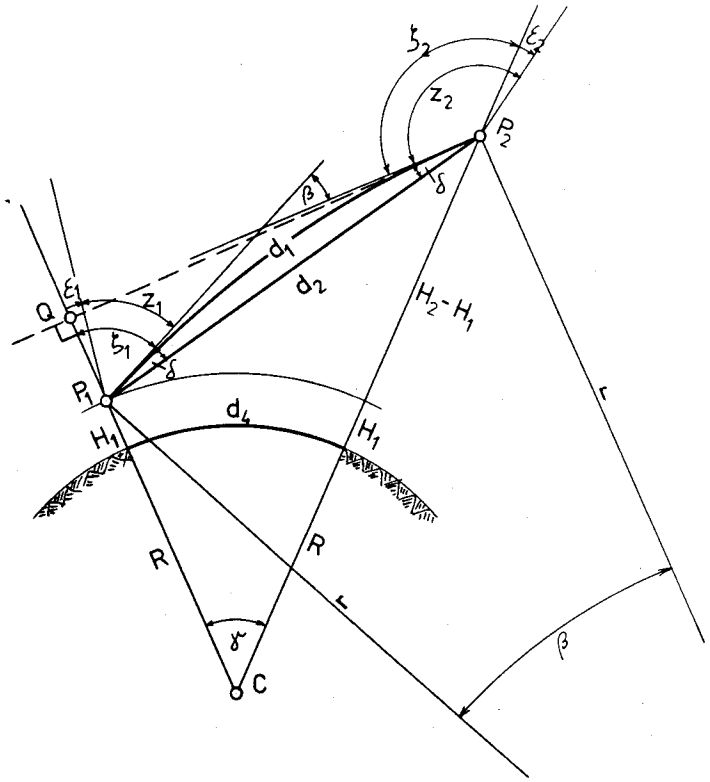

Figure 22

The relationship between the spheroidal zenith distance ζ and the measured zenith distance z is given by

$$\zeta = z + \varepsilon \tag{3.42}$$

Again, two different calculation methods are presented.

3.222 Reduction to the Spheroid in one Step

Following a solution given by Dabrowski & Maier [42] and referring to figure 22, the distance QP_2 may be computed in the right angled triangle P_1P_2Q as

$$QP_2 = d_2 \sin(z_1 + \varepsilon_1 + \delta) \tag{3.43}$$

Considering the right angled triangle QCP_2 the angle γ may be derived as follows

$$\gamma = \arctan\left[\frac{d_2 \sin(z_1 + \varepsilon_1 + \delta)}{R + H_1 + d_2 \cos(z_1 + \varepsilon_1 + \delta)}\right] \tag{3.44}$$

The spheroidal distance d_4 may now easily be computed as

$$d_4 = R \arctan\left[\frac{d_2 \sin(z_1 + \varepsilon_1 + \delta)}{R + H_1 + d_2 \cos(z_1 + \varepsilon_1 + \delta)}\right] \tag{3.45a}$$

The computation of the refraction angle δ follows from figure 22

$$\delta = \frac{\beta}{2} = \frac{d_1}{2r} = \frac{d_1 k}{2R} \qquad (3.46)$$

The wave path chord d_2 is computed from equation (3.23) of section 3.2111 and equation (2.48) of 2.48

$$d_2 = \frac{2R}{k} \sin\left(\frac{d_1 k}{2R}\right) \approx d_1 \qquad (3.47)$$

Equations (3.45a), (3.46) and (3.47) permit a rigorous computation of the spheroidal distance d_4. For $k = 0.13$ and $R = 6370$ km, the difference between d_2 and d_1 (the first arc-to-chord correction according to section 3.2111) amounts to only 0.02 mm for $d = 10$ km, and 0.4 mm for $d = 30$ km. The wave path chord d_2 may therefore be safely replaced by the wave path length d_1 in all practical cases. Equation (3.45a) may subsequently be written as

$$d_4 \approx R \arctan \left[\frac{d_1 \sin\left(z_1 + \varepsilon_1 + \frac{d_1 k}{2R}\right)}{R + H_1 + d_1 \cos\left(z_1 + \varepsilon_1 + \frac{d_1 k}{2R}\right)} \right] \qquad (3.45b)$$

where d_4 = spheroidal distance
d_1 = wave path length
H_1 = spheroidal height of station P_1
z_1 = measured zenith distance at P_1 (in radian)
k = coefficient of refraction of light (= 0.13)
R = radius of curvature of the spheroid along the line P_1P_2
ε_1 = deviation of vertical at P_1 in azimuth of P_1P_2, derived from additional observations (e.g. astronomical observations) (in radians)

The deviation of the vertical is usually unknown which means that ε is very often ignored in computing the spheroidal distance d_4. The effect of ε on d_4 can be derived by taking the total differential of equation (3.45b) (See section 3.224). Replacing spheroidal heights by orthometric heights (geoidal heights) leads to additional errors which have already been discussed in section 3.21.

Note on the use of Pocket Calculators
The use of arc tan in equations (3.45a) and (3.45b) may be critical because the term in brackets is always very small. The accuracy limitations of a particular calculator should be checked for small arguments of this trigonometric function. If necessary, arc tan may be replaced by its series expansion.

3.223 Reduction to the Spheroid in Several Steps, using Measured Zenith Distances

Apart from the one step solution of the problem, given in section 3.222, the reduction of distances can also be evaluated by a similar method as shown previously in section 3.211.

3.2231 First Arc-to-Chord Correction K_1(d_1 to d_2)

This correction has already been discussed in section 3.211. The wave path chord d has been obtained as follows

$$d_2 = d_1 + K_1 \quad \text{where} \quad K_1 = -k^2 \frac{d_1^3}{24R^2} \qquad (3.25)$$

The size of K_1 may be evaluated for $R = 6370$ km and a coefficient of refraction $k_L = 0.13$ (light waves). K_1 then amounts to -0.02mm for $d = 10\,000$ m and to -0.47 mm for $d = 30\,000$ m.

The first arc-to-chord correction may therefore be ignored in almost all cases.

3.2232 Slope Correction $K_5(d_2$ to $d_5)$

The slope correction reduces the wave path chord d_2 to the horizontal distance d_5 at the height H_1. All necessary parameters are depicted in figure 23 and have already been explained in section 3.311. Applying the sine rule to triangle $P_1P_2P_2'$ yields

$$d_5 = d_2 \frac{\sin(z_1 - \frac{\gamma}{2}(2-k))}{\sin(\frac{\pi}{2} + \frac{\gamma}{2})} = d_2 \frac{\sin(z_1 - \frac{\gamma}{2}(2-k))}{\cos\frac{\gamma}{2}} \qquad (3.50)$$

Equation (3.50) is rigorous as long as $\frac{\gamma}{2}$ is correct; it is however usually approximated by

$$\frac{\gamma}{2} \approx \frac{d_2 \sin z}{2(R+H_1)} \qquad (3.51)$$

Using the series expansion of cosine and equation (3.51), it can be shown that the denominator in equation (3.50) may be safely taken as unity for all practical cases. The approximation causes an error of 1 part in 10^8 over 2 km of horizontal distance or 3 parts in 10^7 over 10 km.

Rearrangement of the numerator in equation (3.50) leads to

$$d_5 = d_2 \sin_1 z \cos(\frac{\gamma}{2}(2-k)) - d_2 \cos z_1 \sin(\frac{\gamma}{2}(2-k)) \qquad (3.52)$$

Because $\frac{\gamma}{2}$ is small, the term $(\frac{\gamma}{2}(2-k))$ will also be small.

Substituting

$\cos(\frac{\gamma}{2}(2-k))$ by unity and $\sin(\frac{\gamma}{2}(2-k))$ by $\frac{\gamma}{2}(2-k)$

and considering equation (3.51) yields

$$d_5 = d_2(\sin z_1 - \frac{d_2(2-k)}{2(R+H_1)} \sin z_1 \cos z_1) \qquad (3.53a)$$

Finally, using a theorem of trigonometric functions and neglecting H_1 leads to

$$d_5 = d_2 \sin z_1 - \frac{d_2^2(2-k)}{4R} \sin 2z_1 \qquad (3.53b)$$

where d_5 = horizontal distance at height H_1

d_2 = wave path chord

z_1 = zenith distance in P_1

R = mean radius of curvature of spheroid along the line (R_M = 6370 100 m for NSW I.S.G.)

H_1 = orthometric height of station P_1

The effect on d_5 of neglecting H_1 can be evaluated by multiplying the figures in the table below by the factor H_1/R. The maximum error owing to the disregarding of H_1 in d_5 is smaller than 0.4 mm, if the slope distances d_2 are smaller than 5000 m and the zenith distances between 70^0 and 110^0.

Note: To reduce distances correctly to the spheroid, one would have to use spheroidal zenith distances and spheroidal heights. See section 3.22.

The magnitude of the second term in equation (3.53b) is demonstrated with the aid of a table. It is seen that the term should usually be taken into account.

Table of the value of 2nd term in equation (3.53b)

Slope distance d_2	$z_1 = 80°$	$z_1 = 70°$
100 m	-0.3 mm	-0.5 mm
300 m	-2.3 mm	-4.2 mm
500 m	-6.3 mm	-11.8 mm
1000 m	-25.2 mm	-47.2 mm
2000 m	-100.8 mm	-188.8 mm

For zenith distances of 90°, the second term is zero. The above table assumes $H_1 = 0$ and $k = 0.13$ (light waves).

3.2233 Sea Level Correction $K_6(d_5$ to $d_3)$

The sea level correction K_6 will be slightly different from the solution in section 3.2112 because d_5 is defined at the station height H_1 of P_1 and not at the mean height H_m as before.

$$K_6 = -\frac{H_1}{R} d_5 \qquad (3.54a)$$

$$d_3 = d_5 + K_6 \qquad (3.54b)$$

Equations (3.54a) and (3.54b) are rigorous and can be easily proved in the triangle $P_1P_2'C$ of figure 23

$$d_3 = \frac{d_5 R}{R+H_1}$$

$$= \frac{d_5}{(1+\frac{H_1}{R})}$$

$$\approx d_5(1 - \frac{H_1}{R}) \qquad (3.54c)$$

3.2234 Second Chord-to-Arc Correction $K_4(d_3$ to $d_4)$

This correction has already been discussed in section 3.2113. It can be shown, by using the equation (3.36b) and assuming $R = 6370.1$ km and $k = 0.13$, that the disregarding of this correction causes errors of only 0.1 mm and 1.0 mm on lines of 5 km and 10 km length. K_4 may therefore be ignored in almost all cases.

3.224 Analysis of Errors

The effects of errors in the parameters of equations (3.45a) may be analyzed by the total differential of equations (3.45a, b). After some substitutions and with a radius R = 6 370 000 m the total differential of equation (3.45a) yields, according to [42]:

$$\delta(d_4) = \sin z\, \delta(d_1) - 1.6\times10^{-7} d_4\, \delta(H_1) + \Delta H\, \delta(z) + 7.8\times10^{-8} d_1 \Delta H\, \delta(k) \qquad (3.48)$$

where ΔH is defined by $(H_2 - H_1)$ and all length parameters are taken in metres.

The first two terms will not be discussed further. The third term evaluates the effect of errors in the measured zenith distance or in the omission of the deviation of the vertical. An error of 2 seconds of arc leads to the following errors $\delta(d_4)$:

for ΔH =	50 m	100 m	200 m	1000 m
$\delta(d_4)$ =	0.5 mm	1.0 mm	1.9 mm	9.7 mm

These effects are critical for precise distance meters such as, for example, the Mekometer which has an internal accuracy of 0.2 mm. This may require precise levelling for the determination of the height differences. The knowledge of the deviations of the vertical is essential in this case if the accuracy in measurement is not to be spoiled by inaccurate reduction due to errors in, or ommission of, the deviations of the vertical.

The fourth term in equation (3.48) demonstrates the effect of the difference between the actual coefficient of refraction and the assumed value of $k = 0.13$, which is typically used for EDM reduction. It has been reported in [11] that the coefficient of refraction of "grazing" rays may vary between 2.0 and -1.5 during the day. Assuming an error on the assumed k of $\delta(k)$ equal to 1.0 the following errors $\delta(d_4)$ result in the spheroidal distance:

d_1 =	100 m	300 m	600 m	1000 m	2000 m	3000 m
ΔH =						
100 m	0.8 mm	2.3 mm	4.7 mm	7.8 mm	15.6 mm	23.4 mm
300 m		7.0 mm	14.0 mm	23.4 mm	46.8 mm	70.2 mm
1000 m					156.0 mm	234.0 mm

The resulting errors $\delta(d_4)$ are quite large, due to the large error in k. Smaller $\delta(k)$ may be expected, if distances are measured well above the ground ($\delta(k) = 0.1 - 0.4$). For precise EDM, large height differences should be avoided or the coefficient of refraction should be determined, through reciprocal trigonometric levelling for example.

3.3 Other Reductions and Computations

Apart from the standard EDM reductions which reduce the measured distance to the spheroidal distance, other reductions and computations have to be occassionally used in connection with EDM work. The more frequent problems are discussed below.

3.31 Height Difference from Measured Zenith Distance and Slope Distance

With the introduction of EDM, the determination of height differences by trigonometric levelling has become very convenient. The combination of conventional trigonometric levelling and EDM has led to a survey method, which is a real alternative to spirit levelling, both in precision and in speed (see [30]).

Height differences are also required for a wide range of setting-out work. Several EDM instruments provide a facility for height difference computation. Some of these even measure the zenith distance automatically (Zeiss Reg Elta 14, AGA Geodimeter 700/710, HP 3810A, HP3820A).

Users of instruments with built-in distance reduction and height difference programs should be aware of the particular equations on which the programs are based. The basic equations for the computation of height differences are developed below and these allow a critical review of such built-in programs.

3.311 Single Zenith Distance Measurement

The problem is depicted in figure 23. The deviations of the vertical are ignored because orthometric heights (= geoidal heights) are sought.

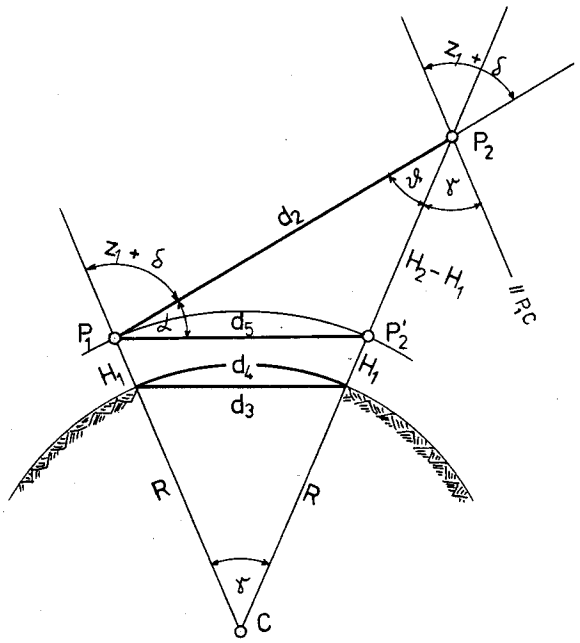

Figure 23

In triangle $P_1P_2P_2'$, the following angles can be computed:

$$\nu = z_1 + \delta - \gamma = z_1 - \frac{\gamma}{2}(2-k) \qquad (3.49a)$$

$$\alpha = \pi - (\frac{\pi}{2} - \frac{\gamma}{2}) - (z_1 + \delta) = \frac{\pi}{2} - (z_1 - \frac{\gamma}{2}(1-k)) \qquad (3.49b)$$

The angle of refraction δ was replaced according to equation (3.46) and figure 22 as follows:

$$\delta = \frac{\beta}{2} = \frac{d_2}{2r} = \frac{d_2 k}{2R} \simeq \frac{k}{2}\gamma \qquad (3.49c)$$

Based on figure 23 and equations (3.49a-c), the sine-rule applied to the triangle $P_1P_2P_2'$ gives

$$H_2 - H_1 = d_2 \frac{\sin(\frac{\pi}{2} - (z_1 - \frac{\gamma}{2}(1-k)))}{\sin(\frac{\pi}{2} + \frac{\gamma}{2})} = d_2 \frac{\cos(z_1 - \frac{\gamma}{2}(1-k))}{\cos\frac{\gamma}{2}} \qquad (3.55a)$$

Considering that γ is very small, cosine $\frac{\gamma}{2}$ is taken as unity.

$$H_2 - H_1 = d_2(\cos z_1 \cos(\tfrac{\gamma}{2}(1-k)) + \sin z_1 \sin(\tfrac{\gamma}{2}(1-k))) \qquad (3.55b)$$

With $\cos(\frac{\gamma}{2}(1-k)) = 1.00$ and $\sin(\frac{\gamma}{2}(1-k)) = \frac{\gamma}{2}(1-k)$ as in 3.2222

$$H_2 - H_1 = d_2 \cos z_1 + \frac{\gamma}{2}(1-k)\, d_2 \sin z_1 \qquad (3.55c)$$

The unknown parameter $\frac{\gamma}{2}$ may be derived from equation (3.44) in section 3.222:

$$\frac{\gamma}{2} = \frac{d_2 \sin z_1}{2(R+H_1) + 2d_2 \cos z_1} \qquad (3.55d)$$

Ignoring the second term of the denominator and setting $H_1 = 0$, produces in conjunction with equation (3.55b) the final form given by Brunner in [31]

$$H_2 - H_1 = d_2 \cos z_1 + \frac{(1-k)}{2R} (d_2 \sin z_1)^2 \qquad (3.56)$$

where $H_2 - H_1$ = orthometric height difference between P1 and P2
d_2 = wave path chord
k = coefficient of refraction of light
R = radius of curvature of spheroid along the line or mean radius as for example R_M = 6 370 100 m in NSW I.S.G.
z_1 = observed zenith distance in P_1

All data are assumed to be measured or reduced to the points P_1 and P_2. The omission of H from the denominator of (3.55d) causes an error in $(H_2 - H_1)$, computed according to (3.56), of only 1 mm for a height above sea level of 1000 m and a horizontal distance of 10 km.

A graph depicting the accuracy of equation (3.56) is given in reference [31]. The maximum error in $(H_2 - H_1)$ is < 0.1 mm for slope distances < 2.5 km and height differences < 1000 m.

The coefficient of refraction in equation (3.56) refers to theodolite observations and not to the EDM measurement. It has been reported in [11] and discussed in section 2.46, that the actual coefficient of refraction for "grazing" rays (close to the ground) may vary between (-2.0) and (+1.50). Grazing rays are usually encountered in short range EDM. As the actual coefficient of refraction is usually unknown, the height differences are computed assuming a mean coefficient of refraction of 0.13. The difference $\delta(k)$ between the mean and the actual value of the coefficient of refraction will then affect the computed height difference $(H_2 - H_1)$ by an error $\delta(H_2 - H_1)$:

$d_2 \sin z_1$ =	$\delta (H_2 - H_1)$ for $\delta k = 1.0$	$\delta(H_2 - H_1)$ for $\delta k = 2.0$
100 m	0.8 mm	1.6 mm
300 m	7.0 mm	14.1 mm
500 m	19.6 mm	39.2 mm
1000 m	78.5 mm	157.0 mm

The equation for $\delta(H_2 - H_1)$ is obtained by differentiating equation (3.56) with respect to k:

$$\delta(H_2 - H_1) = \frac{(d_2 \sin z_1)^2}{2R} \delta k \qquad (3.57)$$

The above table should be kept in mind when assessing the reliability of heights obtained by electronic tacheometry.

3.312 Reciprocal Zenith Distance Measurement

The uncertainty in the coefficient of refraction k can be greatly reduced if reciprocal, simultaneous zenith distances are observed. The counterpart of equation (3.56) in the case of reciprocal zenith distance observations reads, according to [30]:

$$H_2 - H_1 = \frac{d_2}{2} (\cos z_{12} - \cos z_{21}) \qquad (3.58)$$

where $H_2 - H_1$ = orthometric height difference between P1 and P2
d_2 = wave path chord
z_{12} = zenith distance at P1 to P2
z_{21} = zenith distance at P2 to P1
H_1 , H_2 = orthometric(= geoidal) heights.

Equation (3.58) can be derived easily from equation (3.56). Instrument and target heights are again assumed equal. The equation for the determination of spheroidal height differences has been explained in [30].

It was assumed in equation (3.58), that the coefficients of refraction are equal for the reciprocal observations. This will rarely eventuate. The uncertainty of the height difference $(H_2 - H_1)$ caused by the uncertainty of the difference of reciprocal coefficients of refraction $(k_1 - k_2)$ may be calculated as follows [30]:

$$\sigma_{(H_2 - H_1)} = \frac{(d_2 \sin z_1)^2}{4R} \sigma_{(k_1 - k_2)} \qquad (3.59)$$

where $\sigma_{(H_2 - H_1)}$ and $\sigma_{(k_1 - k_2)}$ denote the appropriate standard deviations.

The following values have been estimated for $\sigma_{(k_1 - k_2)}$ by Brunner [30]:

$\sigma_{(k_1 - k_2)} = \pm 0.3$ for simultaneous, reciprocal zenith distance observations, and

$\sigma_{(k_1 - k_2)} = \pm 0.5$ for non-simultaneous, reciprocal zenith distance observations.

A short table may illustrate the effect of the standard deviation of Δk on the standard deviation of the height difference ΔH:

$d_2 \sin z_1$	$\sigma_{\Delta H}$ for $\sigma_{\Delta k} = \pm 0.3$	$\sigma_{\Delta H}$ for $\sigma_{\Delta k} = \pm 0.5$
100 m	±0.1 mm	±0.2 mm
300 m	±1.0 mm	±1.8 mm
500 m	±2.9 mm	±4.9 mm
1000 m	±11.8 mm	±19.6 mm

3.32 Corrections for Unequal Instrument, Target and Reflector Heights

An increasing number of short range EDM instruments and their associated reflectors are designed in such a way that corrections for unequal heights of theodolite, EDM instrument, theodolite target and reflector are unnecessary. This has the advantage not only of saving time but also of increasing the precision. As preparation for the discussion of such EDM instrument designs, the basic reduction equation is derived. This equation will also be applicable for the reduction of EDM distances if zenith distances are measured independently.

The correction is best applied after the application of velocity corrections (see sections 3.11 and 3.12) and the first arc-to-chord correction (see 3.2) but before the slope correction. The situation is depicted in figure 24, where the following elements are denoted as:

d_{EDM} = wave path chord (d_2)
d_{TH} = distance along zenith distance ray
h_{EDM} = height of trunnion axis of EDM instrument (above survey mark P1)
h_{TH} = height of trunnion axis of theodolite (above survey mark P1)
h_T = height of target (above survey mark P2)
h_R = height of reflector (above survey mark P2)
z_{TH} = measured zenith distance at station P1 between theodolite and target.

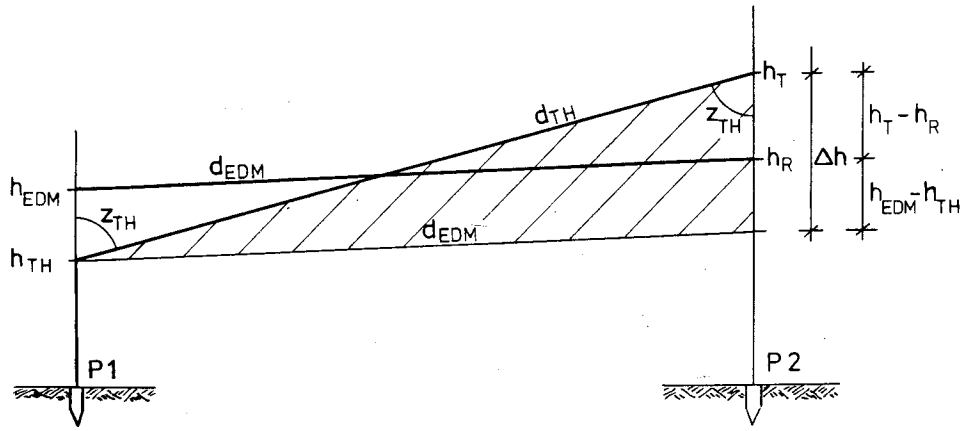

Figure 24

Application of the cosine rule in the hatched triangle together with the equation for Δh:

$$\Delta h = h_{EDM} - h_{TH} + h_T - h_R \tag{3.60}$$

leads to

$$d_{EDM}^2 = d_{TH}^2 + \Delta h^2 - 2 d_{TH} \Delta h \cos z_{TH} \tag{3.61a}$$

and

$$d_{TH}^2 = d_{EDM}^2 + 2 d_{TH} \Delta h \cos z_{TH} - \Delta h^2 \tag{3.61b}$$

The distance d_{TH} may be replaced, with sufficient accuracy, by d_{EDM} in the second term of equation (3.61b), because the value of the term is very small and because the difference between d_{TH} and d_{EDM} is small.

$$d_{TH} = d_{EDM}\left(1 + \frac{2\Delta h \cos z_{TH}}{d_{EDM}} - \frac{\Delta h^2}{d_{EDM}^2}\right)^{\frac{1}{2}} \tag{3.63}$$

With a series expansion for the square root and neglecting terms of third and higher order

$$d_{TH} = d_{EDM} + \Delta h \cos z_{TH} - \frac{\Delta h^2}{2 d_{EDM}} \tag{3.63}$$

where Δh is defined by equation (3.60).

The above reduction procedure is used if, for example, the theodolite observations are carried out independently of the EDM measurements (viz. with different equipment, on different days). On steep and short lines, the heights above the survey mark of theodolite, EDM instrument, target and reflector have to be measured carefully and accurately. The volume of computations may be reduced at least for the reduction of the distance, by using constrained centring. The relationships between h_{TH} and h_{EDM} as well as between h_T and h_R become constant and may be measured with high accuracy, thus reducing the errors of Δh in equation (3.63).

If the height difference $H_2 - H_1$ between the survey mark P1 and P2 is required, it is computed according to equation (3.56) as follows:

$$H_2 - H_1 = d_{TH} \cos z_{TH} + \left(\frac{1-k}{2R}\right) (d_{TH} \sin z_{TH})^2 + h_{TH} - h_T \tag{3.64}$$

Here, the introduction of constrained centring would reduce errors in the first two terms. However, errors in h_T and h_{TH} produce errors in $(H_2 - H_1)$ of the same magnitude.

3.33 Reduction to Centre of Distances

Distances (and angles) are sometimes measured from a satellite station, because for example the permanent mark is occupied by a beacon or another instrument. Two cases are discussed. The first deals with distances which are measured between satellite station and a target on a permanent mark. The second explains the problem when distances are measured between two satellite stations.

3.331 Single Centring of Distances

Again, two different possibilities have to be considered. The zenith distances and horizontal directions may be measured at the permanent mark or at the satellite station. A three dimensional solution is given, assuming that the correction for unequal heights has already been applied, where necessary.

3.3311 Angles and Distances Measured at Satellite Station S

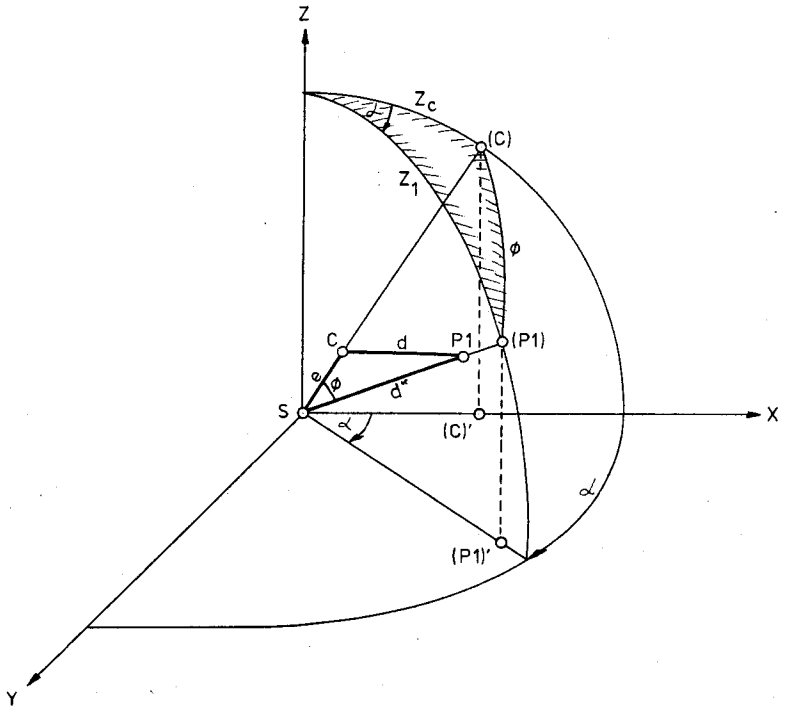

Figure 25a.

The problem is depicted in figure 25a, where

S = satellite station
C = permanent station
P_1 = target (reflector) station number one
(P_1) = projection of P_1 on sphere of radius $r = 1$
(C) = projection of C on sphere of radius $r = 1$
z_C = measured zenith distance from S to C
z_1 = measured zenith distance from S to P_1
e = measured slope distance between S and C (eccentric distance)
d^* = measured slope distance between S and P_1
d = centred slope distance between C and P_1
α = measured horizontal angle $(C)'S(P_1)'$, clockwise from x axis
$(C)'$ = projection of (C) on xy-plane
$(P_1)'$ = projection of (P_1) on xy-plane
Φ = angle $(C)S(P_1)$ = angle CSP_1

The slope distance d between C and P_1 is unknown and must be determined.

In figure 25a, the three dimensional coordinate system has its origin at S and its x-z plane through C; an application of the cosine rule of spherical trigonometry to the hatched triangle yields:

$$\cos \phi = \cos z_c \cos z_1 + \sin z_c \sin z_1 \cos \alpha \qquad (3.65)$$

Applying the cosine rule to the plane triangle SCP_1 gives

$$d^2 = d^{*2} + e^2 - 2d^* e \cos \phi \qquad (3.66a)$$

$$d = d^* \left(1 + \frac{e^2}{d^{*2}} - \frac{2 e \cos \phi}{d^*}\right)^{\frac{1}{2}} \qquad (3.66b)$$

Combining equations (3.66b) and (3.65) leads to:

$$d = d^* \left(1 + \frac{e^2}{d^{*2}} - \frac{2e}{d^*}(\cos z_c \cos z_1 + \sin z_c \sin z_1 \cos \alpha)\right)^{\frac{1}{2}} \qquad (3.67)$$

Equation (3.67) is a rigorous formula for the slope distance d between the two permanent stations C and P_1.

The zenith distance at S to P_1 has also to be centred. This is achieved by forming the sum of height differences:

$$\Delta H\ (CP_1) = \Delta H(SP_1) - \Delta H(SC) \qquad (3.68a)$$

$$d \cos z_{c_1} = d^* \cos z_1 - e \cos z_c \qquad (3.68b)$$

The centred zenith distance from C to P_1 (z_{c_1}) now becomes:

$$\cos z_{c_1} = \frac{d^*}{d} \cos z_1 - \frac{e}{d} \cos z_c \qquad (3.69)$$

where d^*, e, z_1, z_c are measured and d is known from equation (3.67).

3.3312 Angles Measured at Centre Station, Distances at Satellite Station

This situation occurs in tacheometry when an EDM instrument cannot be fitted to a theodolite. Distances and angles to radiation points are taken simultaneously at the EDM and theodolite stations.

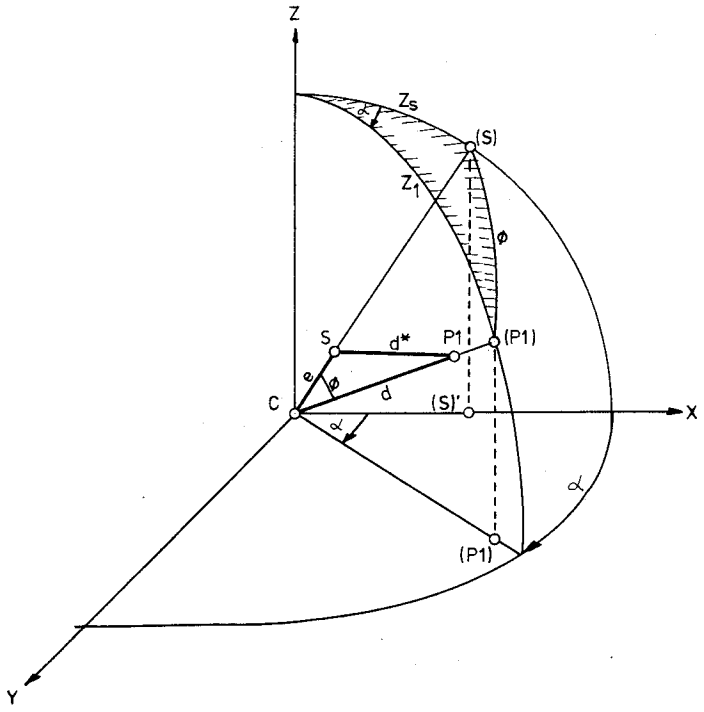

Figure 25b.

The notation in figure 25b is the same as in figure 25a. As in the previous section, a three-dimensional co-ordinate system is assumed. In this case, the origin is coincident with station C. The unknown slope distance d between centre station C and target station P_1 may be found as

$$d = d^* \left[1 - \frac{e^2}{d^{*2}} + \frac{2ed}{d^{*2}} (\cos z_s \cos z_1 + \sin z_s \sin z_1 \cos \alpha)\right]^{\frac{1}{2}} \qquad (3.70)$$

where d^* = measured slope distance between satellite S and P_1

e = measured slope distance between satellite S and centre station C (eccentric distance)

z_s = measured zenith distance from C to S

z_1 = measured zenith distance from C to P1

α = measured horizontal angle $(S)'C(P_1)'$, clockwise from x-axis.

The equation (3.70) is rigorous. Since d appears on both sides of equation (3.70) an approximate value d^* is taken for d and improved by iteration, if necessary.

The subsequent slope reduction uses the zenith distance z_1.

3.332 Double Centring of Distances

A plane solution is given for this rare case where the EDM instrument and reflector are each set up at satellite stations. The distances have to be reduced to the map grid before the centring is executed.

3.3321 Theodolite at Permanent Stations 1 and 2

A solution may be found in Rinner & Benz [17], p.853. See figure 26.

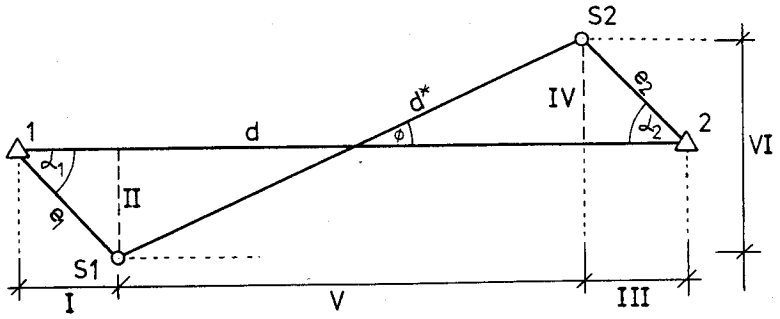

Figure 26.

The following terms and parameters apply:

d	=	centred distance between permanent marks 1 and 2
d*	=	distance between satellite stations
ϕ	=	unknown angle
1,2	=	permanent stations
S1,S2	=	satellite stations
α_1,α_2	=	angles at centre station between direction of main line and direction to satellite, clockwise from main line
e_1,e_2	=	eccentric distances between permanent and satellite stations

I	=	$e_1 \cos \alpha_1$	IV	=	$e_2 \sin \alpha_2$
II	=	$e_1 \sin \alpha_1$	V	=	$d^* \cos \phi$
III	=	$e_2 \cos \alpha_2$	VI	=	$d^* \sin \phi$

It follows from figure 26 that

$$d^* \sin \phi = e_1 \sin \alpha_1 + e_2 \sin \alpha_2 \qquad (3.71a)$$

$$d = e_1 \cos \alpha_1 + e_2 \cos \alpha_2 + d^* \cos \phi \qquad (3.71b)$$

$$= e_1 \cos \alpha_1 + e_2 \cos \alpha_2 + d^* \cos \left(\arcsin\left(\frac{e_1 \sin\alpha_1 + e_2 \sin\alpha_2}{d^*}\right)\right) \qquad (3.72)$$

Equation (3.72) is a rigorous solution.

3.3322 Theodolite at Satellite Stations S1 and S2

See figure 27. The following variables have to be considered, according to Rinner & Benz [17], p. 853:

α_1^*, α_2^* = angles at satellite stations between the adjacent centre and the distant second satellite station, clockwise from the latter.

I	= $e_1 \cos \alpha_1^*$	II	= $e_1 \sin \alpha_1^*$
III	= $e_2 \cos \alpha_2^*$	IV	= $e_2 \cos \alpha_2^*$
V	= $d \cos \phi$	VI	= $d \sin \phi$

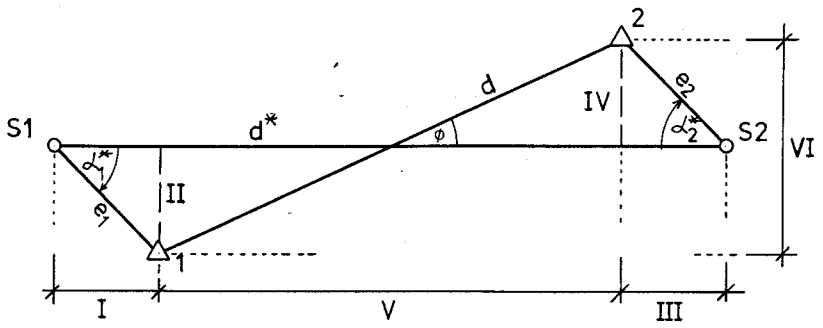

Figure 27.

Considering figure 27 yields:

$$d \cos \phi = d^* - e_1 \cos \alpha_1^* - e_2 \cos \alpha_2^* \qquad (3.73a)$$

$$d \sin \phi = e_1 \sin \alpha_1^* + e_2 \sin \alpha_2^* \qquad (3.73b)$$

With $\sin^2 \phi + \cos^2 \phi = 1$, the final rigorous solution becomes:

$$d = [(d^* - e_1 \cos \alpha_1^* - e_2 \cos \alpha_2^*)^2 + (e_1 \sin \alpha_1^* + e_2 \sin \alpha_2^*)^2]^{1/2} \qquad (3.74)$$

3.34 Determination of the Coefficient of Refraction from Reciprocal Zenith Distance Measurements

Reciprocal and simultaneous zenith distances are sometimes measured at the same time as EDM observations in order to determine the coefficient of refraction k for the prevailing atmospheric conditions. This is because the uncertainty of the coefficient of refraction determines the accuracy of the combined correction for K'', K_1, K_4 (see equation 3.38) and therefore the accuracy of the distance reduction.

Considering the triangle CP_1P_2 in figure 22, the following equations may be derived

$$\gamma + (\pi - \zeta_1 - \delta) + (\pi - \zeta_2 - \delta) = \pi \qquad (3.78a)$$

$$\gamma + \pi = 2\delta + \zeta_1 + \zeta_2 \qquad (3.78b)$$

All angles are to be taken in radians.

From figure 22 and section 3.2111 it follows

$$\delta = \frac{\beta}{2} = \frac{d_1}{2r} = \frac{d_1 k}{2R} \qquad (3.46)$$

that substitution of equation (3.46) in equation (3.78b) leads to

$$\gamma + \pi = \zeta_1 + \zeta_2 + \frac{d_1 k}{R} \qquad (3.79a)$$

$$= z_1 + z_2 + \frac{d_1 k}{R} + (\varepsilon_1 - \varepsilon_2) \qquad (3.79b)$$

Considering equation (3.34), the above equation may be written as

$$\frac{d_1 k}{R} = \frac{d_4}{R} + \pi - (z_1 + z_2) - (\varepsilon_1 - \varepsilon_2)$$

thus leading to the final equation for k

$$k = \frac{d_4}{d_1} + \frac{R}{d_1}\{\pi - (z_1 + z_2) - (\varepsilon_1 - \varepsilon_2)\} \qquad (3.80)$$

where all angles are in radians and where

k = coefficient of refraction

d_1 = wave path length

d_4 = spheroidal distance

R = radius of curvature of spheroid along the line (or mean radius as for example R_M = 6 370 100 in N.S.W. I.S.G.)

z_1, z_2 = observed zenith distances at P_1 and P_2 respectively

$\varepsilon_1, \varepsilon_2$ = deviation of vertical at P_1 and P_2 respectively (Refer to figure 22 for sign of ε).

The rigorous equation (3.80) can be simplified in most cases [39] to

$$k = 1 + \frac{R}{d_1}\{\pi - (z_1 + z_2) - (\varepsilon_1 - \varepsilon_2)\} \qquad (3.81)$$

It is evident that an omission of the (usually unknown) deviations of the vertical will not affect the value of k as long as the deviations are equal at both terminals of the line.

Error Analysis

The total differential of equation (3.81) yields

$$\delta k = -\left(\frac{R}{d_1}\right)\delta z_1 - \left(\frac{R}{d_1}\right)\delta z_2 - \left(\frac{R}{d_1}\right)\delta \varepsilon_1 + \left(\frac{R}{d_1}\right)\delta \varepsilon_2 \qquad (3.82)$$

where δz, $\delta \varepsilon$ are in radians. An error of one second of arc in z_1, z_2, ε_1 or ε_2 produces the following errors δk in k

$$\begin{aligned} d_1 = 10 \text{ km} \quad & \delta k = 0.003 \\ 30 \text{ km} \quad & = 0.001 \\ 50 \text{ km} \quad & = 0.0006 \\ 70 \text{ km} \quad & = 0.0004 \end{aligned} \qquad (3.83)$$

Assuming that

$$\sigma_{z_1} = \sigma_{z_2} \quad \text{and}$$

$$\sigma\varepsilon_1 = \sigma\varepsilon_2 = 0$$

equation (3.82) may be expressed as

$$\sigma_k = \sqrt{2}\left(\frac{R \sin(1'')}{d_1}\right)\sigma_z \qquad (3.84)$$

where σ_z is now to be taken in seconds of arc.

To investigate the effect of the accuracy of measured zenith distances on the derived coefficient of refraction and the combined correction $(K'' + K_1 + K_4)$, equation (3.38) is differentiated to give

$$\sigma_{(K'' + K_1 + K_4)} = \frac{{d_1}^3}{12R^2}(1 - k)\sigma_k \qquad (3.85)$$

To achieve an accuracy of, say, 0.3 ppm in the combined correction $(K'' + K_1 + K_4)$, the accuracy of the coefficient of refraction should not be less than the values listed below

d_1	= 10 km	σ_k	= ± 1.46
	= 30 km		= ± 0.16
	= 50 km		= ± 0.06
	= 70 km		= ± 0.03

The worst case of $(1 - k) = 1.0$ has been considered in the above table.

On longer EDM lines, the determination of the coefficient of refraction is therefore justified if large deviations of the coefficient of refraction from its mean value of 0.13 are expected. The necessary accuracy of the zenith distance measurements may be computed from

$$\sigma_{(K'' + K_1 + K_4)} = \frac{\sqrt{2}\ d_1^2 \sin(1'')}{12R}\ (1 - k)\sigma_z \qquad (3.86)$$

This equation can be simply derived from equations (3.84) and (3.85).

To obtain the combined correction $(K'' + K_1 + K_4)$ to an accuracy of ± 0.3 ppm, the reciprocal and simultaneous zenith distances must be measured with the following accuracies

d_1	= 10 km	σ_z	= ± 5.6'
	= 30 km		= ± 1.9'
	= 50 km		= ± 1.1'
	= 70 km		= ± 0.8'

Again, the term (1 - k) has been taken as one.

3.4 Numerical Examples

The process of reduction of EDM distances is explained with the aid of two numerical examples. The first example explains the reduction scheme for long distances, the second for short distances.

3.41 Reduction of a Long Distance

A distance was measured six times with a Siemens Albis SIAL MD 60 microwave distance meter between the trigonometric stations Perth and Ovens in the vicinity of Bathurst. Three observations were taken in the "Master" mode and another three in the "Remote" mode of each instrument. The following data set was recorded:

Measured distance d' = 22 395.667 m (Mean of six observations, corrected for instrumental constants)

Meteorological data:

Perth	p	= 921.3 mb
	t	= 6.1°C dry
	t'	= 3.2°C wet
Ovens	p	= 882.6 mb
	t	= 5.3°C dry
	t'	= 3.1°C wet

All pressure and psychrometer readings, corrected for instrumental constants of barometers and psychrometers, are mean values for the period of distance measurement. The station coordinates (ISG) and heights (AHD) are as follows

	E(m)	N(m)	Elevation(m)	
Perth Pillar	350 579.53	1295 238.04	879.71	top of pillar
Ovens Pillar	372 099.22	1301 416.35	1273.90	" " "

Instrument heights above the top of the pillar may be ignored for this case as they are equal on both sides.

First Step: First Velocity Correction

Applying equation (3.12)

$$K' = \{320.0 - \frac{77.64(p-e)}{(273.16 + t)} - (1 + \frac{5748}{(273.16 + t)}) \frac{64.68\ e}{273.16 + t}\} 10^{-6}\ d'$$

and equation (2.50a)

$$e = E'_W - 0.000\ 662\ p\ (t - t')$$

allows the computation of the first velocity correction K' on both stations:

	Perth	Ovens
t	6.1°C	5.3°C
t-t'	+2.9°C	+2.2°C
p	921.3 mb	882.6 mb
E'_W	7.68 mb	7.63 mb
e	5.91 mb	6.34 mb
p-e	915.4 mb	876.3 mb
K'	+0.8060 m	+0.9816 m

Mean of first velocity corrections K' = +0.8938 m

According to equation (3.5) the wave path length d may be computed as

$$d = d' + K' = 22\ 395.667 + 0.8938 \text{ m}$$

$$= 22\ 396.5608 \text{ m}$$

Second Step: Slope Correction

$$K_2 = -\frac{(H_2 - H_1)^2}{2d_2} - \frac{1}{8}\frac{(H_2 - H_1)^4}{d_2^3} \quad \text{(from equation (3.32a))}$$

$H_2 - H_1 = 394.19$ m

$d_2 \simeq d = 22\ 396.5608$ m

$K_2 = -3.4690$ m $- 0.0003$ m

$K_2 = -3.4693$ m

Third Step: Sea Level Correction

According to equation (3.33c) and adopting R = 6 370 100 m yields

$$K_3 = -\frac{H_1 + H_2}{2R} d_2 + \frac{(H_1 + H_2)}{4R}\frac{(H_2 - H_1)^2}{d_2}$$

$$K_3 = -\frac{(1273.900 + 879.71)}{2(6370\ 100)}(22\ 396.5608) + \frac{(2153.6100)\ (394.19)^2}{4\ (6370100)\ (22396.5608)}$$

$K_3 = -3.7859 + 0.0006$ m

$K_3 = -3.7853$ m

Fourth Step: Combined Second Velocity and Arc-to-Chord Corrections

The combined correction is defined by equation (3.38): $K'' + K_1 + K_4 = (1-k)^2 \frac{(d_1)^3}{24R^2}$

Assuming k = 0.25 (mean value for microwaves) and R_M = 6 370 100 m (N.S.W., I.S.G.) yields:

$$K'' + K_1 + K_4 = (0.75)^2 \frac{(22\ 396.560)^3}{24(6\ 370\ 100)^2} = +0.0065 \text{ m}$$

Fifth Step: Sea Level Distance

Combining all former steps:

d	=	22 396.5608 m
K_2	=	− 3.4693 m
K_3	=	− 3.7853 m
$K'' + K_1 + K_4$	=	+ 0.0065 m
d_4	=	22 389.3127 m

Sixth Step: Reduction to Map Grid

This step is an example applicable to NSW Integrated Survey Grid calculations. The line scale factor is obtained according to [29], p.24, as

$$K = k_o\left(1 + \frac{y_1^2 + y_1 y_2 + y_2^2}{6r_m^2}\right) \qquad (3.75)$$

where K is the line scale factor, k_o the central scale factor (0.999940), $r_m = k_o R_m$ = 6 369 700 m, R_m = 6 370 100 m, the mean radius of curvature of spheroid (N.S.W. I.S.G.) and y = Easting − 300 000 m.

Thus: $K = 0.999\,940\,(1 + 0.000\,046\,839)$

$= 0.999\,986\,836$

According to [29] the plane distance on grid (grid distance) S may be written as:

$$S = K\,d_4 \qquad (3.76)$$

$= 0.999\,986\,836\,(22\,389.3127)$ m

$= 22\,389.018$ m

This is the grid distance on the ISG Grid, zone 55/3, equivalent to the measured EDM distance between "Ovens" and "Perth".

3.42 Reduction of a Short Distance

A distance was measured from station A to station B with a HP3805A Distance Meter. The following observations were recorded:

measured distance	d'_{AB}	= 587.134 m
height of EDM instr.	h_{EDM}	= 1.652 m
height of reflector	h_R	= 1.724 m
measured zenith distance	z_{TH}	= 85°41'53"
height of theodolite	h_{TH}	= 1.673 m
height of target	h_T	= 1.534 m
temperature at A	t	= 23.8°C
pressure at A	p	= 1008.3 mb

The following coordinates of station A are given for the NSW I.S.G. System, zone 56/1:

	E	N
Station A:	236 637.897 m	1 271 028.524 m

The elevation of A (A.H.D.) is:

$$H_A = 1058.21 \text{ m}$$

Both distance and zenith distance were measured at station A.

First Step: First Velocity Correction

Equation (3.10) reads:

$$K' = \left(278.7 - \frac{79.148\,p}{(273.16 + t)}\right) 10^{-6} d'$$

$$= \left(278.7 - \frac{(79.148)(1008.3)}{(273.16 + 23.8)}\right) 10^{-6} (587.134)$$

$$= +0.0058 \text{ m}$$

Substituting K' in equation (3.5) leads to:

$$d = d' + K' = 587.134 + 0.0058 = 587.1398 \text{ m}$$

The fourth decimal place is carried through the computation in order to obtain reductions correct to three decimal places. For the reduction of distances accurate only to several mm the fourth decimal place may be omitted.

Second Step: Correction for Unequal Heights

Equation (3.60) in section 3.32 reads:

$$\Delta h = h_{EDM} - h_{TH} + h_T - h_R = -0.211 \text{ m}$$

and equation (3.63)

$$d_{TH} = d_{EDM} + \Delta h \cos z_{TH} - \frac{\Delta h^2}{2d_{EDM}}$$

Substituting $d_{EDM} = 587.1398$ m and $z_{TH} = 85°41'53''$ yields:

$$d_{TH} = 587.1398 - 0.0158 - 0.00004 = 587.1240 \text{ m}$$

Third Step: Reduction to Sea Level

Repeating equation (3.45b) of section 3.222:

$$d_4 = R \arctan \left[\frac{d_1 \sin (z_1 + \varepsilon_1 + \frac{d_1 k}{2R})}{R + H_1 + d_1 \cos (z_1 + \varepsilon_1 + \frac{d_1 k}{2R})} \right] \qquad (3.45b)$$

Assuming a coefficient of refraction of light $k = 0.13$, a mean radius $R_m = 6\ 370\ 100$ m and a deviation of the vertical $\varepsilon_1 = 0$ (and with $d_1 = d_{TH}$ and $H_1 = H_A + h_{TH}$) the above equation becomes:

$$d_4 = 6\ 370\ 100 \arctan (\frac{585.47009}{6\ 371\ 203.9}) = 585.3687 \text{ m}$$

The second velocity correction and the two arc-to-chord corrections can be combined according to section 3.2114. The combined correction only amounts to 1.5×10^{-7} m; it may be ignored.

Fourth Step: Reduction to Map Grid

It is sufficient to replace the *line scale factor* by the *point scale factor* for relatively short distances. The point scale factor is given by ([29], p.24)

$$K = 0.99994 + 1.23(10^{-7}y)^2 \qquad (3.77)$$

for the N.S.W. I.S.G. projection and y = Easting - 300 000 m. Considering equation (3.76) in section 3.41 leads to:

$$\begin{aligned} S &= K\, d_4 \\ &= (0.99994 + (1.23)\ (0.0063)^2)\ 585.3687 \\ &= 585.363 \text{ m} \end{aligned}$$

where S is the grid distance on ISG, zone 56/1.

4. Electrooptical Distance Meters

Distance meters featuring visible light or near infrared (NIR) radiation as carrier waves are called electrooptical EDM instruments. These carrier waves may be explained in terms of geometrical optics; normal telescopes are used for transmitting and receiving the signals.

4.1 Classification of Electrooptical Distance Meters

Several criteria may be used to classify electrooptical distance meters. A few are mentioned here:

(1) Range

(2) Precision

(3) Degree of integration with a theodolite

Other criteria for classification have been discussed in sections 2.313 (phase measurement), 2.311 (light source) and 2.312 (modulation technique).

4.11 Classification according to Range

Two classes of instruments may be distinguished with respect to range:

(1) Short range EDM instruments

(2) Long range EDM instruments

Short range instruments have a range from around 0.1 metres to between 300 m and 2000 m using a single prism. They are usually equipped with infrared (IR) emitting diodes.

Long range instruments may have a larger minimum distance (For example, for the Geodimeter 8, 15 m) and are usually equipped with a laser. The maximum range of such instruments depends very much on visibility (see section 2.41) and the number of prisms used. With a large number of prisms (20-40) distances up to 70 km may be measured on clear days.

A class of medium range instruments with a maximum range of 5-10 km, is also available; manufacturers usually classify these as "long range" instruments. Medium range instruments may eventually disappear, because the maximum range of short range instruments is steadily increasing toward the medium range.

4.12 Classification according to Precision

Three categories of instruments are distinguished with regard to the precision obtained from standard observation procedures:

(1)	Instruments with a standard deviation of one observation greater than	$\pm$(5 mm + 5 ppm)
(2)	Instruments with a standard deviation of one observation around	$\pm$(5 mm + 1 ppm)
(3)	Instruments with a standard deviation of one observation smaller than	$\pm$(1 mm + 1 ppm)

Group (1) includes almost all short range instruments. Group (2) consists of short and long range instruments which are precise in scale. The instruments belonging to group (3) may be called *precision instruments*. The word *precision* is usually used in conjunction with a particular instrument viz. the Mekometer ME 3000 with a stated standard deviation of one observation of $\pm$(0.2 mm + 1 ppm). Other instruments of group (3) are presently the Tellurometer MA100 and the Geodolite 3Gr (see appendix D for details).

4.13 Classification according to the Degree of Integration with Theodolites

Several degrees of integration of EDM instruments with theodolites are available. The merits of the different systems are discussed below:

4.131 Full Electronic Tacheometers

Electronic tacheometers are fully integrated EDM instruments and electronic theodolites featuring coaxial optics and digital output of all measured data. They are best used in conjunction with electronic data processing and plotting in large detail or contour surveys and also for large setting-out surveys. Electronic tacheometers have become smaller, lighter and more versatile during the last few years. Such instruments are presently:

Zeiss Reg Elta 14 (1970)
AGA Geodimeter 700/710 (1971)
Hewlett Packard HP 3820A (1978)
Wild Tachymat TC 1 (1978)
Zeiss Elta 2 (1978)
Zeiss Elta 4 (1978)

The reduction of distances causes no problem because of the coaxial design which integrates the EDM instrument and theodolite. The centre of the reflector is used as a target for the measurement of horizontal directions and zenith distances. For more precise angular work the precision of pointing the reflector to the electronic tacheometer becomes critical. The virtual displacement of the reflector's glass cube corner due to refraction at the reflector's front surface depends on its size, construction and pointing facilities. It will not exceed a few millimeters as shown in section 4. 3243.

4.132 Partial Electronic Tacheometers

A large number of different designs may be mentioned under this heading:

(1) Fully integrated EDM instrument and theodolite with glass circles having coaxial EDM and theodolite telescopes.
Instruments: ZEISS SM 11 (1970)
ZEISS SM 4 (1977)

(2) Fully integrated EDM instrument and theodolite, featuring an electronic zenith distance measuring device, a glass circle for horizontal directions and parallel but not coaxial optical axes of EDM instrument and theodolite.
Instrument: Hewlett-Packard HP 3810A (1976)

(3) EDM instrument mounted on an electronic theodolite with accessory units for on-line recording of all data and on-line computations of horizontal distances, and height differences.
Instruments: Keuffel & Esser AUTORANGER and
Keuffel & Esser VECTRON Digital Surveying Instrument

4.133 Telescope Mounted Instruments

This group includes all EDM instruments which are mounted on the telescope of a theodolite. The advantage of this system is the combined pointing for EDM, zenith distances and directions, and the virtual absence of any additional corrections. The weight of such instruments is kept low because of the strain on the vertical and horizontal axis of the theodolite. Three designs may be distinguished:

(1) Only one pointing for angles and distances is necessary. The offset of the EDM instrument axis relative to the theodolite's telescope axis is taken into account by a special reflector-target-system with the same offset between reflector and theodolite target. The reflector-target has to be tiltable to compensate for the tilt of the EDM instrument around the horizontal axis of the theodolite.

(2) EDM instruments with the transmitter and receiver on opposite sides of the theodolite telescope need only one pointing to the centre of the reflector for direction, zenith distance and distance, as described in section 4.131. (Kern DM 500/501).

(3) EDM instrument-theodolite combinations, using a reflector as target, normally require two pointings, one for zenith distance and direction and one for distance. The zenith distance measured to the reflector centre, is subsequently used for distance reduction. Theoretically, a small additional correction should be applied to the measured distance on a very close range. However, this correction is so small that it may be neglected in practice. The problem is explained in figure 28, which depicts a vertical section through the theodolite (T), EDM instrument (E) and reflector (R).

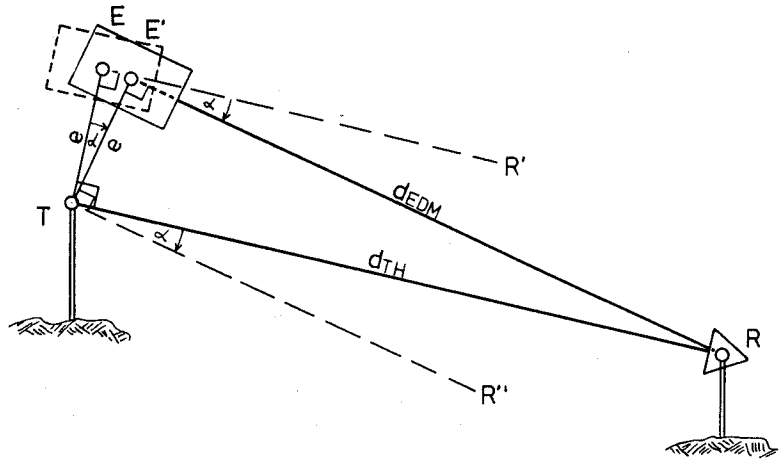

Figure 28.

Assuming that the EDM axis (ER', E'R) is always parallel to the optical axis of the theodolite (TR, TR''), the telescope is first pointed at R, taking the zenith distance and the direction, then the EDM instrument is aligned with R. This tilt causes the EDM instrument centre E to move to E'. The distance d_{EDM} is then measured from E'. Terming the eccentricity of the EDM instrument e, the corrected distance d_{TH} between the horizontal axis of the theodolite T and that of the reflector R may be computed according to

$$d_{TH} = (d_{EDM}^2 + e^2)^{\frac{1}{2}} \qquad (4.1a)$$

$$= d_{EDM}(1 + \frac{e^2}{d_{EDM}^2})^{\frac{1}{2}} \qquad (4.1b)$$

Expanding the root term yields

$$d_{TH} = d_{EDM}(1 + \frac{e^2}{2d_{EDM}^2} - \cdots) \qquad (4.2a)$$

$$= d_{EDM} + \frac{e^2}{2d_{EDM}} \qquad (4.2b)$$

The correcting term in (4.2b) depends on the eccentricity of the EDM instrument and the measured distance. A numerical example illustrates the magnitude of the correction. Assuming an eccentricity of 0.1 m, the correction is +0.5 mm for d = 10 m and +1 mm for d = 5 m and therefore smaller than the usual precision of such instruments.

The following EDM instrument-theodolite combinations allow a change of face whilst the EDM instrument is mounted:

Kern DM500/501 with Kern DKM2A and K1S

Wild DI3S with Wild T16 and T1.

4.134 Theodolite Mounted Instruments

EDM instruments which are fixed on the telescope supports of a theodolite are called theodolite mounted instruments. They feature a horizontal axis and a sighting telescope of their own, because the EDM pointing has to be independent of the theodolite pointing. Transitting of the theodolite telescope is possible and the advantage of such a design is that no strain is put onto the transit axis. The vertical axis system of the theodolite has to carry the additional weight. Because of the fact that the EDM instrument has a large eccentricity relative to the horizontal axis of the theodolite and does not tilt with the telescope of the theodolite, the distance correction will be larger.

This necessary correction may be derived from equations (3.60) and (3.63) in section 3.32.

$$d_{TH} = d_{ETH} + \Delta h \cos z_{TH} - \frac{\Delta h^2}{2 d_{EDM}} \qquad (3.63)$$

$$\Delta h = h_{EDM} - h_{TH} + h_T - h_R \qquad (3.60)$$

Because h_T is equal to h_R and $(h_{EDM} - h_{TH})$ may be renamed as eccentricity e, equation (3.63) may be replaced by

$$d_{TH} = d_{EDM} + e \cos z_{TH} - \frac{e^2}{2 d_{EDM}} \qquad (4.3)$$

where d_{TH} = distance along zenith distance ray

d_{EDM} = measured distance (wave path chord)

e = eccentricity of EDM instrument

= height of EDM instrument minus height of theodolite

z_{TH} = measured zenith distance.

The correcting terms in (4.3) are functions of the zenith distance and the distance. Their magnitude is worked out in a short example. Assuming an eccentricity e = 0.2 m the following correction terms are obtained:

z_{TH}	e cos z_{TH}
70°	+68 mm
80°	+35 mm
85°	+17 mm
90°	0 mm
95°	-17 mm
100°	-35 mm
110°	-68 mm

d_{EDM}	$-\frac{e^2}{2 d_{EDM}}$
5 m	- 4 mm
10 m	- 2 mm
20 m	- 1 mm

Some theodolite mounted EDM instruments are also available with a tribrach mounting thus obviating the need for a theodolite. Such instruments are at present:

ZEISS Eldi2, Eldi 3

Tellurometer CD6

Keuffel & Esser Autoranger

4.135 Separate EDM Instruments

Most instruments in this category are long range instruments; at long distances simultaneous angle measurements are not required because distances are reduced with the aid of given station heights and directions are measured with first order theodolites, avoiding the additional weight of an EDM instrument. A few short range instruments belong to this class as well as some theodolite mounted instruments, which may be bought separately. The measurement of zenith distances, if required, may be achieved by

either (1) replacing an EDM instrument by a theodolite which fits the same constrained centring system and measuring the zenith distance to the centre of the reflector

or (2) replacing an EDM instrument by a theodolite, and a reflector by a traverse target in a common constrained centring system and then measuring the zenith distance to the target.

The first method requires distance corrections according to equation (4.3) in section 4.134. The second method needs no corrections for unequal instrument and target heights, if the target has the same "height" as the theodolite and the reflector the same "height" as the EDM instrument; "height" relates to the common constrained centring system. Such a system was adopted for the precision distance meter Mekometer ME3000 in conjunction with Kern theodolites (DKM2A, DKM3), and a combined reflector-target. If the second method is used in conjunction with equipment, which does not fulfil the conditions of corresponding "heights" laid down above, corrections according to equation 3.63 have to be applied (see section 4.134 or 3.32).

4.14 Special Features of Modern EDM Instruments

Most short range EDM instruments include a wide range of facilities to simplify their operation. Details of instruments which are equipped with such facilities may be found in appendix D. Some special features will be explained here.

4.141 Environmental Correction Dial

This device makes it possible to dial the appropriate first velocity correction into the system so that the displayed distance includes this correction. Temperature and pressure are measured at the instrument station and the first velocity correction (in $\pm$ppm) is usually derived from a correction chart. The dial is graduated in steps of 10 ppm for the HP 3805A and 30 ppm for the Wild DI3; maximum errors in the displayed distances are 5 ppm (HP 3805A) and 15 ppm (DI3). To achieve higher accuracy by elimination of these rounding-off errors, the dial may be set to zero and the first velocity correction applied by computation.

On longer distances, atmospheric data are recorded at both terminals. A mean correction could be dialled into the instrument although the zero dial position and subsequent computations are usually preferred. The environmental correction system of a distance meter may be easily checked by measuring a 1 km distance with differing dial settings; a change of 1 mm in distance corresponds then to 1 ppm and the internal accuracy of the instrument (e.g. $\pm$ 5mm) affects the test result by an insignificant amount (e.g. $\pm$ 5 ppm). The environmental correction dial may also be used for a combined correction consisting of

(1) the first velocity correction

(2) the sea level correction

(3) the point scale factor of the map projection.

This combination corresponds to the "SST correction" mentioned in [29] (p.26) for application in the NSW Integrated Survey Grid. It is important to note that all parameters demanding a correction are booked in the field, as well as the applied correction itself, to allow a checking in the office.

The full advantage of environmental correction dials is only gained in setting out if other computations (e.g. slope correction) are also carried out by the distance meter. Distance reductions which are executed on office computers may well include all parameters and corrections and thus render separate field reductions less efficient and accurate.

4.142 Computation of Horizontal Distance and Height Difference

An increasing number of short range instruments provide the facility of computing the horizontal distance and the height difference. Electronic tacheometers provide these data automatically; with other instruments, the zenith distance has to be dialled-in manually. Automation is very convenient for setting-out work in which horizontal plane distances are provided. Users of such instruments should know exactly how the internal programs determine the horizontal distance and height difference and the accuracy of the determination. For longer distances and higher accuracies it may be better to reduce the measured slope distances with formulae in section 3.22.

4.143 Tracking Mode

The tracking mode of an EDM instrument is that measuring routine which measures the distance to a moving reflector continuously or at constant time intervals (e.g. every 2 seconds), if continuous pointing is provided. This facility is therefore very useful for setting-out. Distances obtained in the tracking mode are usually less accurate than those in the normal mode because the distances are based on smaller observation samples. The full advantage of the tracking mode is only obtained if the instrument reduces slope distances automatically to horizontal distances thus providing the tracking of horizontal distances and possibly the tracking of height differences.

4.144 Audio Signal

An audio signal may supplement or replace the traditional galvanometer for the display of the return signal strength. The pitch of a tone becomes a measure for the strength of the return signal. The volume of an audio signal should be adjustable. The audio signal may be transmitted by radio to the reflector-man thus enabling him to align the reflector. This possibility should be very helpful in setting-out.

4.145 Other Features

A few other distinguishing properties of modern instruments should be mentioned, because they might be important in choosing an instrument. Such information, related to specific instruments, is given in appendix D.

The execution of distance measurement can be more or less automatic after the initial pointing. Some instruments still need an adjustment for aperture diaphragm or neutral filter or an attachment of an attenuator to reduce signal strength. Manual tuning is also often required.

Changing face of the theodolite is possible with some telescope mounted EDM instruments but not with others. For lower accuracy work, this criterion is not really important because the measurement of directions and zenith distances on two faces may not be required.

The advantage of having no obstructing cables between the rotary part of the EDM instrument or the EDM instrument-theodolite combination and the tripod or ground may be another factor affecting the ease of EDM and angular measurements. Cables cause additional unbalanced strain on the instrumental axes. Of the two types of interfering cables, namely power supply and data transfer (electronic tacheometers), the former may be easier to replace by better design.

The degree of integration of an EDM instrument with a theodolite, target and reflector is another very important property of an instrument. It was discussed in section 4.13.

4.2 Block Diagram of an Electrooptical Distance Meter

The working principle and some components of electrooptical EDM instruments were discussed in section 2.31. The design of such an instrument is now explained in more detail to demonstrate the interaction of different components. Although instruments vary in their design according to the differing techniques employed, only one instrument can be discussed in this text. A wider range of instruments is covered in textbooks and numerous technical papers [4], [6], [7], [35].

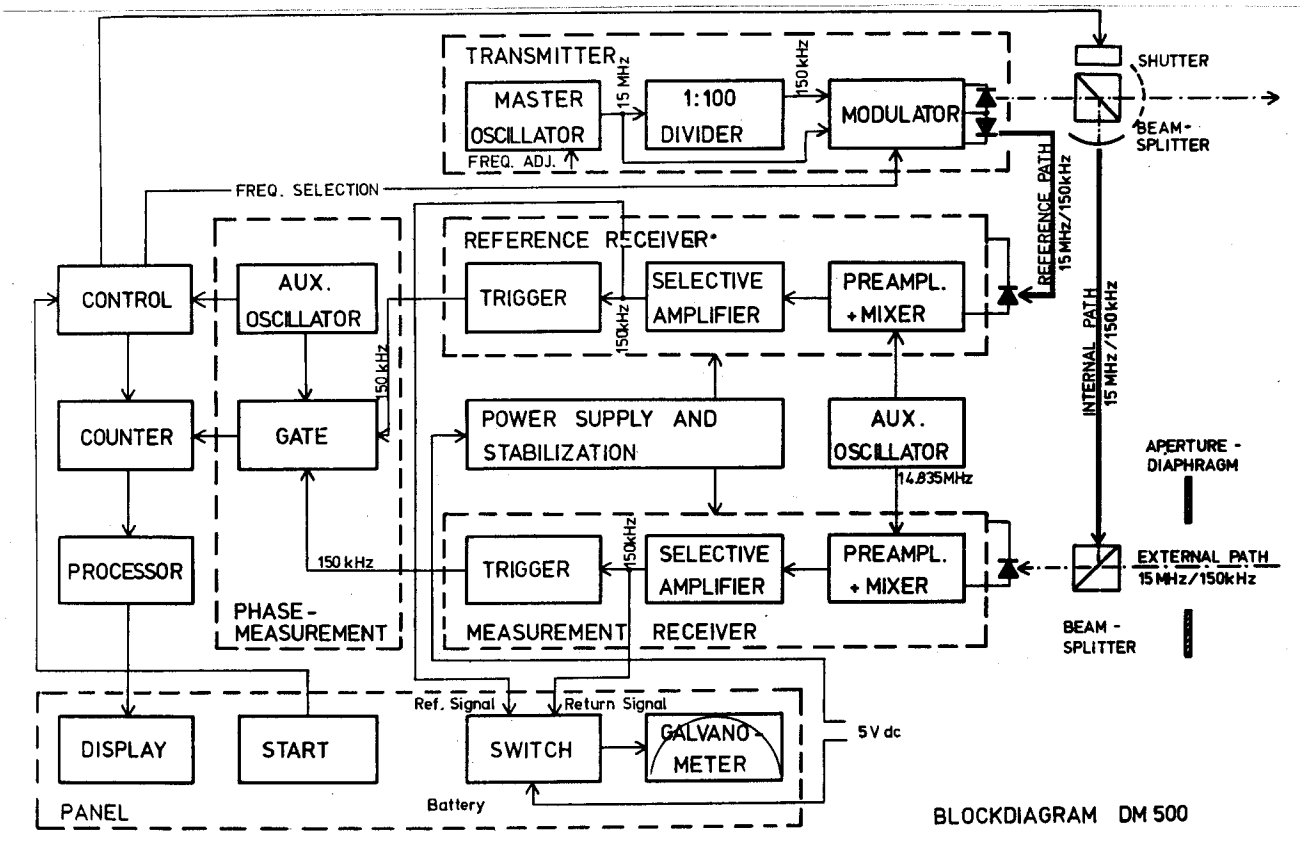

Figure 29.

The large group of electrooptical distance meters employing techniques such as *direct modulation, direct demodulation* and *digital phase measurement* is represented here by the Kern DM500 short range EDM instrument. The block diagram of this specific instrument is depicted in figure 29, neglecting the transmitter and receiver optics [36], [37], [38].

The transmitter includes a master-oscillator, a digital divider (1:100), a modulator and two infrared emitting diodes. The master-oscillator produces the fine measurement frequency of 14.985 400 MHz (~ 15 MHz) corresponding to a unit length of 10 m. The coarse measurement frequency of 149.854 kHz (~ 150 kHz) is then derived by the divider. The modulator has an input for both frequencies and selects one of them according to the commands coming from the program control through a "light pipe" (glass fibre). The power supply of the transmitter block is not shown in figure 29. The modulator drives two infrared emitting diodes. The radiation of the first travels either through the external or the internal light path, the second one through a light pipe to the reference signal receiver thus providing an optical coupling between the transmitter and receiver. Optical coupling has the advantage of full electrical isolation.

In front of the first emitting diode, a turning shutter opens either the interval or external light path according to commands from the program control. The measuring as well as the reference beam are amplitude modulated by the 15 MHz or 150 kHz signal.

Two almost identical receiver blocks process the measuring or reference signal. Avalanche photodiodes transform the incident IR beams into modulated electrical currents which pass first through preamplifiers and then through mixers. In the mixers a signal from an auxiliary oscillator, having a frequency of 150 kHz below the master oscillator's frequency (14.835 MHz), is multiplied with the 15 MHz or 150 kHz signal coming from the preamplifier thus causing signals of different frequencies. In the following selective amplifier, only the low frequency (LF) signal of 150 kHz is amplified. The output of the selective amplifier has therefore always a LF of 150 kHz irrespective of the modulation frequency (either 15 MHz or 150 kHz) received at the photo diode. It can be proved that the phase difference between the signals in the reference and the measurement channel, both either LF or HF, does not change through the frequency transformation in the mixers [37]. Low frequencies are easier to handle in a digital phase measurement and are therefore preferred for that purpose.

The reference and measurement signals pass a trigger before they enter the block of the digital phase measurement as rectangular waves. This type of phase measurement is described in section 2.3133 and depicted in figures 16 and 17. The auxilliary oscillator of the phase measurement section is also used as a time base for the program control of the distance meter.

The program control organizes the entire distance measurement once the start button has been pressed. It controls the selection of the frequencies, the selection of the measurement signal path (turning shutter) and the counter.

The processor subtracts the number of counts of the internal path from those of the external path for the fine measurement, converts counts into length units, adds the additive constant (built-in) and brings all three digits after the decimal point onto the display. The number of full metres within the unit length of 10 m is stored, until the internal and external path of the coarse measurement (150 kHz) is also measured and processed. The value of full metres in the zero to ten metre interval is then compared between the coarse and the fine measurement and the former adjusted. The digits of the coarse measurement go then onto the display.

The adjustment of the two values for the first digit on the left of the decimal point has to be made in such a way that no error can occur for phase measurements around zero [37]. In order to always get a positive correction to the 0 to 10 m value of the coarse measurement, 5 m is subtracted from the coarse measurement first by setting the start value of the display at 995 m. The reduced coarse value is then compared with the fine value and the necessary additional and integer terms computed. This system corrects for errors of up to 5 m in the coarse measurement. An example may illustrate the procedure:

Fine measurement	4.328 m
Coarse measurement	268.6 m
	- 5 m
Red. coarse measurement	263 m

The 3 m in 263 has to be increased by 1 to match the fine measurement. The sequence of the displayed data is:

(1) 995.328 m
(+268)
(2) 263.328 m
(+ 1)
(3) 264.328 m

The subtraction of the *internal* light path distance from the *external* light path distance cancels phase drifts caused by electronic circuits; in other words, this procedure keeps the additive constant (see section 4.51) of the instrument stable.

The galvanometer has differing functions which may be selected by turning a switch located on the instrument panel. It measures the battery voltage, the strength of the reference or return signal as may be seen on the different inputs on the block diagram in figure 29. The aperture diaphragm is used to adjust the strength of the return signal to that of the reference signal by changing the aperture of the receiver optics.

The two beam splitters and the connecting light pipe are part of the internal light path. The measuring sequence of the instrument is as follows:

(1) 2 seconds of time: fine measurement (15 MHz), external path

(2) 2 seconds of time: fine measurement (15 MHz), internal path

(3) 2 seconds of time: coarse measurement (150 kHz), external path

(4) 2 seconds of time: coarse measurement (150 kHz), internal path.

The equal time intervals for all four measurements result from the use of the same phase measurement routine for all four steps. About 300 000 phase measurements can be made in two seconds of time at a frequency of 150 kHz.

4.3 Reflectors

4.31 Introduction

Apart from military laser rangers electrooptical EDM instruments need a device at the target station which reflects the light (or infrared) beam back to the instrument. Reflecting devices should have the following properties:

(1) good reflectivity,

(2) complete illumination of the receiver optics of the instrument,

(3) no change of direction of emerging rays through small movements of the reflecting device, thus rendering a continuous alignment unnecessary.

Such devices are:

(1) plane front surface mirror

(2) spherical reflector

(3) glass prism reflector (corner cube reflector, retrodirective prism)

(4) cat's eye reflector (plastic reflector)

(5) reflecting tape.

Plane front surface mirrors were used in conjunction with the Geodimeter NASM2. Although they had the best reflective properties, their use was soon discontinued because of the requirements for a very stable and precise alignment. Spherical reflectors allow for a misalignment of ±30 minutes of arc and consist basically of a spherical mirror and a small plane mirror in its focal point. Their reflectivity (65%) is much smaller than that of the plane mirrors (90%) due to the greater number of optical parts involved. Spherical reflectors were used in conjunction with early Geodimeter models. Glass prism reflectors have proved to be the most suitable reflector system . They were first employed by the U.S. Army Map Service in 1953 [17], and are now almost exclusively used in terrestrial EDM as well as in satellite and lunar laser ranging (see section 2.212). They are discussed in more details in section 4.32 and have a reflectivity of about 80%.

Cat's eye reflectors consist of an array of very small corner cubes as used on cars or bicycles and are much cheaper than the glass prisms of corner cube reflectors. They have a smaller reflectivity than glass prisms but still allow the measurement of reasonable distances, especially in conjunction with laser instruments (Geodimeter 600: 1500 m, Geodimeter 710: 300 m). Plastic cat's eye reflectors are suitable as permanent marks in setting-out and measuring displacements. The reflecting tape is an even cheaper reflecting device but requires a powerful beam, such as a laser . Using reflecting tapes as targets the Geodimeter models 600 and 710 reach a range of about 200 m and 100 m respectively. Reflecting tapes are self-adhesive and may be stuck on walls as temporary reference marks for setting-out or displacement surveys.

4.32 Glass Prism Reflectors

These common reflectors consist of a corner of a glass cube which was cut in such a way that the plane of the cut is perpendicular to the cube diagonal (equilateral cube corner). It can be shown that if the angles between the cube planes are exactly equal to 90 degrees, all incident rays are reflected in such a way that incident and emerging rays are exactly parallel and symmetrical to the centre ray (ray to the prism corner), independent of the alignment of the reflector. The alignment has however an effect on the effective aperture of the reflector and therefore on the retro-reflected radiant power. Figure 30 shows how the effective aperture A_{eff} expressed as a percentage of the aperture A varies with the angle of incidence α for a prism of circular aperture and a refractive index of 1.5 [9].

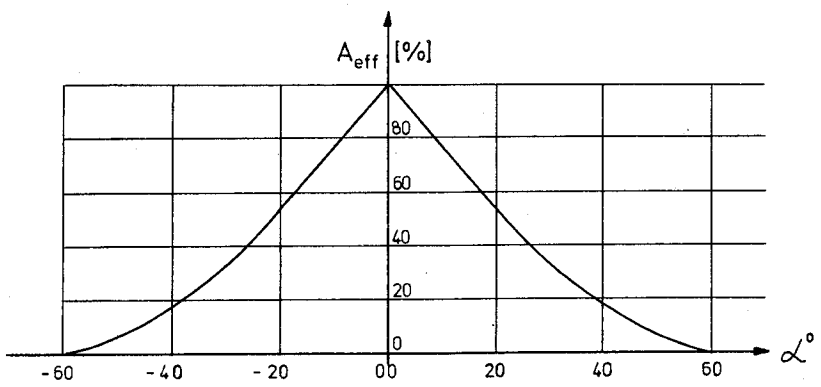

Figure 30.

The reflecting faces of most prisms are coated and do not require cleaning. Those of uncoated prisms may need any condensed water to be cleaned off, to retain full reflectivity.

4.321 Accuracy of Reflectors

Glass prism reflectors may be classified according to their accuracy and their shape. The accuracy of a prism may be defined in terms of the maximum deviation of the angle between its faces from the ideal, theoretical angle of exactly 90° and the maximum deviation of its faces from a ideal plane. AGA long range prisms are ground to 2 seconds of arc maximum deviation from a true right angle, AGA short range prisms only to 20 seconds [40]. The facing of Keuffel and Esser prisms is true to within $\pm$ 546 nm and is at right angles within 4 seconds of arc [41]. Prisms are costly. For example, the cost of single prism reflectors is between 6 and 14% of the price of the EDM instrument. It is therefore wise to be perfectly clear about the required range, accuracy and number before ordering them. Their performance is checked by manufacturers through inspecting interference patterns in an interferometer [56].

4.322 Shape and Size of Reflectors

The shape of the reflectors is determined in advance by the relative position of the transmitter and receiver optics of the corresponding EDM instrument because it is required that the return beam always fully illuminates the receiver optics. EDM instruments with coaxial transmitter and receiver optics require reflectors with a circular aperture; instruments with parallel but separated transmitter and receiver optics need prisms with a rectangular aperture to displace the rays at the reflector by an offset equal to that of the two instrument optics. Reflectors of rectangular aperture are used in conjunction with the following instruments: Wild DI3, DI3S, Kern DM500, DM501, and Keuffel & Esser Autoranger. It may be mentioned that differing solutions were adopted for the prisms of earlier Geodimeters (models 2, 3, 4). The prisms were either ground to a larger angle than 90° or were fitted with a special wedge in front of the prism to spread the beam in order to reach the eccentric receiver optics.

The reflector's size is fixed by the diameter of transmitter and receiver optics and by the requirement that the receiver optics must always be fully illuminated by the reflected beam. It can be easily proved, for an instrument with coaxial optics, that

$$\phi_B = \phi_T + 2\phi_{REFL} \tag{4.4}$$

where ϕ_B is the diameter of the return beam at the receiver, ϕ_T the diameter of the transmitter optics and ϕ_{REFL} the diameter of the reflector's aperture. Denoting the diameter of the receiver optics by ϕ_{REC} the above condition may be written in the form:

$$\phi_B \geq \phi_{REC} \tag{4.5}$$

The minimal reflector diameter may then be computed as

$$\phi_{REFL} = \tfrac{1}{2}(|\phi_{REC} - \phi_T|) \tag{4.6}$$

The actual diameter of reflectors is usually larger than the minimal value given in equation (4.6) thus increasing the radiant power of the return signal.

Circular reflectors may also be used with EDM instruments having separated otpics as long as the displacement Δ between the axis of the two optic systems is small. In this case, the following equation for the minimal reflector diameter applies:

$$\phi_{REFL} = \tfrac{1}{2}(\phi_{REC} + 2\Delta - \phi_T) \qquad (4.7)$$

A few of the instruments in this category are the Mekometer, the Geodimeter models 8, 10, 12A, 14, the Ranger V and the Rangemaster II. See appendix D for details.

EDM instruments featuring a larger displacement Δ between transmitter and receiver axis require a reflector of rectangular aperture of about $(\Delta + \phi_T)$ length and width ϕ_T, assuming transmitter and receiver optics to be of equal diameter $(\phi_T = \phi_{REC})$.

4.323 Reflector constant

If only one particular type of reflector is used in conjunction with a particular EDM instrument the reflector constant is combined with the additive constant for the EDM instrument. The determination of this combined constant is described in section 4.61.

Various types of reflectors may be employed if their relative or absolute constants are determined. The relative reflector constant may be determined by measuring a large number of different distances with all reflectors. The mean differences of distances using two reflectors is a measure of the *relative reflector constant*. In practice, relative constants are usually computed in relation to one specified reflector (reference reflector). The *absolute reflector constant*, which refers to the vertical axis of a reflector, may be worked out from the known or measured dimensions of a reflector. Technical data of a selection of reflectors is given in Appendix F. Figure 31 illustrates the situation:

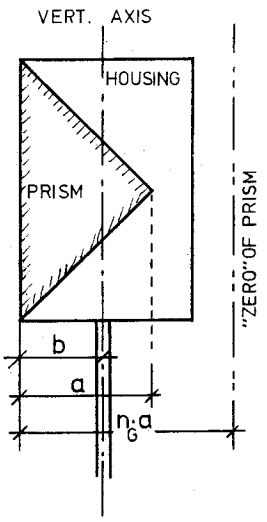

Figure 31.

$$\text{Absolute reflector constant} = -\left\{\frac{n_G}{n_A}\, a - b\right\} \qquad (4.8a)$$

where a is the height of the cube corner above the front surface, n_G the group refractive index of light in glass, n_A the group refractive index of light in air and b the distance between the front surface of reflector and the vertical axis of reflector assembly. The refractive index of glass prisms depends on the type of glass and the carrier wave (dispersion). For crown glass BK 7, for example, the phase refractive index is 1.519 for a wave length of 546 nm and 1.510 for a wave length of 852 nm [43]. (See Appendix F for more information on the refractive index in glass and on the constants a and b for various types of reflectors.) The reflector constant should be added to the distance measurement to obtain the corrected distance. It follows from figure 31 that it is possible to build so-called zero constant prisms which can be fixed on ranging rods. The front surface of the reflector is then at a distance of $(n_G/n_A)a$ from the centre line of the ranging rod (zero of prism).

The method of measuring absolute reflector constants can also be used to derive relative constants. The reflector constants of several reflectors of the same design and brand can be expected to be within a range of $\pm$ 1 mm [56].

4.324 Effects of Errors of Reflector Alignment

4.3241 Tiltable Reflector-Target with Eccentric Prism(s)

It was mentioned in section 4.133 that several telescope mounted instruments employ reflector-target combinations which compensate for the offset between telescope and distance meter. The horizontal axis of such reflector-targets is usually located through the centre of the target. Any erroneous vertical pointing of the reflector-target leads to a small error in the measured distance. The effect on distance of an error in vertical pointing α together with an eccentricity e of the reflector centre from the tilting axis may be written as follows:

$$\Delta d = e \sin \alpha \qquad (4.8b)$$

where d is the error in distance and α is given in degrees. An angle α of 5° and an eccentricity e of 45 mm (Wild DI3) would lead to a distance error of 4 mm. It can be seen that reflectors need to be aligned carefully in cases where the axis of the prism has an eccentricity relative to the tilting axis of the reflector-target.

4.3242 Effect of the Reflector's Alignment on the Measured Distance

Another effect of inaccurate alignment, which affects all prisms whether they are tiltable or not, is that the EDM rays travel a longer distance within the glass of the prism if the prism's front surface is not exactly perpendicular to the EDM rays. Because of the different refractive indices of glass and air a different distance is then measured. The situation is depicted in figure 32, where the broken lines depict a properly aligned prism and the unbroken lines a misaligned prism.

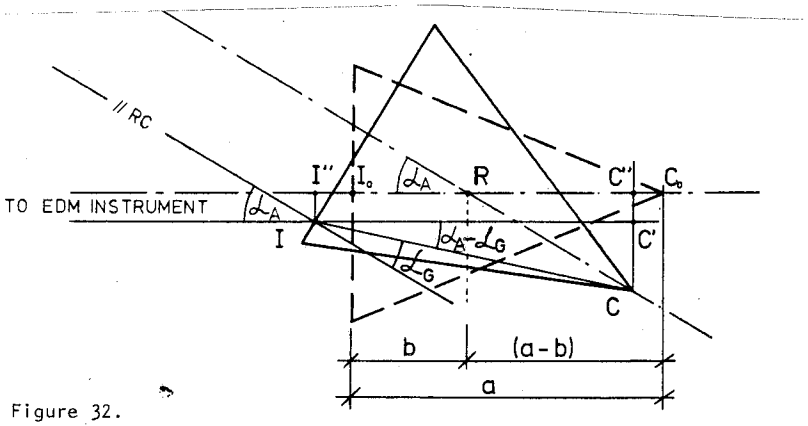

Figure 32.

The corner of the aligned prism is denoted by C_o and that of the misaligned one by C. The point of incidence of the EDM ray which travels to the prism corner C_o and back is termed I_o and that of the ray which proceed to the prism corner C (and back) is denoted by I. Only the corner rays are considered because they allow a two dimensional solution of the problem. The final statement however holds for all rays in the three dimensional case.

The vertical or horizontal axis is denoted by R and the dimension of the reflector and its relationship to the axis are given by the parameters a and b. The *angle of incidence* α_A and the *angle of refraction* α_G refer to the maladjusted prism (A = air, G = glass). The corresponding angles in the case of the correctly aligned prism are zero.

The *law of refraction* is defined by the formula

$$\frac{n_A}{n_G} = \frac{\sin \alpha_G}{\sin \alpha_A} \tag{4.9}$$

It permits the computation of the unknown angle of refraction α_G for a given angle of incidence α_A, equal to the error angle in alignment, as

$$\alpha_G = \text{arc sin } (\frac{n_A}{n_G} \sin \alpha_A) \tag{4.10}$$

In order to compare the distance measurements in the cases of an aligned and a deflected prism, the measured lengths $I''C_o$ and IC are compared. Considering the appropriate refractive indices the difference Δd between the measured distances to the aligned and the deflected prisms amounts to

$$\Delta d = I''I_o + (I_oC_o)\frac{n_G}{n_A} - (IC)\frac{n_G}{n_A} \tag{4.11}$$

If Δd is added to the distance measured to the deflected prism, the correct distance, equal to the distance measured to the aligned prism, is obtained. In equation (4.11), the refractive indices of glass and air are denoted by n_G and n_A, respectively.

The line elements in equation (4.11) may be derived from figure 32 as

$$IC = (a) \sec \alpha_G \tag{4.12}$$

$$IC' = IC \cos (\alpha_A - \alpha_G)$$
$$= (a) (\sec \alpha_G) \cos (\alpha_A - \alpha_G) \tag{4.13}$$

$$RC'' = (a-b) \cos \alpha_A \tag{4.14}$$

$$I''I_o = IC' - RC'' - b$$
$$= (a) \sec \alpha_G \cos (\alpha_A - \alpha_G) - (a-b) \cos \alpha_A - b \tag{4.15}$$

Substitution of equations (4.12) and (4.15) in equation (4.11) yields

$$\Delta d = a \sec \alpha_G \cos (\alpha_A - \alpha_G) - (a-b) \cos \alpha_A - b + a\frac{n_G}{n_A} - a\frac{n_G}{n_A} \sec \alpha_G$$

$$= a(\cos (\alpha_A - \alpha_G) - \frac{n_G}{n_A}) \sec \alpha_G - (a-b) \cos \alpha_A + a\frac{n_G}{n_A} - b \tag{4.16}$$

where α_G is defined by equation (4.10). It can be seen that the possible errors in distance depend largely on the size of the prism and on the position of the vertical or horizontal axis (R) in relation to the prism.

A numerical example may illustrate the magnitude of the error in distance Δd caused by the misalignment of the reflector. The following parameters are assumed (Wild GDR11 reflector):

a	= 60 mm	n_A	= 1.00
b	= 22 mm	n_G	= 1.52 (λ = 900 nm)
α_A	= 1°	Δd	= 0.00 mm
	= 5°		= 0.07 mm
	= 10°		= 0.27 mm
	= 15°		= 0.59 mm
	= 20°		= 1.03 mm
	= 25°		= 1.56 mm
	= 30°		= 2.16 mm

An alignment of the reflector to $\pm 15°$ will lead to a maximum error in distance of only 0.5 mm (Wild reflector GDR11). The alignment of a centrally supported reflector is therefore not critical at all with regard to the distance measurement. See section 4.3241 for additional errors of eccentrically supported prisms and appendix F for technical data of other reflectors.

4.3243 Effect of the Reflector's Alignment on Angular Measurement

The corner of a prism is sometimes used as a target for the measurement of zenith distances and horizontal directions. Because the prism corner is observed through the glass, the ray is refracted at the incident plane of the prism, if the reflector is not exactly aligned. As can be seen from figure 32, the image of C appears in I, which has an offset of II'' from the true direction to the axis of the reflector R.

Considering equations (4.10) and (4.12) of the previous section and inspection of figure 32 lead to

$$II'' = CC'' - CC' \tag{4.17}$$

$$CC' = IC \sin(\alpha_A - \alpha_G)$$

$$= a \sec \alpha_G \sin(\alpha_A - \alpha_G) \tag{4.18}$$

$$CC'' = (a-b) \sin \alpha_A \tag{4.19}$$

The displacement of the ray is then given by:

$$II'' = (a-b) \sin \alpha_A - a \sec \alpha_G \sin(\alpha_A - \alpha_G) \tag{4.20}$$

where the angle of refraction α_G is computed according to equation (4.10):

$$\alpha_G = \arcsin\left(\frac{n_A}{n_G} \sin \alpha_A\right) \tag{4.10}$$

The displacement II'' procudes the following error Δz in a zenith distance measured at the EDM instrument station or $\Delta\alpha$ in a measured direction:

$$\Delta z''(\text{or } \Delta\alpha'') = \frac{11''}{d \sin(1'')}$$

$$= \frac{(a-b) \sin \alpha_A - a \sec \alpha_G \sin (\alpha_A - \alpha_G)}{d \sin(1'')} \qquad (4.21)$$

where α_A is the vertical or horizontal misalignment of the reflector and d the distance between EDM instrument and reflector. A numerical example illustrates the magnitudes of errors in the observed zenith distances or directions. With reference to the AGA reflector (old type), a is taken as 41 mm, b as 35 mm, n_A as 1.00 and n_G as 1.55 (λ = 546 nm).

α_A =	11'' =	$\Delta z(\Delta\alpha)$ for d=50 m	$\Delta z(\Delta\alpha)$ for = 100 m	$\Delta z(\Delta\alpha)$ for 500 m
1°	0.31 mm	0.6''	0.3''	0.1''
3°	0.93 mm	1.8''	0.9''	0.2''
5°	1.54 mm	3.0''	1.5''	0.3''
10°	3.02 mm	6.0''	3.0''	0.6''
15°	4.39 mm	9.3''	4.7''	0.9''
20°	5.59 mm	12.9''	6.5''	1.3''
25°	6.55 mm	17.0''	8.5''	1.7''
30°	7.23 mm	21.5''	10.8''	2.2''

The table above indicates clearly that, for example, the cube corner of a non-tiltable AGA reflector (old type) should not be used as theodolite target if accurate zenith distance observations are required over short ranges. Angular errors caused by the misalignment of other types of reflectors may be computed using equation (4.21). The technical data of some reflectors are given in appendix F.

In order to avoid the problems involved in theodolite pointings to cube corners of reflectors, many reflectors are equipped with additional targets for angular measurements.

4.325 Temperature Effects

The reflectivity of a reflector is only optimal if its entire glass mass has the same temperature. Unequal temperature distribution in the prism causes deformations of the faces and thus divergence of the emerging beam. Prisms need one hour or more to adapt to a new temperature after a change in ambient temperature [59]. Naturally, the larger the prism the longer it will take to settle down in new temperature conditions. If distances at the upper limit of the range of an EDM instrument and its reflectors are attempted, it may be advisable to shade not only the instrument but also the reflector and to expose the reflector to (shade) field temperatures well before the measurement.

4.326 Care of Reflectors

Basically, reflectors should be treated with the same care as theodolites. Wet or dusty surfaces should be cleaned with a soft cloth, avoiding scratching the glass surface. Wet prisms should be allowed to dry before they are stored. Fingerprints on the glass should be avoided, but may be cleaned with a soft cloth dampened with ether or alcohol.

During measurements in rain or snow, the reflector should be protected to avoid water drops on the front surface of the prism. Water drops on the plane of incidence of the prism decrease the reflectivity and thus the range of the EDM instrument. In wet conditions the front surface of the reflector may also be treated with a "antimist" towel or covered with a

thin soap layer to produce a thin layer of water rather than water drops [5].

4.4 Batteries

4.41 Batteries Used in EDM

Three types of batteries are presently used in conjunction with EDM instruments:

(1) general purpose batteries (primary batteries)

(2) Nickel-Cadmium rechargable batteries

(3) Lead-Acid batteries (car batteries).

The first group of primary batteries is not yet widely used in EDM. It may however become more common in future because EDM instruments require less and less power and because they provide the cheapest form of power. Sealed Ni-Cd batteries are at present used almost exclusively as the power supply in EDM because of their low weight and high capacity. Lead-acid batteries are still used in long range EDM where the power requirements are higher. They also provide, in form of car batteries, a reserve power supply for instruments which are usually operated by Ni-Cd batteries. However, a 12V dc input at the EDM instrument is necessary for this purpose.

The Ni-Cd batteries are further discussed in the following section. Details of lead-acid batteries may be found in reference [4].

4.42 Sealed Ni-Cd Batteries

4.421 Construction and Principle

Most EDM instruments employ batteries which are series combinations of individual cyclindrical cells assembled in packs. The individual cells are usually rated at 1.2V dc. They consist of a nickel-plated steel case as the negative terminal and a cell cover a the positive terminal. The positive and negative electrode plates are wound to form a compact roll and are isolated from each other by a porous separator. An electrolyte furnishes the ions for conduction between the positive and negative electrodes. As safety measure, a high-pressure vent is usually incorporated in the button of the cell cover. The construction of a sealed Ni-Cd cell is depicted in figure 33 [44].

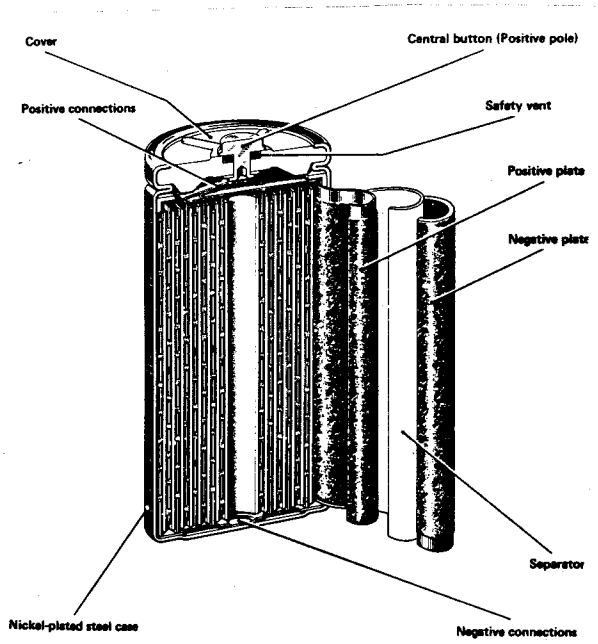

Figure 33: Sealed Ni-Cd Cell (Courtesy of Plessey)

The electrodes in Ni-Cd cells undergo changes in oxidation state without any change in physical state and, because of this, have a long life. Nickel hydroxide is the active material in the positive plate. The changed Nickel hydroxide (NiOOH) is transformed to a lower valence state, namely $Ni(OH)_2$, during discharge. In the negative plate, Cadmium (Cd) metal is the active material and is oxidized to Cadmium hydroxide, $Cd(OH)_2$ during a discharge of the cell. The reactions in the electrolyte (KOH, potassium hydroxide), during charge and discharge may be summarised according to [45] as

$$Cd + 2H_2O + 2\,NiOOH \underset{\text{Charge}}{\overset{\text{Discharge}}{\rightleftharpoons}} 2Ni(OH)_2 + Cd(OH)_2$$

The pressure relief safety vent opens if the internal pressure of the cell, caused by hydrogen and oxygen gases, exceeds 1 to 2 MPa [45].

A note of Caution

Ni-Cd batteries should not be incinerated or mutilated because they may burst or release toxic materials. They should not be short circuited either because this may cause burns. Even a small amount of the electrolyte causes serious problems if it gets in the eye. Immediate flushing with water for 15 minutes and subsequent medical attention is absolutely necessary in this case [45].

4.422 Discharge Characteristics

The discharge characteristics depend on various operation variables such as discharge rate, discharge duration, temperature during the discharge and the previous charge, previous charge rate and time and the previous cycling history.

The capacity of Ni-Cd cells of 1.2V nominal voltage is given in Ah and is based upon a discharge down to 1.0 or 1.1V at a specified discharge rate. At lower drain rates, the actual capacity of a cell will be greater than the rated capacity; at higher drain rates the available capacity will be smaller. The temperature during the discharge as well as during the previous charge also has an effect on the available capacity. Both effects are depicted in figure 34 [45]. The drop in available capacity at low temperatures is considerable. However, the low temperature performance of Ni-Cd batteries is better than that of most other battery types. A decrease in available capacity also occurs at temperatures above 40° to 50° C.

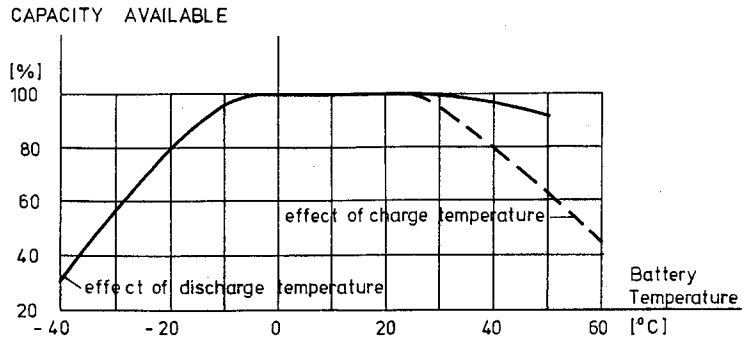

Figure 34

The voltage of Ni-Cd cells remains relatively flat throughout most of the discharge period, with only a 100 mV drop for the rated discharge current. Higher drain rates produce curves of steeper slopes and at lower voltage levels. The discharge voltage is also affected by previous long term overcharging. The effect called *voltage depression* may lead to a 0.1 V smaller

discharge voltage during the entire discharge. One or more discharge/charge cycles will remove the effects of this voltage depression.

A multi-cell battery should never be discharged down to zero voltage because it may cause reverse charging of the lowest capacity cells within the battery, leading to a build-up of pressure in these cells. It is recommended that the discharge should be terminated when the battery voltage reaches a value equivalent to the product (cell voltage) x (n-1) where n is the number of cells in a battery. A ten-cell battery (12V) should therefore not be discharged below 10.8V.

4.423 Charge Characteristics

Four types of charge may be distinguished:

(1) Slow charge (14-16 hours, "overnight") Charge current = 0.1 C

(2) Quick charge (3-7 hours) Charge current = 0.3 C

(3) Rapid charge (15-60 minutes), Charge current = 1.0 C

(4) Ultra-rapid charge (1-3 minutes)

The parameter C is the current in amperes equal to the numerical value of the nominal ampere-hour capacity of the cell. In EDM the technique of overnight charge is usually adopted because overcharging of batteries is not critical at low charge rates of 0.1 C and because charging during field work is usually not possible. A few high rate cells allow overcharging at quick charge rates. Quick, rapid and ultra-rapid charging may be possible with normal Ni-Cd cells but requires a sophisticated charge control to avoid overcharging which would cause excessive temperatures and pressures in the cells.

Nickel-Cadmium batteries should not be charged at temperatures below 5°C unless the charge rate is reduced according to specifications. The batteries can be fully charged at temperatures between 5° and 25°C and partially charged ($\leq$70%) at higher temperatures ($\leq$45°C). Long periods of overcharging should be avoided because they produce the effect of voltage depression, discussed in the previous section, during the next discharge. If batteries are overcharged beyond thier design capability, a permanent loss in capacity will result.

The *charge retention* of Ni-Cd batteries is depicted in figure 35 for new cells [45].

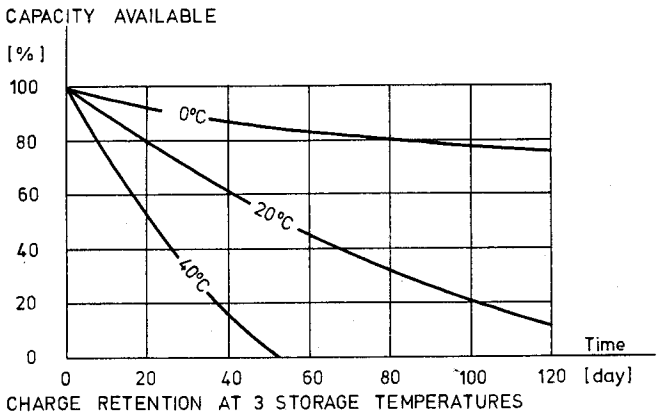

Figure 35.

It is the ability of a stored battery to retain its energy once it has been charged and this is both time and temperature dependent as shown in figure 35. The *self-discharge* may be reduced and the charge retention increased by storing batteries below 20°C. Charged Ni-Cd batteries will

eventually lose all of their charge through this chemical self-discharge which is however in no way harmful either to their life or to their storage characteristics.

The *memory effect* is an almost constant reduction of the discharge voltage level (about 0.1 V) during the discharge period and subsequently a reduction in the stated capacity to a predetermined discharge voltage cut-off point and is developed in the battery from repetitive use patterns. If repeated partial charge and discharge cycles of exact magnitudes are applied, the cell may become so conditioned that it will deliver only slightly more capacity than in the previous repetitive cycles. The memory effect does not occur when the battery is discharged to random end-voltages or overcharged for random amounts of time as is usually the case in EDM applications.

4.424 Capacity and Life of Battery

The capacity rating of a cell is generally stated in terms of ampere-hours and is referred to as an operating variable, indicating the integral of the discharge current - time relationship under certain qualifying conditions, rather than as a rating of total electrical charge capability. The qualifying conditions define the charge current and time, the discharge current and the end-of-discharge voltage after a discharge.

The only way to measure the capacity of a battery accurately is to discharge it while measuring and integrating time and current of discharge. This should be done under the qualifying conditions specified for the battery. The battery is usually discharged at a constant current rate (specified by qualifying conditions) to the cut-off voltage (end-of-discharge voltage) laid down for the battery. The calculation of the ampere-hour capacity is simply obtained by multiplication of time and current.

Two types of loss of capacity may be distinguished:

(1) temporary (reversible) loss

(2) permanent loss.

Temporary loss results from continuous overcharging at high temperatures, programmed cyclic charges and discharges (memory effect) of repetitive nature and other long-term constants in the manner of operation. The full capacity of the battery may be restored by simply discharging the battery completely at a low rate of discharge and recharging it at the 0.1C rate for 20 hours at 25°C [45]. Only one or two of these cycles are generally needed. It is possible to extend the useful battery life by such periodic *reconditioning*.

Permanent loss of capacity may result from an internal short circuit (physical contact of two plates of opposite polarity after decomposition of the separator material) or from an open circuit caused by loss of water in the electrolyte (dry-outs). The life span of a battery to its permanent failure is affected by a large number of factors. The battery temperature is one such factor. Temperatures above room temperature (20-25°C) accelerate the degradation of the separator and seal of a cell. Frequent exposure to high temperatures will therefore shorten the life expectancy, as will charging at very low temperatures. The time element is also very important, both on its own (electrolyte loss) and in conjunction with temperature (separator decomposition). High pressure may cause venting and thus loss of electrolyte. However, only frequent venting will have an effect on the life and performance of a battery. The depth of discharge also has an impact on the life expectancy because the probability of an internal short circuit is greater during a low state of charge than during a partial or full state of charge.

The end of the useful life of a battery is reached when the available capacity is at 50% (General Electric [45]) or 80% (Union Carbide [46]) of its original capacity. It is usually

given in time and/or number of charge/discharge cycles. Plessey [44] state a cycling life for SAFT/VR cells of approximately 500 cycles with 100% depth of discharge and 2000 cycles with 50% depth of discharge. General Electric [45] state a range of life expectancy from 500 cycles to more than 30 000 cycles depending on the conditions of use. The expected life may amount to more than 10 years with regard to the loss of electrolyte through gas diffusion [45]. To achieve the above values the following operating conditions have to exist [44] [45] [46]:

Storage	-40°C to 45° (+65°)
Discharge	(-40) -20°C to +45° (+65°)
Charge	+ 5°C to +45° (+65°) (at 0.1C rate)

Data in brackets refer to specific cells only.

4.5 Major Instrumental Errors and Constants of Electrooptical EDM Instruments

The magnitude of instrumental errors and constants are kept small by the manufacturers and their effects are included in the rated accuracy of a type of instrument. However the main errors and constants of EDM instruments have to be known by the user because the constants have to be verified periodically and errors sometimes exceed the stated accuracy of an instrument.

4.51 Additive Constant

Because the virtual electrooptical origin or zero of an EDM instrument is usually not located on the vertical axis of the instrument, a small correction has to be added to all distance measurements to refer the distance to the instrument's vertical axis. This correction is usually called the additive constant. Zero error is a less favoured term for the same correction. A correction which combines the additive constant of the distance meter and the constant of the corresponding reflector (see section 4.323) is usually determined by the manufacturer and incorporated in the instrument. This built-in correction is usually correct to 1 or 2 mm for instruments with an internal accuracy of ± 5 mm at the time of the factory adjustment.

The remaining additive constant can change with time and should be determined periodically. Some instruments allow the updating of the internal constant by the user, however, most do not. In the latter case, the additive constant must be applied during the computation of the reduced distance.

4.52 Cyclic Errors

Two types of cyclic errors may be distinguished, according to Kahmen [35], with respect to their dependency on the return signal strength.

4.521 Cyclic Error, Dependent on the Return Signal Strength

This cyclic error is caused by electrical coupling between the reference signal and the measurement signal and by optical crosstalk between the transmitter and receiver optics in electrooptical distance meters. It occurs in all distance meters to a greater or lesser degree, and is independent of the type of phase measuring system. The manufacturers reduce the amplitude of cyclic errors by rigorous electrical shielding of transmitter and receiver, separation of optical channels, special anti-reflex coating of common optical parts and/or electronic compensation. The amplitude of cyclic errors in short-range instruments with ± 5 mm internal accuracy is usually smaller than 5 mm. [48] [74]

The effect of electrical or optical crosstalk may be explained by a mathematical model. Considering equation (2.5a) and equation (2.7a,b) the reference signal y_1 and the return signal y_2 may be written as

$$y_1 = A_1 \sin(\omega t) \tag{4.22}$$

$$y_2 = A_2 \sin(\omega t + \Delta\Phi) \tag{4.23}$$

A component y_3 of the reference signal y_1 is superimposed on the return signal y_2. The contaminating signal y_3 has the same phase and frequency as the reference signal, but a much smaller amplitude:

$$y_3 = A_3 \sin(\omega t) \tag{4.24}$$

where $A_3 << A_1$. The superimposed return signal in the receiver channel then becomes

$$\begin{aligned} y &= y_2 + y_3 \\ &= A_3 \sin(\omega t) + A_2 \sin(\omega t + \Delta\Phi) \end{aligned} \tag{4.25}$$

Because two waves of equal frequency are superimposed, the resulting wave has the same frequency but different phase and amplitude

$$y = A \sin(\omega t + \psi) \tag{4.26}$$

Under the condition of $A_3 << A_2$, equation (4.26) may be written as

$$y = (A_2 + A_3 \cos\Delta\Phi) \sin\{\omega t + (\Delta\Phi - \frac{A_3}{A_2} \sin\Delta\Phi)\} \tag{4.27}$$

Because electrooptical EDM instruments are based on the measurement of phase differences, only the last term of equation (4.27) is important:

$$\Delta\Phi' = \Delta\Phi - \frac{A_3}{A_2} \sin\Delta\Phi \tag{4.28}$$

where $\Delta\Phi'$ is the time lag of the contaminated return signal. Using the terms unit length U and fraction of unit length L, equation (2.15b) of section 2.221 yields

$$L' = L - \frac{A_3}{A_2} \left(\frac{U}{2\pi}\right) \sin\left(\frac{2\pi L}{U}\right) \tag{4.29}$$

where L' = measured fraction of unit length of the contaminated return signal

L = fraction of unit length of return signal

U = unit length of EDM instrument

A_2 = amplitude of the return signal

A_3 = amplitude of the contaminating part of the reference signal.

The second term in equation (4.29) is called the cyclic error because it is mainly a function of the fraction of the unit length and thus repeats itself every U metres. The cyclic error is however also a function of the return signal strength A_2 which decreases with increasing distance. It increases with distance. Assuming a unit length U of 10 m and an amplitude of the contaminating signal $A_3 = 0.003\ A_2$ the amplitude of the cyclic error will be

$$\frac{A_3}{A_2} \left(\frac{U}{2\pi}\right) = 0.003 \left(\frac{10\ m}{2\pi}\right) = 4.8\ mm \tag{4.30}$$

4.522 Cyclic Error, Dependent on the Analogue Phase Measurement System

Instruments which use a resolver in the phase measurement may display another cyclic and sinusoidal error with two full wave lengths within one unit length of the instrument (see section 2.3132 and Kahmen [35]). Analogue phase measuring systems other than resolvers may display non-sinusoidal cyclic errors within a unit length of the instrument. The Hewlett-Packard HP 3800B belongs to this category of instrument, for example. The amplitudes of cyclic errors produced by the analogue phase measurement are constant and thus independent of distance.

4.53 Scale Errors

Scale errors in EDM are caused for the most part by frequency errors in the modulation frequencies. The magnitudes of and reasons for frequency errors have been discussed in section 2.311 (oscillator). Scale errors however are also produced by a limited environmental correction setability (see section 4.141), an error in the given carrier wavelength (section 2.43) and errors in measured temperature, pressure and humidity (sections 2.44, 2.45 and 2.474).

4.54 Phase Inhomogeneities of Emitting and Photo Diodes

Phase inhomogeneities are a property of emitting and photo diodes (see sections 2.3121 and 2.3122) and lead to unequal phase information in a plane perpendicular to the radiation axis. The phase inhomogeneities cause non-cyclic and non-linear errors dependent on distance because the reflector returns a decreasing part of the total radiation cone with increasing distance. The resulting errors are called *non-cyclic errors* and are plotted as a function of distance. They are naturally dependent on the shape, size and number of reflectors used and usually determined with the additive constant of an EDM instrument [35] [47] [48]. Poor pointing of the EDM instrument to the reflector (either electronically or optically) leads to additional errors due to phase inhomogeneities because edge rays may be reflected instead of centre rays of the radiation cone.

Phase inhomogeneities may be easily checked by deliberate mispointings in steps of several minutes of arc, to the left, to the right, upwards and downwards (horizontal and vertical scans). The resulting distance measurements may be plotted in so-called *error pointing diagrams* [35] [47] [48].

4.6 Calibration and Standardization

In this text calibration is defined as the determination of instrumental constants and standardization as the determination of the scale of an instrument. Every instrument should be calibrated at regular intervals e.g. fortnightly in the first months after purchase and once per month or two months thereafter. Calibration should also be executed after any maintenance work on the EDM instrument. It is advisable to keep a file for all calibration measurements of every instrument to monitor the variability of all instrumental constants and errors, and to always use the same standard observation program for the determination of constants.

4.61 Determination of the Additive Constant

The only reliable methods of additive constant determination are methods which use a large number of redundant observations over a large range of distances. The standard approach is to use distance measurements in all combinations on baselines of between 6 and 8 stations. The maximum distance should correspond to the maximum range of the EDM instrument to one prism under fair atmospheric conditions [49]. The spacing of the baseline stations should be multiples of the unit length of the instrument, in order to eliminate or at least reduce the effects of cyclic errors [49] [50]. Formulae for the geometric design of EDM baselines are given in Appendix H.

Several methods are available for the computation of the additive constant. They depend on the availability of highly accurate known baseline distances and of computing facilities. The table below gives a summary of different solutions. A more detailed description is given by Rueger [49].

	Baseline of Known Length	Baseline of Unknown Length
Computation with Pocket Calculator	Method: Linear Regression (=least square adjustment) for example: standard pocket calculator programs. Unknowns: - additive constant - scale factor	Method: Least square adjustment (equal weight for all observations), for example: Halmos/Kadar Method [49]. Unknowns: Additive constant + (N-1) baseline distances (N=number of stations on baseline)
Computation with desk-top or large computer	Method: Least square adjustment, with correct weighting of observations. Unknowns: - additive constant - scale factor	Method: Least square adjustment with correct weighting of observations. Unknowns: - additive constant - (N-1) baseline distances

The residuals and the standard deviation of the additive constant should be computed in all four cases. The residuals are plotted against distance and lead to the diagram of *non-cyclic errors* [49]. It has been reported that correct weighting of observations yields more consistent additive constants in repeated determinations [51].

4.62 Determination of the Cyclic Error Correction

Cyclic errors need to be determined over one unit length of an instrument (see sections 4.521 and 4.522). A test line for cyclic errors can be easily established according to figure 36 [49].

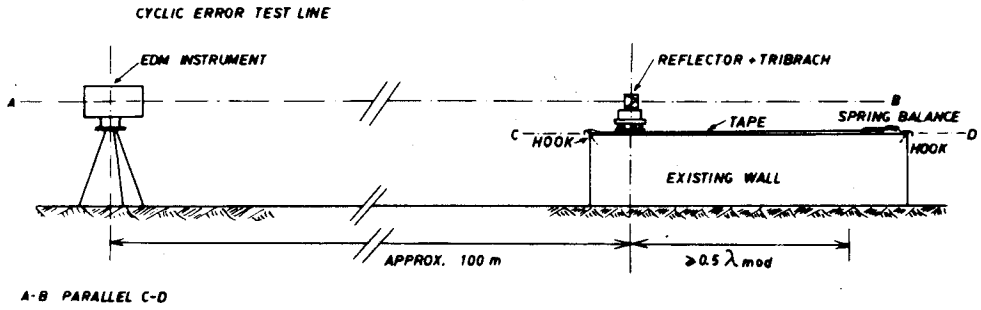

Figure 36.

A low wall with a more or less horizontal top surface, such that it is possible to set up the EDM instrument on line at a distance of say 100 m, is selected [52]. A steel tape (graduated to 1 cm) is fixed temporarily at standard tension so that it is fully supported on top of this wall. The reflector in its tribrach is then moved along the tape at exact intervals of for example 1 m or 0.5 m or 0.25 m (according to the required precision and unit length of the instrument) over a total distance equivalent to one unit length of the EDM instrument in use. If the instrument's line of sight to the reflector is parallel to the top surface of the wall, no slope corrections have to be applied. Corrections for

temperature and pressure need not be taken into account, providing the conditions remain unchanged over the short time period of the test measurements.

The reductions are made according to the table below and the resulting s* values are subsequently plotted as a function of distance as shown in figure 37 (unit length in this example is 10 m).

Tape mark	s	Subtract	s*
1 m	100.032 m	0 m	100.032 m
2 m	101.032 m	1 m	.032 m
3 m	102.026 m	2 m	.026 m
4 m	103.022 m	3 m	.022 m
5 m	104.018 m	4 m	.018 m
6 m	105.016 m	5 m	.016 m
7 m	106.016 m	6 m	.016 m
8 m	107.020 m	7 m	.020 m
9 m	108.026 m	8 m	.026 m
10 m	109.030 m	9 m	.030 m
		Mean s* =	100.0238m

s = observed distance

s* = observed distance, reduced to first observed tape mark.

In figure 37, s* is plotted as a function of s and the mean of s* is drawn as a line. A sine curve of 10 m wavelength (unit length in this example) with its axis as s* mean is now fitted to the data. The correction to the original additive constant dc for a given s being an exact multiple of the unit length (here 10 m) is obtained as the difference, in ordinate s*, between the estimated sine curve of the cyclic error and s* mean. The correction dc is taken as positive if the curve for this abscissa is above the line of s* mean and negative if the curve at this point is below s* mean. In this example (see figure 37), dc is equal to +8 mm for s = 100 m or for s = 110 m (multiple of unit length = 10 m). Together with the additive constant c determined according to section 4.61 the total additive constant c_{tot} then yields

$$c_{tot} = c + dc \qquad (4.31)$$

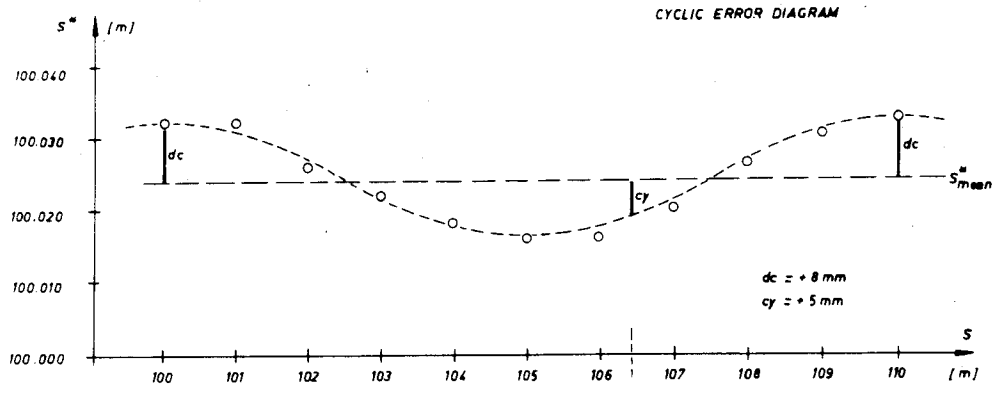

Figure 37.

The total additive constant c_{tot} would now be applied to all distances measured subsequently, as would corrections for the cyclic error c_y. The c_y are derived from figure 37 as well. c_y is defined as the interval between the estimated cyclic error curve and s^* mean for a certain fraction of the unit length. c_y is taken positive if the curve is below s^* mean and negative if the curve is above the s^* mean line.

The full correction of a measured distance would then be

$$s_{corr} = s + c_{tot} + c_y \tag{4.32}$$

Although corrections for cyclic error may be applied to all field observations, it is much more convenient to have the cyclic error eliminated by the manufacturer. Fortunately, as shown by many publications, most modern EDM instruments will only have cyclic errors of small amplitudes (0 - 10 mm). Cyclic errors of amplitudes well below the level of the stated precision of an instrument may be ignored. Since larger cyclic errors do sometimes occur [48], and because cyclic errors may change their amplitude and phase with time, the determination of cyclic errors must be included in periodic calibrations of EDM instruments. The reliability of the determination of the cyclic error may be increased by moving the reflector in shorter steps and by replacing the graphical interpretation by a rigorous least square adjustment [53] [65].

4.63 Standardization

There are two completely different ways of standardizing an EDM instrument, namely, measuring frequencies or determining a scale factor from a baseline of known length. The measurement of frequencies is also the more precise way of standardizing instruments as no instrumental errors or errors in reductions affect the result. The only problem arising is that calibrated frequency counters, sufficiently accurate for EDM standardization, are normally not available to surveyors. If frequencies are measured they should be measured with the EDM instrument at different temperatures, in order to get information about the drift of the frequency with temperature. If the *actual frequency* (f_{act}) shows any significant deviation from the *nominal frequency* (f_{nom}) for which the instrument is designed, the measured distance (s_{meas}) can be corrected by the formulae

$$s_{corr} = \frac{f_{nom}}{f_{act}} s_{meas} \tag{4.33}$$

or

$$s_{corr} = s_{meas} + \left(\frac{f_{nom} - f_{act}}{f_{act}}\right) s_{meas} \tag{4.34}$$

where s_{corr} is the distance corrected for scale errors. Information as to where and how frequencies should be measured on a specific instrument can be obtained from the manufacturer. Some EDM instruments even have a built-in frequency output [48] so that the instruments need not be opened. Frequency tests are described in [68] [69].

Example: f_{act} = 14 985 412.0 Hz (HP 3800 S/N 1141A00110 on 6th October 1976, at 20°C, after 60 minutes continuous operation)

f_{nom} = 14 985 453.0 Hz

Using equations (4.33) and (4.34) yields

$$s_{corr} = 1.000\ 002\ 736\ s_{meas}$$

and

$$s_{corr} = s_{meas} + 2.736 \times 10^{-6} s_{meas}$$

Another method of testing the scale of an EDM instrument is by comparison with known distances in conjunction with a determination of the additive constant on a baseline of known length. To get the known distances, the baseline must be measured by either invar taping, observations with an interferometer or by a precision EDM instrument. All these methods of obtaining accurate values for the baseline are expensive especially as these accurate values must be updated at regular intervals. More details on this method are given in [49] [64] [67].

Finally it should be mentioned that scale errors may not be as critical as they may appear from the above comments, especially in Integrated Surveys. Consider, for example, traverses between two control stations of a state survey not occupying more than one day. It may be assumed that the scale of the EDM instrument will be fairly constant during the period of observation. The Bowditch adjustment of the traverse will automatically adjust the actual mean scale of the EDM instrument to the grid scale defined by the two control points and their coordinates. Naturally, a large scale error in the EDM instrument (or errors in the coordinates of the two control points) will increase the misclosures. This leads to another reason for the periodic standardization of EDM instruments, since survey regulations generally specify maximum misclosures. With respect to traverses it should be further noted that other systematic errors, e.g. additive constant and cyclic error are not eliminated by the usual Bowditch adjustment and may cause systematic errors in the coordinates of traverse points if not accounted for.

5. Microwave Instruments

5.1 Introduction

Microwave instruments, like optical instruments, measure along the shortest path between the two instruments and therefore need intervisibility between the stations. (It is however possible to measure long distances a few metres above the sea without the requirement of intervisibility). Several carrier wavelengths have been used in microwave EDM, 8 mm (Q band), 30 mm (X band) and 100 mm (S band). S band instruments display very large ground swing effects, while Q band instruments have less power to penetrate haze and cloud and therefore have a reduced range. For these reasons X band instruments have proved to be the most popular.

Microwave instruments are mainly used for the measurement of long distances, up to 150 km, although their all-weather capability may justify even medium or short range applications. The accuracy of microwave distances is mainly dependent on the accuracy of the refractive index. With measurement of atmospherical parameters at the terminals only, an accuracy of 2-3 ppm may be expected. Higher accuracies may be achieved by using better atmospheric models (see sections 2.48 and 3.13).

The basic working principle of microwave instruments has been given in section 2.32. The reader may refer to the literature for a more detailed discussion of such instruments [4] [6] [7] [17] [35]. The main technical data of a few instruments are listed in table 3 of appendix D.

5.2 Effects of Reflections in Microwave EDM

Because microwave instruments have a much larger beam divergence than optical instruments (see table 3 of appendix D), certain parts of the beam may reach the ground or other reflecting surfaces and may be reflected there. The reflected wave travels a longer distance and, being received with the direct wave, has an effect on the measurement of the distance. The effect is usually called *ground swing*. The amplitude of the ground swing is dependent on the reflectivity of the specific ground surface. Water, snow and street surfaces may be highly reflective [54].

The effect has been expressed in mathematical terms by Poder [4] and Küpfer [54]. Ground swing is mainly a function of the excess path length, the reflectivity of the reflecting surface, the modulation frequency and the carrier frequency. The last two parameters can be chosen by the designer of such instruments, and this has led to two different instrumental designs for the reduction of ground swing:

(1) One such design involves the measurement of a distance with up to 20 slightly different *carrier* wavelengths. The resulting distances may then exhibit slight variations, which may be plotted. If a sine curve eventuates, the mean may be taken and this will be free from ground swing effects. For very large and small (< 1.3 m) excess path lengths however, no full "swing" curve is obtained and the mean is hard to estimate [54]. Different carrier waves are, for example, used in the Tellurometers MRA-5 and CA1000. (See table 3 of appendix D).

(2) Another method of reducing ground swing is the use of higher modulation frequencies. This method was adopted in the Siemens-Albis MD60 (equivalent to the former Wild DI60), where a modulation frequency of 150 MHz (unit length = 1 m) is employed [55] and to a lesser extent in the Tellurometer MRA-5 [35].

Ground swing may be further reduced by setting up instruments in positions where the reflected beam is prevented from reaching the antenna by a hump in front of the instrument or by ensuring that the beam cone never reaches any reflecting surfaces (peak to peak, tower to tower) [17]. On flat ground, the effect may be reduced by setting-up very close to the ground [35], or by

variation of the height of instrument. Küpfer has derived formulae indicating the necessary variation of the height of instrument in order to obtain a full period of the ground swing for various excess path lengths and distances ([54], p.339, figure 16).

5.3 Instrumental Constants and Errors of Microwave Instruments

The instrumental errors of microwave instruments are basically the same as those of electrooptical instruments:

(1) additive constant

(2) cyclic error

(3) scale error

They may be determined in the same way. The test lines however should be chosen in such a way that no lateral or ground reflections falsify the results. Küpfer has investigated the reflection problems involved in the determination of the additive constant and has given a solution in reference [54]. Cyclic errors in older instruments have been quite large (up to 100 mm [7]).

APPENDIX A

First Velocity Correction Chart for HP 3800B and HP 3805A

The formula on which this chart is based has been given in section 3.111, A constant term of + 0.4 ppm for humidity is included.

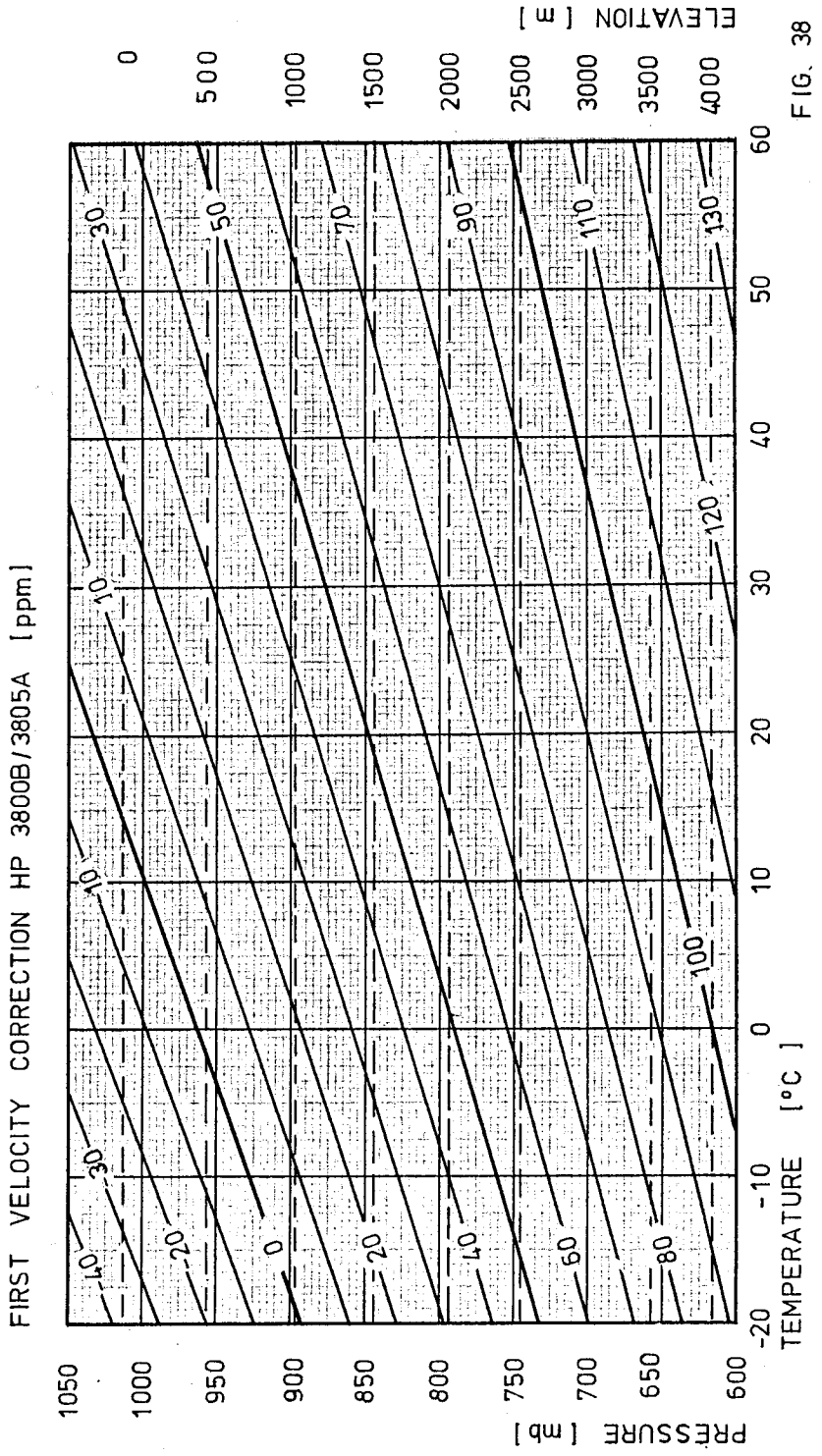

FIG. 38

APPENDIX B

First Velocity Correction Nomogram for AGA Geodimeter Model 6A

The nomogram is based on equation (3.13) in section 3.113 and includes an average correction of - 0.6 ppm for humidity. To determine the first velocity correction in parts per million (ppm) on the centre scale of figure 39, a rule is placed so that it intersects the temperature and the pressure scale at the values of measured temperature and pressure. [5]

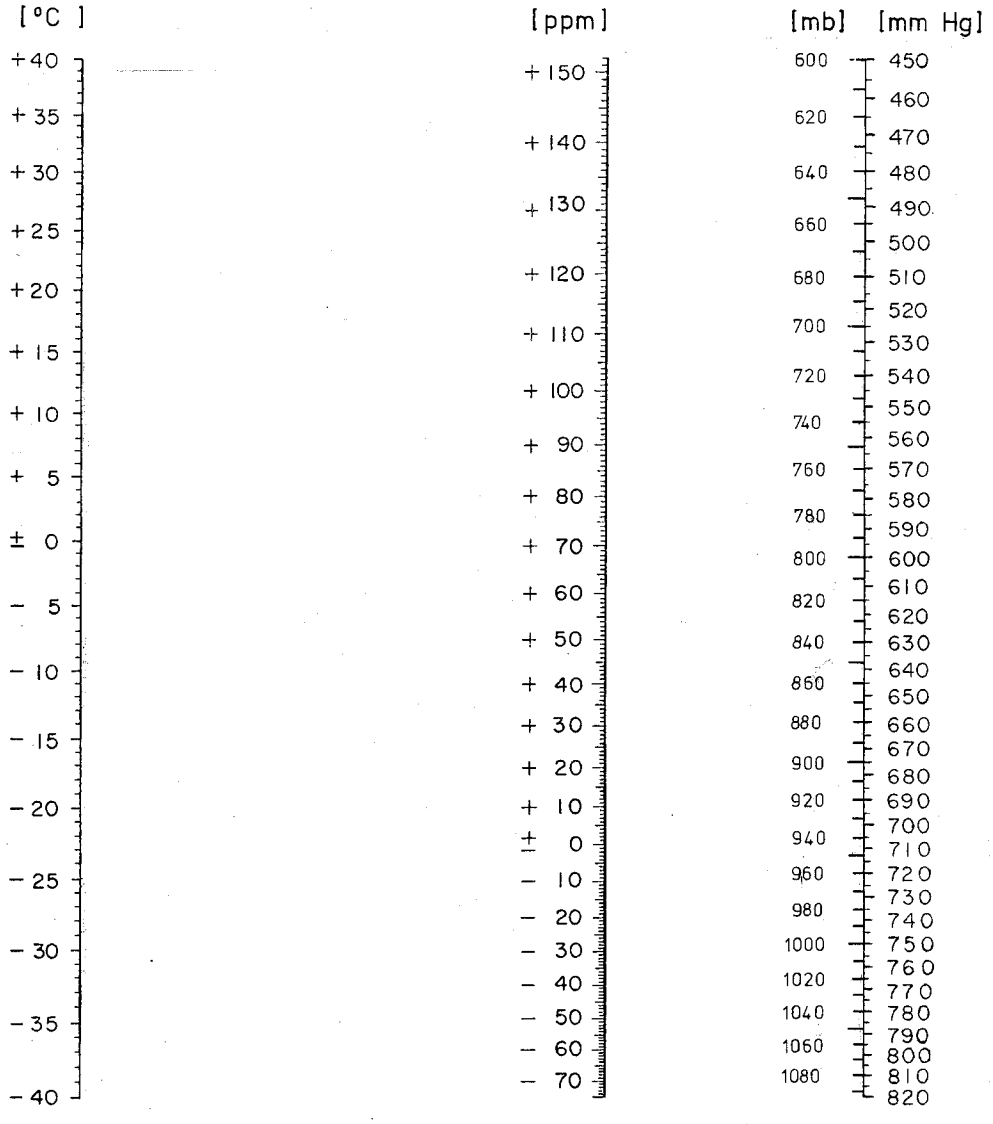

FIG. 39

APPENDIX C

Computation of Distance from Geodimeter 6 A Measurements

It was explained in section 2.2213 that the Geodimeter 6 A measurements are based on three main unit lengths, namely

$$U_1 = 5.000\ 000 \text{ m}$$

$$U_2 = 4.987\ 532 \text{ m}$$

$$U_3 = 4.761\ 905 \text{ m}$$

Because fine measurements are obtained with all three unit lengths the unknown distance may be computed independently three times:

$$d = m_1 U_1 + L_1 \qquad (2.17a)$$

$$d = m_2 U_2 + L_2 \qquad (2.17b)$$

$$d = m_3 U_3 + L_3 \qquad (2.17c)$$

where m_1, m_2 and m_3 are unknown integers and L_1, L_2 and L_3 the measured fractions of the unit lengths U_1, U_2 and U_3 respectively. The unit lengths are related as follows

$$400\ U_1 = 401\ U_2 = 2000 \text{ m} \qquad (2.18a)$$

$$20\ U_1 = 21\ U_3 = 100 \text{ m} \qquad (2.18b)$$

The result of equations (2.18) is that the differences $A = (L_2 - L_1)$ and $B = (L_3 - L_1)$ display a linear rise from zero to five with an increase in distance. Equal values of $A = (L_2 - L_1)$ occur with a period of 2000 metre and equal values of $B = (L_3 - L_1)$ with a period of 100 m. Further, numbers m_1 and m_2 are equal in the range 0-2000 metres and m_1 and m_2 are equal within 0-100 metres, which leads to

$$m_2 = m_1 + x \qquad (2.19a)$$

$$m_3 = m_1 + y \qquad (2.19b)$$

where x is the number of full 2000 metre intervals (known from other sources) and y is the number of full 100 metre intervals in the distance d. The parameter y will be derived from solving equations (2.17a) and (2.17b).

Prior to the use of the equation group (2.17) for the computation of the distance, the unknown numbers m_1, m_2 and m_3 must be determined. This step corresponds to a "coarse" measurement with other instruments.

From equations (2.17a), (2.17b) and (2.19a) follows

$$\begin{aligned} m_1U_1 + L_1 &= m_2U_2 + L_2 \\ &= (m_1 + x)U_2 + L_2 \\ m_1U_1 - m_1U_2 &= L_2 - L_1 + xU_2 \\ m_1 &= \frac{L_2 - L_1 + xU_2}{U_1 - U_2} \end{aligned}$$

Substituting equation (2.18a) leads to

$$m_1 = \frac{(L_2 - L_1) + x \frac{400}{401} U_1}{U_1 - \frac{400}{401} U_1}$$

$$m_1 = \frac{401(L_2 - L_1) + 400\, U_1 x}{401\, U_1 - 400\, U_1}$$

$$m_1 = 401 \frac{L_2 - L_1}{U_1} + 400\, x \qquad (2.20a)$$

Substitution of (2.20a) in (2.17a) and considering $U_1 = 5$ m exactly yields

$$d = L_1 + 401(L_2 - L_1) + 2000\, x \qquad (2.21a)$$

The second term of the above equation, namely $401(L_2 - L_1)$ or 401A, must be an integer according to (2.17a). Due to the limited accuracy in the measurement of L_2, L_1 and the large multiplication factor (401), the term 401A will not always give the correct answer for m_1. It is therefore only used to determine y* multiples of 100 m within the 2000 m interval of distance d. (The total number of y multiples of 100 m in the distance d is therefore derived from the sum of y* multiples of 100 m, and x multiples of 2000 m). For a higher resolution, a second computation has to follow using equations (2.17a), (2.17c) and (2.19b).

$$m_1 U_1 + L_1 = m_3 U_3 + L_3$$

$$= (m_1 + y) U_3 + L_3$$

$$m_1 U_1 - m_1 U_3 = (L_3 - L_1) + y U_3$$

$$m_1 = \frac{L_3 - L_1 + yU_3}{U_1 - U_3}$$

Considering equation (2.18b), the integer m_1 yields

$$m_1 = \frac{(L_3 - L_1) + \frac{20}{21} U_1 y}{U_1 - \frac{20}{21} U_1}$$

$$= 21 \frac{(L_3 - L_1)}{U_1} + 20\, y \qquad (2.20b)$$

Inserting equation (2.20b) into equation (2.17a) leads to

$$d = L_1 + 21(L_3 - L_1) + 20\, U_1\, y$$

and, considering $U_1 = 5$ m exactly, also to

$$d = L_1 + 21(L_3 - L_1) + 100\, y \qquad (2.21b)$$

The term $21(L_3 - L_1)$ or 21B must be an integer (as the term 401A before) and gives the number of z multiples of the basic unit length U_1 up to 100 metres. The number of y multiples of 100 m are obtained from equation (2.21a); it is derived from the sum of y* multiples of 100 m (within a 2000 m interval) and of x multiples of 2000 m.

The distance may now be computed from the first distance equation

$$d = m_1 U_1 + L_1$$
$$= 2000\,x + 100y^* + 5z + L_1 \qquad (2.22a)$$

where z is the number of 5 m intervals in d. The term $5z$ corresponds to the term $21(L_3 - L_1) = 21B$, rounded to the nearest multiple of 5 metres. The term $100\,y^*$ is obtained from

$$100y^* = 401(L_2 - L_1) - 21(L_3 - L_1)$$
$$= 401A - 21B$$

which has to be rounded to the nearest multiple of 100 m.

Example: Measured: $L_1 = 1.789$ Given: $x = 2$

$L_2 = 5.851$

$L_3 = 3.184$

$$d = 2000\,x + 100y^* + 5z + L_1$$
$$21B = 21(L_3 - L_1)$$
$$= (3.184 - 1.789)21$$
$$21B = 29.295 \text{ m}$$

Considering $21B = U_1 z$, the term $5z$ yields 30 m.

$$401A = 401(L_2 - L_1)$$
$$= 401(5.851 - 1.789)$$
$$= 1628.082$$
$$401A - 21B = 1628 - 29$$
$$= 1599 \text{ m}$$

Refering to $100y^* = 401A\text{-}21B$, the term $100y^*$ becomes 1600 m.

$$d = 4000 + 1600 + 30 + 1.789$$
$$= 5631.789 \text{ m}$$

The distance also can be computed on the bases of equations (2.17b) and (2.17c), using the unit lengths U_2 and U_3. This is usually done and the mean of the three values of d is taken for the final distance value.

Substituting equations (2.18a) and (2.19a) in equation (2.17b) leads to

$$d = (m_1 + x)\,\frac{400}{401}\,U_1 + L_2$$

With (2.20a)

$$d = \left(401\,\frac{(L_2 - L_1)}{U_1} + 400\,x + x\right)\frac{400}{401}\,U_1 + L_2$$
$$= 400(L_2 - L_1) + 400\,U_1 x + L_2$$

Using for U_1 the value 5 m and substituting the rounded value $(100y^* + 5z)$ for $401(L_2 - L_1)$, the second distance equation yields

$$(L_2 - L_1) = \frac{(100y^* + 5z)}{401}$$

$$d = \frac{400}{401}(100y^* + 5z) + 1000x + L_2$$

$$= 0.997506234\ (100y^* + 5z) + 2000x + L_2$$

$$= L_2 - 0.002493766\ (100y^* + 5z) + 100y^* + 5z + 2000x$$

$$= L_2 - 0.002493766\ (100y^* + 5z) + 5z + 100y^* + 2000x \qquad (2.22b)$$

Similarly, by substituting equations (2.18b) and (2.19b) into equation (2.17c)

$$d = (m_1 + y)\frac{20}{21}\ U_1 + L_3$$

and considering equation (2.20b), the last of the three distance equations may be written

$$d = (21\frac{(L_3 - L_1)}{U_1} + 20y + y)\frac{20}{21}\ U_1 + L_3$$

$$= 20(L_3 - L_1) + 20\ U_1 y + L_3$$

Replacing U_1 by 5 m and the rounded value $5z$ by $21B = 21(L_3 - L_1)$ leads to

$$d = \frac{20}{21}(5z) + 100y + L_3$$

$$= L_3 + 0.952380952(5z) + 100y$$

and, with replacing $(100y)$ by $(100y^* + 2000x)$, the final form of the third distance equation yields

$$d = L_3 - 0.047619048(5z) + 5z + 100y^* + 2000x \qquad (2.22c)$$

The usual format of Geodimeter field notes uses a slightly different notation. The following relations exist:

$P = 2000\ x$ $\qquad$ $K_2 = 0.002493766\ (100y^* + 5z)$

$E = 100\ y^*$ $\qquad$ $K_3 = 0.047619048\ (5z)$

$F = 5\ z$

$D = E + F = 5z + 100y^*$

Refering to the previous example, we can now compute d from equations (2.22b) and (2.22c).

Using equation (2.22b) yields

$$d = 5.851 - 0.002493766(1600 + 30) + 30 + 1600 + 4000$$

$$d = 5.851 - 4.065 + 30 + 1600 + 4000$$

$$d = 5631.786\ m$$

and using equation (2.23b)

$$d = 3.184 - 0.047619048(30) + 30 + 1600 + 4000$$

$$d = 5631.755\ m$$

The mean distance $\bar{d}$ therefore would be: $\bar{d} = 5631.777\ m$

APPENDIX D

TABLE 1: Technical Data of a Selection of Short Range EDM Instruments

Manufacturer	Model	Range with 1 prism m	Range with 3 prisms m	Radiation Source	Carrier Wave Length nm	Unit length m	Stand. Dev. mm + ppm		Weight Instr. kg	Weight Battery kg	Power Cons. W	Battery Volt V	Battery Cap Ah	Beam Div. '	Angular Accuracy Hor.	Angular Accuracy Vert.
AGA Geotronics	Geodimeter 710	1700	3500	Laser	632.8	5	5	1	(14.2)	10.9	100	12	60	0.7-35	±2''	±3''
Sweden	Geodimeter 10	700	1400	Diode	910	10	5	10	2.8	4.0	17	6	15	8.5		
	Geodimeter 12A	1000	2000	Diode	910	10	5	5	2.8	4.0	17	6	15	8.5		
	Geodimeter 14	4000	6000	Diode	910	10	5 (5-30)	10 (3)	2.8	4.0	17	6	15	8.5		
Hewlett-Packard USA	HP3805A	500	1600	Diode	910	10	7	10	10.4	1.0	14	12	2	3.0		
	HP3810A	500	1600	Diode	910	10	5	10	11.9	1.0	18	12	2	3.0	±20''	±30''
	HP3820A	1000	3000	Diode	830	10	5	5	10.7	-	(1.5)	3.6		3.0	±2''	±4''
Kern	DM 500	300	500	Diode	875	10	5	5	1.6	2.8		5	10	4		
Switzerland	DM 501	1000	1600	Diode	900	10	5	5	1.6	2.8		5	10	4		
	ME 3000	1500	2500	XENON Lamp	480	0.3	0.2	1	18.7	8.8	18	12	10			
Keuffel & Esser USA	Autoranger	700	1600	Diode	910	10	5	6	2.4	0.9	10.5	12	1.8	8		
Precision	Beetle 500S	300	500	Diode	910	10	10	-	2.7	2.3	17	12	4	8		
International	Beetle 1000S	500	1000	Diode	910	10	10	-	2.7	2.3	17	12	4	8		
USA	Beetle 1600S	700	1600	Diode	910	10	10	-	2.7	2.3	17	12	4	8		
Tellurometer	MA 100		1000	Diode	930	1	1.5	1	17		18	12		15'		
Plessey UK	CD 6	800	1500	Diode	930	10	5	5	3.7		15	12		20'		
Wild	DI 3	400	600	Diode	875	20	5	5	1.8 5.2 (2.0 4.3	3.0 (2.3 3.0	14	12 (12 12	7 (1.8 7.0	5'		
Switzerland	DI 3S	1000	1600	Diode	885	20	5	5			17					
Zeiss	Eldi 1	2000	2500	Diode	910	10	5-10	2	8	0.4	5	9	1.8	2'		
West Germany	Eldi 2	700	1000	Diode	910	10	5	2	4.2	0.4	5	9	1.8	4'		
	Eldi 3	400	700	Diode	910	10	5-10	2	3.8	0.4	5	9	1.8	4'		
	SM 4	700	1000	Diode	910	10	5-10	2	7.8	0.4	5	9	1.8	4'	±3''	±3''
	Reg Elta 14	500	800	Diode	910	10	5-10	-	25	2.5	14	12	6	2'	±3''	±5''

APPENDIX D

TABLE 1(CONTD.): Technical Data of a Selection of Short Range EDM Instruments

Manufacturer	Model	Range with 1 prism m	Range with 3 prisms m	Radiation Source	Carrier Wave Length nm	Unit length m	Stand. Dev. mm + ppm		Weight Instr. kg	Weight Battery kg	Power Cons. W	Battery Volt V	Battery Cap Ah	Beam Div. '	Angular Accuracy Hor.	Angular Accuracy Vert.
AGA Geotronics Sweden	Geodimeter 120	1000	2000	Diode	910	10	5	7	2.6	1.0		12	2	8.6	-	±1'
	Geodimeter 6A		< 5000	Tungsten Lamp	550	5	5	1	16.3	-	30	12	-	V 7.0 H 1.0	-	-
Hewlett-Packard U.S.A.	HP 3800B	1500	2500	Diode	910	10	5	7	7.7	6.0	12	12	8	3.5	-	-
	HP 3808A	3000	6000	Diode	840	10	5	1	9.2	1.0	16	12	2.0	2.0	-	-
Keuffel & Esser U.S.A.	Autoranger S	1600	3200	Diode	865	10	5	6	2.4	0.9	10.5	12	2.5	3.5	-	-
	Autoranger II	1600	3200	Diode	865	10	5	6	3.1		10.5	12	1.5	3.5	-	-
	Vectron	-	-	-	-	-	-	-	6.8	3.0	10.0	12	(2.5 / 6.0)	-	±3"	±3"
Sokkisha Japan	SDM - 1C	1000	1600	Diode	910	10	5	5	2.8	1.5	15	5	3.5	4.0	-	-
	RED - 1 (=SDM-1D)	1300	2000	Diode	830	10	5	5	3.5		<12	12	1.0	3.0	-	-
Topcon Japan	DM - C2	1400	2000	Diode	820	10	5	5	2.8	0.7	7	8.4	1.8	7	-	-
Wild Switzerland	TC 1 (Tachymat)	(700 / 1000)	(1000 / 1600)	Diode	885	30.7692	(5 / 5-15)	5 / 5	9.8	3.0	16	12	7.0	6.0	±2"	±3"
Zeiss	Elta 4	(700 / 1000	(1200 / 1600	Diode	910	10	(5 / 10	2 / 2	6.5		5	9	1.8	1.2	±3"	±3"
Fed. Rep. Germ.	Elta 2	1200	(1600 / 2000	Diode	910	10	(5 / 10	2 / 2	12.0		7	9	1.8	1.0	±0.6"	±0.6"

APPENDIX D

TABLE 1 (CONTD.): Technical Data of a Selection of (Short Range)EDM Instruments

Manufacturer	Model	Range with 1 Prism m	Range with 3 Prisms m	Radiation Source	Carrier Wavelength nm	Unit Length m	Stand. Dev. mm + ppm		Weight Instr. kg	Weight Battery kg	Power Cons. W	Battery Volt V	Battery Cap Ah	Beam Div. "	Angular Accuracy Hor.	Angular Accuracy Vert.
AGA Geotronics Sweden	Geodimeter 14A	6000	8000	Diode	910	10	5-15	3	2.5	1.0	20	6	4	2.5	-	-
	Geodimeter 110	1400	2100	Diode	910	10	5	5	2.5	1.0	10	12	2	2.5	-	-
	Geodimeter 112	2000	3100	Diode	910	10	5	3	2.5	1.0	10	12	2	2.5	-	-
	Geodimeter 116	1000	1400	Diode	910	10	5	5	2.6	1.0	10	12	2	2.5	-	(±1")
Hewlett-Packard U.S.A.	HP 3810B	2000	5000	Laser Diode	840	10	5	1	12.0	1.0	16	12	2	3.0	±5"	±20"
Kern, Switzerland	DM 502	1200	2000	Diode	860	10	5	5	1.6	2.8	3.5	5	7	4.0	-	-
Keuffel & Esser U.S.A.	Autoranger-A	300	500	Diode	865	10	2-3		3.0	1.0	10.5	12	1.8	8.5	-	-
Precision International, Inc. U.S.A.	Super Beetle 1400S	700	1400	Diode	910	10	4.5	5	2.5	1.8	18-24	12	4.0	8.5	-	-
	Super Beetle 2000S	1000	2000	Diode	910	10	4.5	5	2.5	1.8	18-24	12	4.0	8.5	-	-
Sokkisha Japan	SDM 5A	500	800	Diode	865	10	5	5	2.1	0.4	6	12	1.2	6.0	-	-
	SDM 3D	1000	1600	Diode	865	10	5	5	8.5	-	8	8.4	1.5	2.5	±10"	±10"
Topcon Japan	GUPPY GTS-1/GTS-10	700	1000	Diode	820	10	5	10	5.0	0.7	7	8.4	1.8	7	+10"	±10"
Wild, Switzerland	Distomat DI4	1000	1600	Diode	885	30.76	5	5	2.2	2.3(3.0)	5	12	2(7)	4.0	-	-
Terra Technology Corp. U.S.A.	Terrameter LDM 2	1000 to	20000	HeNe Laser + HeCd Laser	632.8 441.6	0.05	0.1	0.1	42.2		575	115	(AC)	0.7	-	-

April 1981.

APPENDIX D

TABLE 1 (CONTD.): Technical Data of a Selection of (Short Range) EDM Instruments

Manufacturer	Model	Range with 1 Prism m	Range with 3 Prisms m	Radiation Source	Carrier Wavelength nm	Unit Length m	Stand. Dev. mm + ppm		Weight Instr. kg	Weight Battery kg	Power Cons. W	Battery Volt. V	Battery Cap. Ah	Beam Div. '	Angular Accuracy Hor.	Angular Accuracy Vert.
AGA Geotronics Sweden	Geodimeter 110A	800	1800	Diode	910	10	5	5	2.5	1.0	8,4	12	2.0	2.5	-	-
Alpha Electronics U.S.A.	Alpha I	700	1500	Diode		10	5	5	2.5	0.6	9.6	12			-	-
	Alpha II	1200	2000	Diode		10	5	5	2.5	0.6	9.6	12			-	-
	Alpha III	2000	3000	Diode		10	5	5	2.5	0.6	9.6	12			-	-
Keuffel & Esser U.S.A.	Autoranger III		3600	Diode	865		5	2	3.1	0.7	14	12	1.0		-	-
	Ranger V-A	up to 25 km		HeNe-Laser	632.8		5	2	20		60	12			-	-
	Rangemaster III	up to 60 km		HeNe-Laser	632.8		5	1	20		60	12			-	-
Nikon Japan	NLD-3	up to 60 km		HeNe-Laser	632.8		5	1	19		47-61	12		4''-62''	-	-
Precision International U.S.A.	Citation CI-450	1600	2300	Diode	905	10	5	5	2,8	2,3/3,0	9	12	2(7)		-	-
	Citation CI-410	1000	1500	Diode	905	10	5	5	2,6	2,3/3,0	9	12	2(7)			
Topcon Japan	DM-S1	1000	1400	Diode	820	10	5	5	2.9	-	7	8.4	1.8	7	-	-
	DM-C3	1600	2500	Diode	820	10	5	5	2.9	-	7	8.4	1.8	7	-	-
Wild Switzerland	DI 4L	2500	3500	Diode	885	30.769	5	5	1.9	0,4/3.0	3.75	12	0,5/7,0	4	-	-
	DI 20	6000	7000	Diode	835	33.333	5	1	3.7	0,4/3.0	5.0	12	0,5/7,0	2,5	-	-
	TC 1L	2500	3500	Diode	885	30.769	5	5	9.8	0.4/3.0	8-19	12	0.5/7.0	4	±2''	±3''

October 1981.

APPENDIX D

TABLE 1 (CONTD.): Technical Data of a Selection of (Short Range) EDM Instruments

Manufacturer	Model	Range with 1 Prism m	Range with 3 Prisms m	Radiation Source	Carrier Wavelength nm	Unit Length	Stand. Dev. mm + ppm		Weight Instr. kg.	Weight Battery kg.	Power Cons. W	Battery Volt. V	Battery Cap. Ah	Beam Div. (')	Angular Accuracy Hor.	Angular Accuracy Vert.
AGA Geotronics Sweden	Geodimeter 140	2500	3600	Diode	910	10	5	3	7.5		12			8	±2"	±2"
Alpha Electronic Corp. U.S.A.	OMNI 1		2500	Diode			5	5	7.5			12			±10"	±10"
Benchmark Inc. U.S.A.	Surveyor I-X		1000	Diode			5	5	2.3	0.5					-	-
	Surveyor II-X		2000	Diode			5	5	2.3	0.5					-	-
	Surveyor III-X		3000	Diode			5	5	2.3	0.5					-	-
COM-RAD U.K.	Geomensor 204DME	5000	8000	Xe Flash Tube	480	~0.3	0.1	0.5	26		24	12		3	-	-
Hewlett-Packard U.S.A.	HP 3850A	2000	8000	Laser Diode	835	10	5	1	12.7		14	12		3	-	-
Kern Switzerland	DM 102	1000	1700	Diode	860	10	5	5	1.7	2.5	3.5	5	7	4	-	-
Nikon Japan	ND-160	1000	1600	Diode			5	5	2.3	0.7	7.6	8.4	1.8		-	-
	ND-250	1600	2500	Diode			5	5	2.3	0.7	7.6	8.4	1.8		-	-
PENTAX Japan	PM- 81	1400	2000	Diode	850	10	5	5	3.0		5.0	8.4	0.6	2.2	-	-
Sokkisha Japan	RED-2	1800	2600	Diode	860	10	5	5	2.0	0.3		6			-	-
	SDM-300 (RED mini)	300	500	Diode	860	10	5	5	>0.9		6.6	6	1.6		-	-

September 1982/JMR.

APPENDIX D

TABLE 1 (CONTD.): Technical Data of a Selection of (Short Range) EDM Instruments

Manufacturer	Model	Range with 1 Prism m	Range with 3 Prisms m	Radiation Source	Carrier Wavelength m	Unit Length m	Stand. Dev. mm	Stand. Dev. ppm	Weight Instr. kg.	Weight Battery kg.	Power Cons. W	Battery Volt. V	Battery Cap. Ah	Beam Div. (')	Angular Accuracy Hor.	Angular Accuracy Vert.
Topcon Japan	GTS-2	1100	1700	Diode	820	10	5	5	6.0	0.8	9.2	8.4	1.1		±10"	±10"
VEB Carl Zeiss Jena, G.D.R.	EOT 2000	1000	1500	Diode	860	10	10	-	10.5			12			±1"	±1"
Zeiss (O'kochen) F.R.G.	Elta 3		1200	Diode	910	10	5	2	13.5	-		9	1.8		±2"	±2"
	Elta 20		1600	Diode	910	10	5	2	13.5	-		9	1.8		±1"	±1"
	RSM 3	1000	1600	Diode	910	10	5	2	7.5	-		9	1.8		±2"	±3"
	SM 41		1000	Diode	910	10	10	2	6.5	-		9	1.8		±3"	±3"

September 1982/JMR.

APPENDIX D

TABLE 1 (CONTD.): Technical Data of a Selection of (Short Range) EDM Instruments

Manufacturer	Model	Range with 1 Prism m	Range with 3 Prisms m	Radiation Source	Carrier Wavelength nm	Unit Length m	Stand. Dev. mm + ppm		Weight Instr. kg	Weight Battery kg	Power Cons. W	Battery Volt V	Battery Cap Ah	Beam Div. '	Angular Accuracy Hor.	Angular Accuracy Vert.
AGA Geotronics Sweden	Geodimeter 16	5000	7000	Diode	910	10	5-15	3	2.5	2.0		6	4.0	7	-	-
	Geodimeter 136	1000	1400	Diode	910	10	5	5	8.5					8	±3"	±3"
	Geodimeter 122	2500	3600	Diode	910	10	5	3	2.8	1.0		12	2.0	8	-	±20"
Kern, Switzerland	DM 503	2500	3500	Diode	860	10	3	2	1.6	2.5	4.5	5	7	4	-	-
Pentax, Japan	PX-06D	1400	2000	Diode	850	10	5	5	6.3	0.8	4.2	8.4	1.1	2.5	±6"	±6"
Sokkisha, Japan	RED-3	1800	2600	Diode	860	10	5	5	2	0.4	5.5	6	1.8	7	±10"	±10"
	SDM-3E	800	1400	Diode	860	10	5	5	7.2	0.4	5.0	6	1.8	7	±10"	±10"
	SDM-3ER	800	1400	Diode	860	10	5	5	7.2	0.4	5.5	6	1.8	7	±10"	±10"
	SET 5	800	1400	Diode	860	10	5	5	7.5	0.4	6.0	6	1.8	7	±5"	±5"
Topcon, Japan	DM-S2	1600	2000	Diode	820	10	5	5	1.5	0.4	6.3	8.4	1	7	-	-
	DM-S3	2200	3900	Diode	820	10	5	5	1.5	0.4	6.3	8.4	1	7	-	-
	ET-1	1400	2000	Diode	820	10	5	5	7.5	0.8	6.3	8.4	1	7	±2"	±3"
Wild, Switzerland	DI 4S	300	500	Diode	885	30.7692	2	5	1.1	0.4	5.0	12	0.5	4	-	-
	DI 5	2500	3500	Diode			3	2	1.9	0.9	5.0	12	2		-	-
VEB Carl Zeiss Jena, G.D.R.	RETA	1000	1500	Diode	860	10	5	2	10.2	0.8	4 - 8	12	1.8	2.5	±3"	±3"
	RECOTA	1000	1500	Diode	860	10	5	2	11.7	0.8	4 - 8	12	1.8	2.5	±1.6"	±1.6"
Zeiss (O'Kochen)	Elta 46		1600	Diode	910	10	5	2	6.5	-	5.6	9	1.8	2.5	±3"	±3"

Compiled from data supplied by manufacturers or their local agents.

March, 1984

APPENDIX D

TABLE 1 (CONTD.) : Technical Data of a Selection of (Short Range) EDM Instruments

Manufacturer	Model	Range with 1 Prism m	Range with 3 Prisms m	Radiation Source	Carrier Wavelength nm	Unit Length m	Stand. Dev. mm + ppm		Weight Instr. kg	Weight Battery kg	Power Cons. W	Battery Volt V	Battery Cap Ah	Beam Div. '	Angular Accuracy Hor.	Angular Accuracy Vert.
Geotronics AB Sweden	Geodimeter 114	8000	10000	Diode	880	10	5	1	2.7	1.0	8.5	12	2	0.7	-	-
	Geodimeter 210	2300	4000	Diode	910	10	5	3	1.1	0.25	<4	12	0.4	2.5	-	-
	Geodimeter 216	1000	1700	Diode	910	10	5	5	1.3	0.25	<4	12	0.4	2.5	-	±30"
	Geodimeter 220	2300	4000	Diode	910	10	5	3	1.3	0.25	<4	12	0.4	2.5	-	±20"
	Geodimeter 420	1000	1600	Diode	910	10	5	3	6.9	1.0	6	12	1.0	2.5	±3"	±3"
	Geodimeter 440	2300	3500	Diode	910	10	3	3	6.9	1.0	6	12	1.0	2.5	±2"	±2
	Geodimeter 142	2500	3600	Diode	910	10	2	3	9.5	1.0	12	12	2.0	2.5	±1"	±1"
KERN Switzerland	DM 104	1000	2000	Diode	860	10	5	5	1.7	2.5	5	5	7	4	-	-
	DM 150	1000	2000	Diode	860	10	5	5	1.8	2.5	6.5	5	7	4	-	10"
	DM 504	2500	3500	Diode	860	10	3	2	1.6	2.5	5	5	7	4	-	-
	DM 550	2500	3500	Diode	860	10	5	2	1.6	2.5	6.5	5	7	4	-	10"
	Mekometer ME 5000	4000	8000	HeNe Laser	632.8	0.30	0.2	0.2	11.0	3.6	24	12	7		-	-
NIKON Japan	ND-20	700	1000	Diode	820	10	5	5	2.2	(0.4)	3	8.4	0.5		N/A	
	ND-21	1000	1600	Diode	820	10	5	5	2.2	(0.4)	3	8.4	0.5		N/A	
	ND-26	2000	3000	Diode	820	10	5	5	2.3	(0.4)	3	8.4	0.5		N/A	
	NTD 2/2S	1600	2300	Diode	820	10	5	5	6.6	(0.4)	3	8.4	0.5		10/5"	10/5"
	NTD 3	1600	2300	Diode	820	10	5	5	6.6	(0.4)	3	8.4	0.5		5"	5"
	NTD 4	1600	2300	Diode	820	10	5	5	6.6	(0.4)	3	8.4	0.5		3"	3"
	DTM-1	1600	2300	Diode	820	10	5	5	8.3	1.1	<5.5	8.4	2	2	2"	3"
	DTM-5	1600	2300	Diode	820	10	5	5	6.4	0.9	<5.0	8.4	1.2		5"	5"
	DTM-20	800	1200	Diode	820	10	5	5		0.9	<5.0	8.4	1.2		10"	10"
PENTAX Japan	MD-14	1000	1400	Diode			5	5				8.4			N/A	
	MD-20	1400	2000	Diode			5	5				8.4			N/A	
	PTS-10	1400	2000	Diode			5	5	7.7	0.6		8.4			<5"	<5"
	PX-20D	1000	1600	Diode	815	10	5	5	7.1	0.8		8.4			20"	20"
	PX-10D	1400	2000	Diode	815	10	5	5	7.1	0.8		8.4			10"	10"

Compiled from data supplied by manufacturers or their local agents.

January 1988

APPENDIX D

TABLE 1 (CONTD.) : Technical Data of a Selection of (Short Range) EDM Instruments

Manufacturer	Model	Range with 1 Prism m	Range with 3 Prisms m	Radiation Source	Carrier Wavelength nm	Unit Length m	Stand. Dev. mm	Stand. Dev. + ppm	Weight Instr. kg	Weight Battery kg	Power Cons. W	Battery Volt V	Battery Cap Ah	Beam Div. "	Angular Accuracy Hor.	Angular Accuracy Vert.
SOKKISHA Japan	RED 2A	2300	3200	Diode	860	10	5	3	2	0.3	5.4	6	1.3	2.0	-	-
	RED 2L	4500	6400	Diode	860	10	5	3	2	0.3	5.4	6	1.3	2.0	-	-
	RED Mini 2	500	1200	Diode	810	10	5	5	1.0	0.2	3.6	6	1	3.4	-	-
	SDM3F/3FR	1300	2100	Diode	860	10	5	3	7.3	0.2	4.8/6.0	6	1	3.4	5"	5"
	SET 2	2300	3100	Diode	860	10	3	2	7.6	0.2	4.2	6	13	3.4	2"	2"
	SET 3	2200	3000	Diode	860	10	5	3	7.6	0.2	4.2	6	13	3.4	3"	3"
	SET 4	1300	2100	Diode	860	10	5	3	7.6	0.2	4.2	6	13	3.4	5"	5"
TOPCON Japan	DM-A2/DM-A3	700	1000	Diode	820	10	5	5	1.3	1.0	0.7	8.4	2	7.0	-	-
	GTS-2B/2S	1400	2000	Diode	820	10	5	5	13.2	1.0	1.0	8.4	2	7.0	6"	6"
	GTS-3B	2000	2800	Diode	820	10	5	3	5.2	1.0	1.0	8.4	2		2"	2"
	GTS-3	2000	2800	Diode	820	10	5	5	5.2	1.0		8.4	2		3"	3"
	ET-2			Diode	820	10	5	3				8.4			7"	1"
	DM-A5	750	1100	Diode	820	10	5	3	0.7	0.2		8.4	1		-	-
WILD Heerbrugg Switzerland	DI5S	2500	3500	Diode	845	30.7692	3	2	1.9		5	12	0.4	2.5	-	-
	DI 1000	800	1200	Diode	865	20	5	5	1.1		2.4	12	0.2	8.3	-	-
	DI 2000	2000	2800	Diode	850	10.10101	1	1	1.2		1	12	0.1	2.5	-	-
	DI 3000	9000	11000	Diode	865	N/A	5	1	1.7		4	12	0.33	2.6	-	-
	TC 2000	2000	2800	Diode	850	30.7692	3	2	22.9		9.5	12	0.8	4.7	0.5"	0.5"
	TC 1600	2000	2800	Diode	850	10.1010	3	2	5.5	0.2	5	12	0.4	4.7	1.8"	1.8"
Carl Zeiss F.R.G.	Series E 'Elta 4'	1000	1500	Diode	910	10	3	2	4.8	0.36	2-3.5	4.8	2	3.5	3"	3"
	Series E 'Elta 3'	1600	2000	Diode	910	10	3	2	5.3	0.36	2-3.5	4.8	2	3.5	2"	2"

Compiled from data supplied by manufacturers or their local agents.

January 1988

APPENDIX D

TABLE 2: Operational Data of a Selection of Short Range EDM Instruments

Instrument Model	Integration with theodolite: None	Integration with theodolite: theodolite mounted telescope mounted	Integration with theodolite: integrated	Environmental Correction Dial	Comp. of ΔH and horizontal Distance: automatic	Comp. of ΔH and horizontal Distance: semi-automatic	Pointing EDM + angles: one pointing only	Pointing EDM + angles: two pointings	Tracking Mode: Slope distance	Tracking Mode: Horizontal distance	Change of face with mounted EDM instrument	No interfering cables	Audio Signal	Operation of EDM: fully automatic	Operation of EDM: manual attenuator	Operation of EDM: manual tuning	Operation of EDM: partially automatic	Circle reading: automatically (electr.)	Circle reading: manually (optical)
Geod 710			X	X		X		X		X		X			X				X
Geod. 10		X		X				X					X		X				
Geod. 12A		X		X				X		X			X		X				
Geod. 14		X		X				X					X		X	X			
HP 3805A	X			X								X				X	X		
HP 3810A			X	X		X		X		X	X	X				X			(X)(X)
HP 3820A			X	X		X		X		X	X	X				X			X
DM 500		X		-				X			X	X				X			
DM 501		X		-				X			X	X			X				
ME 3000	X			comp.													X		
Autoranger	(X)	X	(X)	X		(X)			X	X	X		X		X				
Beetle 500S		(X)	X	X			X		X				X			2X			
Beetle 1000S		(X)	X	X			X		X				X			2X			
Beetle 1600S		(X)	X	X			X		X				X			2X			
MA 100	X			-							X						X		
CD 6		X		X				X	X		X		X			X			
DI 3			X	X		X		X			X			X					
DI 3S			X	X		X		X	X		X			X					
Eldi 1		X		X				X			X	X				X			
Eldi 2		X		X				X			X	X				X			
Eldi 3		X		X				X			X	X				X			
SM 4			X	X			X				X	X				X			X
Reg Elta 14			X	X		X	X				X					X		X	

APPENDIX D

TABLE 2(CONTD.): Operational Data of a Selection of Short-Range EDM Instruments

Instrument Model	Integration with theodolite				Environmental Correction Dial	Comp. of ΔH and horizontal Distance		Pointing for distance and angle		Tracking mode for		Change of face with mounted EDM instrument	No interfering cables	Audio Signal	Operation of EDM Instrument				Circle Reading	
	None	theodolite mounted	telescope mounted	integrated		automatic	semi-automatic	one pointing only	two pointings	Slope distance	Horizontal distance				fully automatic	manual attenuator	manual tuning	partially automatic	automatic (electronic)	manual (optical)
Geodimeter 120			X		X	X		X		X	X			X		X			V	H
Geodimeter 6A	X																X			
HP 3800B	X				X											X	X			
HP 3808A	X				X					X			X		X	X				
Autoranger S (+ Vectron[3])	(X)	X[1]	X[2]		X	X[3]		X[2]	X[1]	X	X[3]	X[1]		X				X	X[3]	
Autoranger II	(X)	X			X	X[3]			X	X	X[3]	X[1]	X	X				X	X[3]	
SDM-IC			X					X									2X			
SDM-ID (=RED-1)		X[1]	X[2]		X			X[2]	X[1]	X		X[1]	X	X			X			
DM-C2		X			X			X		X		X		X			X			
Tachymat TC1				X	X	X		X		X	X	X	X		X				X	
Elta 4				X	X	X		X		X	X	X	X				X		X	
Elta 2				X	X	X		X		X	X	X	X				X		X	

TABLE 2 (CONTD.): Operational Data of a Selection of Short Range EDM Instruments

Manufacturer	Instrument Model	Integration with theodolite			Environmental Correction Dial	Comp. of ΔH and horizontal Distance		Pointing EDM + angles		Tracking Mode			Change of face with mounted EDM instrument	No intefering cables	Audio Signal	Operation of EDM				Circle reading:	
		None	theodolite mounted	telescope mounted	integrated	automatic	semi-automatic	one pointing only	two pointings	Slope distance	Horizontal distance					fully automatic	manual attenuator	manual tuning	partially automatic	automatically (electr.)	manually (optical)
AGA Geotronics Sweden	Geodimeter 14A			X		X			X						X	X	X				
	Geodimeter 16			X		X			X						X	X					
	Geodimeter 110			X		X			X						X	X					
	Geodimeter 112			X		X			X		X				X	X					
	Geodimeter 116			X		X		X			X	X			X	X				V	H
	Geodimeter 122			X		X		X			X	X			X	X				V	H
	Geodimeter 140				X	X		X			X	X	X	X	X	X				X	
FUHRER (Fennel)	FEN 2000		X			X			X		X		X			X	X				
F.R.G.	FEN 4000		X			X			X		X		X			X	X				
	FEN 10000		X			X			X		X		X	X		X	X				
Hewlett Packard	HP 3810B	X				X		X			X	X		X	X	X				V	H
U.S.A.	HP 3850A	X				X					X			X		X					
Kern	DM 102			X					X		X					X	X				
Switzerland	DM 502			X					X		X		X	X		X	X				
	DM 503			X		X			X		X		X	X		X	X				
Precision-International	Citation CI-450		X[1]	X		X		X			X	X	X[1]		X	X	X				
U.S.A.	Citation CI-410		X[1]	X		X		X			X	X	X[1]		X	X	X				
Sokkisha	RED-2		X[1]	X		X		X	X[1]		X	X	X[1]	X	X	X					
Japan	REDmini (SDM-300)		X[1]	X		X		X	X[1]		X		X[1]		X	X					
	RED-3			X		X		X			X	X			X	X				V	
	SDM-3E				X	X	X	X			X	X	X	X	X	X					X
	SDM-3ER				X	X		X			X	X	X	X	X	X				V	X
	SDM-5A		X			X			X		X		X		X	X	X				
	SDM-3D				X	X	X	X			X		X		X	X					X
Topcon	DM-S1		X			X			X		X	X	X	X	X	X					
Japan	DM-C3		X			X			X		X		X	X	X	X					
	GTS-1/10				X	X		X			X		X			X	X				X
	GTS-2				X	X		X			X		X	X	X	X					X
	DM-S2		X[1]	X		X	X	X	X[1]		X		X[1]	X	X	X					
	ET-1				X	X		X			X	X	X	X		X				X	
Wild	DI4/4L/4S			X		X		X			X		X			X					
Switzerland	DI20			X		X			X		X				X	X					
	TC1L				X	X		X			X	X	X	X		X				X	
Zeiss (O'Kochen)	Elta 3/20				X	X		X			X	X	X	X		X	X			X	
F.R.G.	RMS3				X	X		X			X	X	X	X		X	X			V	H
	SM41				X	X		X			X		X	X		X					X
	Elta 46R				X	X		X			X	X	X	X		X	X			X	

Compiled from data supplied by manufacturers or their local agents

March 1984

APPENDIX D

TABLE 2 (CONTD.) : Operational Data of a Selection of Short Range EDM Instruments

Manufacturer	Model	Integration with theodolite: None	Integration with theodolite: theodolite mounted	Integration with theodolite: telescope mounted	Integration with theodolite: integrated	First Velocity Correction Entry	Comp. of ΔH and horizontal Distance: automatic	Comp. of ΔH and horizontal Distance: semi-automatic	Pointing EDM + angles: one pointing only	Pointing EDM + angles: two pointings	Tracking Mode: Slope distance	Tracking Mode: Horizontal distance	Change of face with mounted EDM instrument	No interfering cables	Audio Signal	Operation of EDM: fully automatic	Operation of EDM: manual attenuator	Operation of EDM: manual tuning	Operation of EDM: partially automatic	Circle reading: automatically (electr.)	Circle reading: manually (optical)
Geotronics AB	Geodimeter 114			X		X			X		X				X	X				N/A	
Sweden	Geodimeter 210			X		X			X		X			X	X	X				N/A	
	Geodimeter 216			X		X		X	X		X	X		X	X	X				VA	
	Geodimeter 220			X		X		X	X		X	X		X	X	X				VA	
	Geodimeter 420				X	X		X	X		X	X		X	X	X				X	
	Geodimeter 440				X	X		X	X		X	X		X	X	X				X	
	Geodimeter 142				X	X		X	X		X	X			X	X				X	
Kern	DM 104			X		X			X		X				X	X					
Switzerland	DM 150			X		X		X	X		X	X			X	X				X	
	DM 504			X		X			X		X		X	X	X	X					
	DM 550			X		X		X	X		X	X	X	X	X	X				X	
NIKON	ND-20	X				X		X		X	X	(X)	X		X	X				N/A	
Japan	ND-21	X				X		X		X	X	(X)	X		X	X				N/A	
	ND-26	X				X		X		X	X	(X)	X		X	X				N/A	
	NTD 2/2S				X	X		X	X		X	(X)	X	X	X	X					X
	NTD 3				X	X		X	X		X	(X)	X	X	X	X					X
	NTD 4				X	X		X	X		X	(X)	X	X	X	X					X
	DTM-1				X	X		X	X		X	X	X	X	X	X				X	
	DTM-5				X	X		X	X		X	X	X	X	X	X				X	
	DTM-20				X	X		X	X		X	X	X	X	X	X				X	
PENTAX	MD-14	X				X		X		X	X		X	X		X				N/A	
Japan	MD-20	X				X		X		X	X		X	X		X				N/A	
	PTS-10				X	X	X		X		X	X	X	X	X	X				X	
	PX-20D				X	X		X	X		X		X	X	X	X					X
	PX-10D				X	X		X	X		X		X	X	X	X					X
Sokkisha	RED 2A	X	X			X		X	X		X	X		X	X	X				N/A	
Japan	RED 2L	X	X			X		X	X		X	X		X	X	X				N/A	
	Red Mini 2	X	X						X		X	X				X				N/A	
	SDM 3F/FR				X	X		X	X		X	X	X	X	X	X					X
	SET 2				X	X	X		X		X	X	X	X	X	X				X	
	SET 3				X	X	X		X		X	X	X	X	X	X				X	
	SET 4				X	X	X		X		X	X	X	X	X	X				X	

Compiled from data supplied by manufacturers or their local agents.

January 1988

APPENDIX D

TABLE 2 (CONTD.) : Operational Data of a Selection of Short Range EDM Instruments

Manufacturer	Model	Integration with theodolite: None	Integration with theodolite: theodolite mounted	Integration with theodolite: telescope mounted	Integration with theodolite: integrated	First Velocity Correction Entry	Comp. of ΔH and horizontal Distance: automatic	Comp. of ΔH and horizontal Distance: semi-automatic	Pointing EDM + angles: one pointing only	Pointing EDM + angles: two pointings	Tracking Mode: Slope distance	Tracking Mode: Horizontal distance	Change of face with mounted EDM instrument	No interfering cables	Audio Signal	Operation of EDM: fully automatic	Operation of EDM: manual attenuator	Operation of EDM: manual tuning	Operation of EDM: partially automatic	Circle reading: automatically (electr.)	Circle reading: manually (optical)
Topcon	DM-A2/DM-A3		(X)	X		X		(X)		X (X)		X (X)	(X)	X	X		X				N/A
Japan	GTS-2B/2S				X	X		X		X		X (X)	X	X	X		X				X
	GTS-3B				X	X	X			X		X	X	X	X		X			X	
	GTS-3				X	X	X			X		X	X	X	X		X			X	
	ET-2				X	X	X			X		X	X	X	X		X			X	
	DM-5A		(X)	X		X		(X)		X (X)		X (X)	(X)	X	X		X				N/A
WILD Heerbrugg	DI 5S			X		X		X		X		X (X)	X	X	X		X				N/A
Switzerland	DI 1000			X		X		X		X		X (X)	X	X	X		X				N/A
	TC 1600				X	X	X			X		X (X)	X	X	X		X			X	
	DI 2000			X		X		X		X		X (X)	X	X	X		X				N/A
	DI 3000			X		X		X		X		X (X)	-	X	X		X				N/A
	TC 2000				X	X	X			X		X X	X	X	X		X			X	
Carl Zeiss	Series E ELTA 4				X	X	X			X		X X	X	X	-		X			X	
F.R.G	Series E ELTA 3				X	X	X			X		X X	X	X	-		X			X	

Compiled from data supplied by manufacturers or their local agents

January 1988

APPENDIX D

TABLE 3: Technical Data of a Selection of Long Range Instruments

Manufacturer	Model	Radiation Source	Carrier	Unit length m	Stand. Dev. mm + ppm		Range km	Weight kg	Power Consumption W	Phase Measurement	Beam Divergence
Electrooptical Instruments:			nm								
AGA Geotronics Sweden	Geodimeter 8	5mW laser	632.8	5	5	1	60	23	75	analogue	20''
	Geodimeter 600	1mW laser	632.8	5	5	1	0.015-40	15	26	analogue	10''
AGA USA	Geodimeter 78	1.8mW laser	632.8	10	10	1	10	8.2	60-72	digital	40''
Spectro Physics USA	Geodolite 3G	5mW laser	632.8	3	1	1	70	49	400	digital	
Keuffel & Esser USA	Rangemaster 2	5mW laser	632.8	10	5	1	60	18	60	digital	20''
	Ranger 5	3mW laser	632.8	10	10	2	25	16	57	digital	
Microwave Instruments:			GHz					12			
Tellurometer	MRA5	Gunn-Osc	10-10.5	5	10	3	0.1-50	6	42	digital	6°
Plessey UK	CA1000	Gunn-Osc	10.1-10.4	3	22	5	0.05->30	1.6	4.5	analogue	20°
Siemens-Albis AG Switzerland	SIAL MD60	Klystron	10.3	1	10	3	0.02-150	15	38	digital	6°

APPENDIX D

TABLE 3 (CONTD): Technical Data of a Selection of Long Range Instruments

Manufacturer	Model	Radiation Source	Carrier	Unit length	Stand. Dev.	Range	Weight	Power Consumption	Phase Measurement	Beam Divergence
				m	mm + ppm	km	kg	W		
Microwave Instruments:			GHz							
Microfix South Africa	100C	Gunn-Osc	16.25		15 3	0.02-60	3.4	6.0	analogue	3.5°/6°/45°
Tellumat U.K.	CMW 6		16.0-16.5		10 3	0.1 -50	7	<20	digital	4.5°
	CMW20		34.5-34.9	0.9	5 3	0.02-25	4	12	digital	3°

Compiled from data supplied by manufacturers or their local agent.

March 1984.

APPENDIX D

TABLE 3 (CONT.) : Technical Data of a Selection of Long Range Instruments

Manufacturer	Model	Radiation Source	Carrier	Unit length m	Stand. Dev. mm + ppm		Range km	Weight kg	Power Consumption W	Phase Measurement	Beam Divergence
Geotronics AB Sweden	Geodimeter 6000	Diode	nm 880	10	5	1	0.0002-21	2.7	8.5	digital	2.25
Tellumat U.K	CMW20	?	GHz 34.5-34.9	?	5	3	0.02-25	3	12	?	2.5°/3.0°
	MRA 7	Gunn-Osc	(17.4-17.5 / 16.2-17.3)	1.8737	15	3	0.02-50	4	10	?	6°
Tellurometer U.K.	MRA 6	?	?	?	10	3	0.10-50	4	?	?	?

Compiled from data supplied by manufacturers or their local agent.

January 1988

APPENDIX D

TABLE 4: First Velocity Corrections and Modulation Frequencies of a Selection of Short-Range Instruments.

Manufacturer	Model	Carrier Wave Length	Main Modulation Frequency	Unit Length	Reference Refractive Index	Terms of First Velocity Corr.		Remarks
						C	D	
		nm	Hz	m				
AGA Geotronics	Geodimeter 710	632.8	29 970 000	5	1.000 3086	308.6	81.00	Same Correction for Geodimeter 6BL,8
Sweden	Geodimeter 6A	550	29 970 000	5	1.000 3092	309.2	82.164	
	Geodimeter 10	910	14 985 530	10	1.000 275	275	79.6	
	Geodimeter 12A	910	14 985 530	10	1.000 275	275	79.6	
	Geodimeter 14	910	14 985 530	10	1.000 275	275	79.6	
	Geodimeter 120	910	14 985 530	10	1.000 275	275	79.6	
Hewlett-Packard	HP 3800B	910	14 985 453	10	1.000 2783	278.3	79.15	
U. S. A.	HP 3805A	910	14 987 103*	10	1.000 2783	278.3	79.15	* frequency set to + 110 ppm
	HP 3808A	835	14 987 090*	10	1.000 2794	279.2	79.46	* frequency set to + 110 ppm
	HP 3820A	835	14 987 090*	10	1.000 2794	279.2	79.46	* frequency set to + 110 ppm
Kern	DM 500	875	14 985 400	10	1.000 2816	281.6	79.26	
Switzerland	DM 501	900	14 985 400	10	1.000 2819	281.9	79.19	
	Ranger V	632.8	14 984 980	10	1.000 310	310	81.01	Same Correction for Rangemaster II
Keuffel and	Autoranger I	910	14 983 482*	10	1.000 3104	310.4	79.19	* frequency set to - 100 ppm
Esser U. S. A.	Autoranger S	865	14 983 482*	10	1.000 3104	310.4	79.40	* frequency set to - 100 ppm
	Autoranger II	865	14 983 482*	10	1.000 3104	310.4	79.40	* frequency set to - 100 ppm
Precision Int.	Beetle 500S	910	14 984 979	10	1.000 3100	310.0	79.15	
U. S. A.	Beetle 1000S	910	14 984 979	10	1.000 3100	310.0	79.15	
	Beetle 1600S	910	14 984 979	10	1.000 3100	310.0	79.15	
Sokkisha	SDM - 1C	910	14 985 450	10	1.000 2786	278.6	79.15	
Japan	RED - 1 (=SDM-1D)	830	14 985 450	10	1.000 2786	278.6	79.49	
Tellurometer	MA 100	930	74 927 600	1 (2)	1.000 274	274	79.13	
Plessey U. K.	CD 6	930	14 985 520	10	1.000 274	274	79.17	
Topcon	DM - C2	820	14 985 437	10	1.000 2811	281.1	80.00	** Use environmental correction dial and first velocity correction chart as supplied with instrument; some corrections for the oscillator drift with temperature are then also included.
Japan								
Wild	DI 3	875	7 492 700	20	1.000 282	282	79.2	
Switzerland	DI 3S	885	7 492 700	20	1.000 282	282	79.2	
	TC 1	885	4 871 444	30.7692	1.000 282	282	79.2	
Zeiss	Eldi 1	910	14 985 100	10	1.000 3020	302.0**	79.15**	First Velocity Correction:
Fed. Rep. Ger.	Eldi 2	910	14 985 100	10	1.000 3020	302.0**	79.15**	
	Eldi 3	910	14 985 100	10	1.000 3020	302.0**	79.15**	$K' = (C - \frac{Dp}{(273.16+t)} + \frac{11.20e}{(273.16+t)}) 10^{-6} d$
	SM 4	910	14 985 100	10	1.000 3020	302.0**	79.15**	
	Elta 2	910	14 985 800	10	1.000 2551	255.1**	79.15**	
	Elta 4	910	14 985 800	10	1.000 2551	255.1**	79.15**	p in mb, t in ^oC, e in mb

TABLE 4 (CONTD.): First Velocity Corrections and Modulation Frequencies of a Selection of Short-Range Instruments

Manufacturer	Model	Carrier Wave Length	Main Modulation Frequency	Unit Length	Reference Refractive Index	Terms of First Velocity Corr.		Remarks
						C	D	
		nm	Hz	m				
AGA Geotronics, Sweden	Geodimeter 14A	910	14 985 530	10	1.000 275	275	79.55	
	Geodimeter 110/110A	910	14 985 530	10	1.000 275	275	79.55	
	Geodimeter 112	910	14 985 530	10	1.000 275	275	79.55	
	Geodimeter 116	910	14 985 530	10	1.000 275	275	79.55	
	Geodimeter 122	910	14 985 530	10	1.000 275	275	79.55	
	Geodimeter 140/136	910	14 985 530	10	1.000 275	275	79.55	
	Geodimeter 16	910	14 985 530	10	1.000 275	275	79.55	
Fuhrer (FENNEL) F.R.G.	FEN 2000	905	(14 983 482)	-	1.000 27345	273.45	79.08	Pulse Distance Meter
	FEN 4000	905	(14 983 482)	-	1.000 27345	273.45	79.08	Pulse Distance Meter
	FEN 10000	905	(14 983 482)	-	1.000 27345	273.45	79.08	Pulse Distance Meter
Hewlett-Packard U.S.A.	HP 3801A	910	14 987 103*	10	1.000 2783	278.3	79.15	*frequency set at + 110 ppm
	HP 3859A	840	14 987 090*	10	1.000 2783	278.3	79.15	*frequency set at + 110 ppm
	HP 3810B	840	14 987 090*	10	1.000 2783	278.3	79.15	*frequency set at + 110 ppm
Kern Switzerland	DM 502	860	14 985 400	10	1.000 282	282	79.2	
	DM 102	860	14 985 400	10	1.000 282	282	79.2	
	DM 503	860	14 985 400	10	1.000 282	282	79.2	
Sokkisha Japan	SDM 3D, 5D	860	14 985 453	10	1.000 2789	278.96	79.33	
	RED-2, RED-3	860	14 985 453	10	1.000 2789	278.96	79.33	
	REDmini (SDM-300)	860	14 985 453	10	1.000 2789	278.96	79.33	
	SDM-3E/3ER & SET 5	860	14 985 453	10	1.000 2789	278.96	79.33	
Topcon Japan	DM-S1/S2/S3	820	14 985 437	10	1.000 2796	279.6	79.51	
	DM-C3	820	14 985 437	10	1.000 2796	279.6	79.51	**** Applicable if PM-81 is set to 278 ppm and if a temperature of +15°C and a pressure of 760 mm Hg is entred into the PX-06D.
	GTS-1/GTS 10	820	14 985 437	10	1.000 2796	279.6	79.51	
	GTS-2	820	14 985 437	10	1.000 2796	279.6	79.51	
	ET-1	820	14 985 437	10	1.000 2796	279.6	79.51	
Wild Switzerland	D14/4L/4S	885	4 870 255	30.7692	1.000 282	282	79.2	
	TC 1L	885	4 870 255	30.7692	1.000 282	282	79.2	*** Applicable if PPM value in Citation set to 310 ppm.
	D1 20	835	4 495 620	33.333	1.000 2822	282.2	79.43	
Zeiss (O'Kochen) F.R.G.	Elta 3	910	14 985 800	10	1.000 2555	255.5**	78.96**	**Use environmental correction dial and first velocity correction chart as supplied with instrument; some corrections for the oscillator drift with temperature are then also included.
	Elta 20	910	14 985 800	10	1.000 2555	255.5**	78.96**	
	Elta 46R	910	14 985 800	10	1.000 2555	255.5**	78.96**	
	RSM 3	910	14 985 800	10	1.000 2555	255.5**	78.96**	
	SM 41	910	14 985 800	10	1.000 2555	255.5**	78.96**	
Precision-Intern. U.S.A.	Citation CI-410	905	14 984 980	10	1.000 310	310.0***	79.21***	First Velocity Correction: $K' = (C - \frac{Dp}{(273.16+t)} + \frac{11.20e}{(273.16+t)})10^{-6} d$ p in mb, t in ^{o}C, e in mb
	Citation CI-450	905	14 984 980	10	1.000 310	310.0***	79.21***	
VEB Carl Zeiss Jena, G.D.R.	RETA	860	14 985 570	10	1.000 2705	270.5	79.35	
	RECOTA	860	14 985 570	10	1.000 2705	270.5	79.35	
Pentax, Japan	PM-81 & PX-06D	850	14 985 450	10	1.000 2785	278.5****	79.2****	

Compiled from data supplied by manufacturers or their local agents.

March, 1984.

APPENDIX D

TABLE 4 (CONT.) : First Velocity Corrections and Modulation Frequencies of a Selection of Short-Range Instruments

Manufacturer	Model	Carrier Wave Length	Main Modulation Frequency	Unit Length	Reference Refractive Index	Terms of First Velocity Corr.		Remarks
						C	D	
		nm	Hz	m				
WILD Heerbrugg	DI 5S	845	4 870 255	30.7692	1.000 282	282	79.2	
Switzerland	DI 1000	865	7 492 700	20	1.000 282	282	79.2	
	DI 2000	850	14 835 546	10.10101	1.000 2818	281.8	79.4	
	DI 3000	865	15 000 000	N/A	1.000 2815	281.5	79.3	
	TC 2000	850	4 870 255	30.7692	1.000 282	282	79.2	
	TC 1600	850	14 835 546	10.1010	1.000 282	282	79.4	
Carl Zeiss	Series"E" ELTA 4	910	14 985 800	10				
F.R.G.	Series"E" ELTA 3	910	14 985 800	10				

First Velocity Correction:

$$K' = (C - \frac{Dp}{(273.15+t)} + \frac{11.20e}{(273.15+t)})10^{-6}d$$

p in mb, t in ^{o}C, e in mb

NOTE: This first velocity correction applies only if the distance meter is set to zero ppm (or equivalent) during measurement.

Compiled from data supplied by manufacturers or their local agent.

January 1988

TABLE 4 (CONT.) : First Velocity Corrections and Modulation Frequencies of a Selection of Short-Range Instruments

Manufacturer	Model	Carrier Wave Length	Main Modulation Frequency	Unit Length	Reference Refractive Index	Terms of First Velocity Corr.		Remarks
						C	D	
		nm	Hz	m				
Geotronics AB	Geodimeter 114	880	14 984 651	10	1.000 275	275	79.55	
Sweden	Geodimeter 210	910	14 984 629	10	1.000 275	275	79.55	
	Geodimeter 216	910	14 984 629	10	1.000 275	275	79.55	
	Geodimeter 220	910	14 984 629	10	1.000 275	275	79.55	
	Geodimeter 420	910	14 984 629	10	1.000 275	275	79.55	
	Geodimeter 440	910	14 984 629	10	1.000 275	275	79.55	
	Geodimeter 142	910 (880)	14 985 543	10	1.000 275	275	79.55	
	Geodimeter 6000	880	14 984 651	10	1.000 275	275	79.55	
Kern & Co.	DM 104	860	14 985 400	10	1.000 282	282.2	79.4	
Switzerland	DM 150	860	14 985 400	10	1.000 282	282.2	79.4	
	DM 504	860	14 985 400	10	1.000 282	282.2	79.4	
	DM 550	860	14 985 400	10	1.000 282	282.2	79.4	
	Mekometer ME5000	632.8	460-510MHz	~0.30	1.000 284515	284.515	~80.91	
PENTAX	MD-14							
Japan	MD-20							
	PTS-10				1.000 2798	279.8	79.56	
	PX-20D	815	14 985 450	10	1.000 2798	279.8	79.56	
	PX-10D	815	14 985 450	10	1.000 2798	279.8	79.56	
NIKON	ND-20	820	14 972 947	10	1.000 280	280	79.5	
Japan	ND-21	820	14 972 947	10	1.000 280	280	79.5	
	ND-26	820	14 972 947	10	1.000 280	280	79.5	
	NTD 2/2S	820	14 972 947	10	1.000 280	280	79.5	
	NTD 3	820	14 972 947	10	1.000 280	280	79.5	
	NTD 4	820	14 972 947	10	1.000 280	280	79.5	
	ND-30	820	14 972 947	10	1.000 280	280	79.5	
	ND-31	820	14 972 947	10	1.000 280	280	79.5	
	DTM-1	820	14 972 947	10	1.000 280	280	79.5	
	DTM-5	820	14 972 947	10	1.000 280	280	79.5	
	DTM-20	820	14 972 947	10	1.000 280	280	79.5	
Sokkisha	RED 2A	860	14 985 5453	10	1.000 27896	278.96	79.33	
Japan	RED 2L	860	14 985 5453	10	1.000 27896	278.96	79.33	
	RED MINI 2	810	14 985 5453	10	1.000 27896	278.96	79.33	
	SDM 3F/3FR	860	14 985 5453	10	1.000 27896	278.96	79.33	
	SET 2	860	14 985 5453	10	1.000 27896	278.96	79.33	
	SET 3	860	14 985 5453	10	1.000 27896	278.96	79.33	
	SET 4	860	14 985 5453	10	1.000 27896	278.96	79.33	
TOPCON	DM-A2/DM-A3	820	14 985 437	10	1.000 2796	279.6	79.51	
Japan	GTS-2B/2S	820	14 985 437	10	1.000 2796	279.6	79.51	
	GTS-3B	820	14 985 437	10	1.000 2796	279.6	79.51	
	GTS-3	820	14 985 437	10	1.000 2796	279.6	79.51	
	ET-2	820	14 985 437	10	1.000 2796	279.6	79.51	
	DM-A5	820	14 985 437	10	1.000 2196	279.6	79.51	

First Velocity Correction:

$$K' = (C - \frac{Dp}{(273.15+t)} + \frac{11.20e}{(273.15+t)})\ 10^{-6} d$$

p in mb, t in ^{o}C, e in mb

NOTE: This first velocity correction applies only if the distance meter is set to zero ppm (or equivalent) during meas.

Compiled from data supplied by manufacturers or their local agents

January 1988

APPENDIX D

TABLE 5: Technical Data of a Selection of Pulse Distance Meters

Manufacturer	Model	Range with Reflector			Radiation	Carrier	Standard		Weight		Power	Battery		Beam	Pulse	
		Passive	Plastic	Triple Prism	Source	Wavelength	Deviation		Instr.	Battery	Cons.	Volt.	Cap.	Div.	Length	Repetition Rate PRR
		m	m	m		nm	mm	ppm	kg.	kg.	W	V	Ah	(')	ns	Hz
Eumig Austria	LP8010-01µP	80	-	-	laser diode	890	10	-	9.5		85	12		22	30	2500
	LP8015-03	15	-	-	laser diode	900	30	-	7.2		60	12		22	30	800
	LP80130-10	100	300	-	laser diode	900	100	1000	6.9		30	12		12	30	120
	LP80200-10	120	300	-	laser diode	890	100	1000	6.9		30	12		10	30	120
	LP80300-10	150	300	-	laser diode	890	100	1000	6.9		25	12		22	35	120
	LP80400-20	250	500	-	laser diode	900	200	1000	6.9		30	12		22	35	120
	LP80130/1000-20	80	-	1000	laser diode	900	200	1000	6.9		30	12		12	30	120
	LP80200/2000-20	120	-	2000	laser diode	890	200	1000	6.9		30	12		9	30	120
Fennel (Führer) Fed.Rep. of Germany	Fen 2000		150	2000	laser diode	905	5	5	3.5	-	10	12	1.1	6.0	5	var.
	Fen 10000			3000	laser diode	905	100	-	3.1	-	10	12	1.1	6.0	5	var.
	Fen 4000			3000	laser diode	905	5	5	3.5	-	10	12	1.1	6.0	5	var.
Keuffel & Esser U.S.A.	Pulseranger	100		>3000	laser diode	905	30	30	3.6	-		12				
D.J. Vyner U.K.	RF2K	50	300	2500		904	500	100	3.0	3.0		12		7.0	25	400
	RF4K	100	500	4500		904	500	100	3.0	3.0		12		7.0	25	300

September 1982/JMR.

APPENDIX E

TABLE 1: Saturation Vapour Pressure Over Water [14]

Temperature °C.	.0 mb.	.1 mb.	.2 mb.	.3 mb.	.4 mb.	.5 mb.	.6 mb.	.7 mb.	.8 mb.	.9 mb.
-10	2.8627	2.8402	2.8178	2.7956	2.7735	2.7516	2.7298	2.7082	2.6868	2.6655
- 9	3.0971	3.0729	3.0489	3.0250	3.0013	2.9778	2.9544	2.9313	2.9082	2.8854
- 8	3.3484	3.3225	3.2967	3.2711	3.2457	3.2205	3.1955	3.1706	3.1459	3.1214
- 7	3.6177	3.5899	3.5623	3.5349	3.5077	3.4807	3.4539	3.4272	3.4008	3.3745
- 6	3.9061	3.8764	3.8468	3.8175	3.7883	3.7594	3.7307	3.7021	3.6738	3.6456
- 5	4.2148	4.1830	4.1514	4.1200	4.0888	4.0579	4.0271	3.9966	3.9662	3.9361
- 4	4.5451	4.5111	4.4773	4.4437	4.4103	4.3772	4.3443	4.3116	4.2791	4.2468
- 3	4.8981	4.8617	4.8256	4.7897	4.7541	4.7187	4.6835	4.6486	4.6138	4.5794
- 2	5.2753	5.2364	5.1979	5.1595	5.1214	5.0836	5.0460	5.0087	4.9716	4.9347
- 1	5.6780	5.6365	5.5953	5.5544	5.5138	5.4734	5.4333	5.3934	5.3538	5.3144
0	6.1078	6.1523	6.1971	6.2422	6.2876	6.3333	6.3793	6.4256	6.4721	6.5190
1	6.5662	6.6137	6.6614	6.7095	6.7579	6.8066	6.8556	6.9049	6.9545	7.0044
2	7.0547	7.1053	7.1562	7.2074	7.2590	7.3109	7.3631	7.4157	7.4685	7.5218
3	7.5753	7.6291	7.6833	7.7379	7.7928	7.8480	7.9036	7.9595	8.0158	8.0724
4	8.1294	8.1868	8.2445	8.3026	8.3610	8.4198	8.4789	8.5384	8.5983	8.6586
5	8.7192	8.7802	8.8416	8.9033	8.9655	9.0280	9.0909	9.1542	9.2179	9.2820
6	9.3465	9.4114	9.4766	9.5423	9.6083	9.6748	9.7416	9.8089	9.8765	9.9446
7	10.013	10.082	10.151	10.221	10.291	10.362	10.433	10.505	10.577	10.649
8	10.722	10.795	10.869	10.943	11.017	11.092	11.168	11.243	11.320	11.397
9	11.474	11.552	11.630	11.708	11.787	11.867	11.947	12.027	12.108	12.190
10	12.272	12.355	12.438	12.521	12.606	12.690	12.775	12.860	12.946	13.032
11	13.119	13.207	13.295	13.383	13.472	13.562	13.652	13.742	13.833	13.925
12	14.017	14.110	14.203	14.297	14.391	14.486	14.581	14.678	14.774	14.871
13	14.969	15.067	15.166	15.266	15.365	15.466	15.567	15.669	15.771	15.874
14	15.977	16.081	16.186	16.291	16.397	16.503	16.610	16.718	16.826	16.935
15	17.044	17.154	17.264	17.376	17.487	17.600	17.713	17.827	17.942	18.057
16	18.173	18.290	18.407	18.524	18.643	18.762	18.882	19.002	19.123	19.245
17	19.367	19.490	19.614	19.739	19.864	19.990	20.117	20.244	20.372	20.501
18	20.630	20.760	20.891	21.023	21.155	21.2888	21.422	21.556	21.691	21.827
19	21.964	22.101	22.240	22.379	22.518	22.659	22.800	22.942	23.085	23.229
20	23.373	23.518	23.664	23.811	23.959	24.107	24.256	24.406	24.557	24.709
21	24.861	25.014	25.168	25.323	25.479	25.635	25.792	25.950	26.109	26.269
22	26.430	26.592	26.754	26.918	27.082	27.247	27.413	27.580	27.748	27.916
23	28.086	28.256	28.428	28.600	28.773	28.947	29.122	29.298	29.475	29.652
24	29.831	30.011	30.191	30.373	30.555	30.739	30.923	31.109	31.295	31.483
25	31.671	31.860	32.050	32.242	32.434	32.627	32.821	33.016	33.212	33.410
26	33.608	33.807	34.008	34.209	34.411	34.615	34.820	35.025	35.232	35.440
27	35.649	35.859	36.070	36.282	36.495	36.709	36.924	37.140	37.358	37.576
28	37.796	38.017	38.239	38.462	38.686	38.911	39.137	39.365	39.594	39.824
29	40.055	40.287	40.521	40.755	40.991	41.228	41.466	41.705	41.945	42.187
30	42.430	42.674	42.919	43.166	43.414	43.663	43.913	44.165	44.418	44.672
31	44.927	45.184	45.442	45.701	46.961	46.223	46.486	46.750	47.016	47.283
32	47.551	47.820	48.091	48.364	48.637	48.912	49.188	49.466	49.745	50.025
33	50.307	50.590	50.874	51.160	51.447	51.736	52.026	52.317	52.610	52.904
34	53.200	53.497	53.796	54.096	54.397	54.700	55.004	55.310	55.617	55.926
35	56.236	56.548	56.861	57.176	57.492	57.810	58.129	58.450	58.773	59.097
36	59.422	59.749	60.077	60.407	60.739	61.072	61.407	61.743	62.081	62.421
37	62.762	63.105	63.450	63.796	64.144	64.493	64.844	65.196	65.550	65.906
38	66.264	66.623	66.985	67.347	67.712	68.078	68.446	68.815	69.186	69.559
39	69.934	70.310	70.688	71.068	71.450	71.833	72.218	72.605	72.994	73.385
40	73.777	74.171	74.568	74.966	75.365	76.767	76.170	76.575	76.982	77.391
41	77.802	78.215	78.630	79.046	79.465	79.885	80.307	80.731	81.157	81.585
42	82.015	82.447	82.881	83.316	83.754	84.194	84.636	85.079	85.525	85.973
43	86.423	86.875	87.329	87.785	88.243	88.703	89.165	89.629	90.095	90.564
44	91.034	91.507	91.981	92.458	92.937	93.418	93.901	94.386	94.874	95.363
45	95.855	96.349	96.845	97.343	97.844	98.347	98.852	99.359	99.869	100.38
46	100.89	101.41	101.93	102.45	102.97	103.50	104.03	104.56	105.09	105.62
47	106.16	106.70	107.24	107.78	108.33	108.88	109.43	109.98	110.54	111.10
48	111.66	112.22	112.79	113.36	113.93	114.50	115.07	115.65	116.23	116.81
49	117.40	117.99	118.58	119.17	119.77	120.37	120.97	121.57	122.18	122.79
50	123.40	124.01	124.63	125.25	125.87	126.49	127.12	127.75	128.38	129.01
51	129.65	130.29	130.93	131.58	132.23	132.88	133.53	134.19	134.84	135.51
52	136.17	136.84	137.51	138.18	138.86	139.54	140.22	140.91	141.60	142.29
53	142.98	143.68	144.38	145.08	145.78	146.49	147.20	147.91	148.63	149.35
54	150.07	150.80	151.53	152.26	152.99	153.73	154.47	155.21	155.96	156.71
55	157.46	158.22	158.97	159.74	160.50	161.27	162.04	162.82	163.59	164.38
56	165.16	165.95	166.74	167.53	168.33	169.13	169.93	170.74	171.55	172.36
57	173.18	174.00	174.82	175.65	176.48	177.31	178.15	178.99	179.83	180.68
58	181.53	182.38	183.24	184.10	184.96	185.83	186.70	187.58	188.45	189.34
59	190.22	191.11	192.00	192.89	193.79	194.69	195.60	196.51	197.42	198.34
60	199.26	200.18	201.11	202.05	202.98	203.92	204.86	205.81	206.76	207.71

APPENDIX E

TABLE 2: Saturation Vapour Pressure Over Ice [14]

Temperature C.	.0	.1	.2	.3	.4	.5	.6	.7	.8	.9
Unit	mb.	mb.	mb.	mb.	mb.	mb.	mb.	mb.	mb.	mb.
-50	0.03935	0.03887	0.03839	0.03792	0.03745	0.03699	0.03653	0.03608	0.03564	0.03520
-49	0.04449	0.04395	0.04341	0.04289	0.04236	0.04185	0.04134	0.04083	0.04033	0.03984
-48	0.05026	0.04965	0.04905	0.04846	0.04788	0.04730	0.04673	0.04616	0.04560	0.04504
-47	0.05671	0.05603	0.05536	0.05470	0.05405	0.05340	0.05276	0.05212	0.05150	0.05087
-46	0.06393	0.06317	0.06242	0.06168	0.06095	0.06022	0.05950	0.05879	0.05809	0.05740
-45	0.07198	0.07113	0.07030	0.06947	0.06865	0.06784	0.06704	0.06625	0.06547	0.06469
-44	0.08097	0.08003	0.07909	0.07817	0.07725	0.07635	0.07546	0.07457	0.07370	0.07283
-43	0.09098	0.08993	0.08889	0.08786	0.08684	0.08584	0.08484	0.08386	0.08289	0.08192
-42	0.1021	0.1010	0.09981	0.09866	0.09753	0.09641	0.09530	0.09420	0.09312	0.09204
-41	0.1145	0.1132	0.1119	0.1107	0.1094	0.1082	0.1070	0.1057	0.1045	0.1033
-40	0.1283	0.1268	0.1254	0.1240	0.1226	0.1212	0.1198	0.1185	0.1171	0.1158
-39	0.1436	0.1420	0.1404	0.1389	0.1373	0.1358	0.1343	0.1328	0.1313	0.1298
-38	0.1606	0.1588	0.1571	0.1553	0.1536	0.1519	0.1502	0.1485	0.1469	0.1452
-37	0.1794	0.1774	0.1755	0.1736	0.1717	0.1698	0.1679	0.1661	0.1642	0.1624
-36	0.2002	0.1980	0.1959	0.1938	0.1917	0.1896	0.1875	0.1855	0.1834	0.1814
-35	0.2233	0.2209	0.2185	0.2161	0.2138	0.2115	0.2092	0.2069	0.2047	0.2024
-34	0.2488	0.2461	0.2435	0.2409	0.2383	0.2357	0.2332	0.2307	0.2282	0.2257
-33	0.2769	0.2740	0.2711	0.2682	0.2653	0.2625	0.2597	0.2569	0.2542	0.2515
-32	0.3079	0.3047	0.3014	0.2983	0.2951	0.2920	0.2889	0.2859	0.2828	0.2799
-31	0.3421	0.3385	0.3350	0.3315	0.3280	0.3246	0.3212	0.3178	0.3145	0.3112
-30	0.3798	0.3759	0.3720	0.3681	0.3643	0.3605	0.3567	0.3530	0.3494	0.3457
-29	0.4213	0.4170	0.4127	0.4084	0.4042	0.4000	0.3959	0.3918	0.3877	0.3838
-28	0.4669	0.4621	0.4574	0.4527	0.4481	0.4435	0.4390	0.4345	0.4300	0.4256
-27	0.5170	0.5118	0.5066	0.5014	0.4964	0.4913	0.4863	0.4814	0.4765	0.4717
-26	0.5720	0.5663	0.5606	0.5549	0.5493	0.5438	0.5383	0.5329	0.5276	0.5222
-25	0.6323	0.6260	0.6198	0.6136	0.6075	0.6015	0.5955	0.5895	0.5836	0.5778
-24	0.6985	0.6916	0.6848	0.6780	0.6713	0.6646	0.6580	0.6515	0.6450	0.6386
-23	0.7709	0.7634	0.7559	0.7485	0.7412	0.7339	0.7267	0.7195	0.7125	0.7055
-22	0.8502	0.8419	0.8338	0.8257	0.8176	0.8097	0.8018	0.7940	0.7862	0.7785
-21	0.9370	0.9280	0.9190	0.9101	0.9013	0.8926	0.8840	0.8754	0.8669	0.8585
-20	1.032	1.022	1.012	1.002	0.9928	0.9833	0.9739	0.9645	0.9553	0.9461
-19	1.135	1.124	1.114	1.103	1.092	1.082	1.072	1.062	1.052	1.042
-18	1.248	1.236	1.225	1.213	1.201	1.190	1.179	1.168	1.157	1.146
-17	1.371	1.358	1.345	1.333	1.320	1.308	1.296	1.284	1.272	1.260
-16	1.506	1.492	1.478	1.464	1.451	1.437	1.424	1.410	1.397	1.384
-15	1.652	1.637	1.622	1.607	1.592	1.577	1.562	1.548	1.534	1.520
-14	1.811	1.795	1.778	1.762	1.746	1.730	1.714	1.698	1.683	1.667
-13	1.984	1.966	1.948	1.930	1.913	1.895	1.878	1.861	1.844	1.827
-12	2.172	2.153	2.133	2.114	2.095	2.076	2.057	2.039	2.020	2.002
-11	2.376	2.355	2.334	2.313	2.292	2.271	2.251	2.231	2.211	2.191
-10	2.597	2.574	2.551	2.529	2.506	2.484	2.462	2.440	2.419	2.397
- 9	2.837	2.812	2.787	2.763	2.739	2.715	2.691	2.667	2.644	2.620
- 8	3.097	3.070	3.043	3.017	2.991	2.965	2.939	2.913	2.888	2.862
- 7	3.379	3.350	3.321	3.292	3.264	3.236	3.208	3.180	3.152	3.124
- 6	3.685	3.653	3.622	3.591	3.560	3.529	3.499	3.468	3.438	3.409
- 5	4.015	3.981	3.947	3.913	3.879	3.846	3.813	3.781	3.748	3.717
- 4	4.372	4.335	4.298	4.262	4.226	4.190	4.154	4.119	4.084	4.049
- 3	4.757	4.717	4.678	4.638	4.600	4.561	4.523	4.485	4.447	4.409
- 2	5.173	5.130	5.087	5.045	5.003	4.961	4.920	4.878	4.838	4.797
- 1	5.623	5.577	5.530	5.485	5.439	5.394	5.349	5.305	5.260	5.217

APPENDIX F

Technical Data of Reflectors

F.1 Dimensions of Reflectors

Manufacturer	Reflector type	a mm	b mm
AGA	old ("30 mm const")	41	35
	new ("zero const")	40.5	62
Hewlett Packard	single prism	50.3	47.8
Kern	DM 500/501 prism	81.0	34.5
Sokkisha	PR-1, PR-3, PR-9	57.6	57.0
Topcon	prism on holder	48	72.4
WILD	GDR 11	60	22
	GDR 31	60	22
	GPR 1	39.6	26.2
ZEISS (Oberkochen)	TR 2, TR 7, TR 19	40	27

The parameters are defined as follows:

a = height of prism corner above front plane of prism (refer to figure 31, section 4.323).

b = distance between horizontal and vertical axis of reflector and front plane of prism.

The manufacturing tolerances of parameters a and b are better than 0.5 mm.

F.2 Refractive Index of Glass

Prisms used in EDM are usually made of BK 7 optical glass. The refractive index of BK 7 may be computed from the dispersion formula [61] [62]

$$n^2_{G_{ph}} = A_0 + A_1\lambda^2 + A_2\lambda^{-2} + A_3\lambda^{-4} + A_4\lambda^{-6} + A_5\lambda^{-8} \qquad \text{(F.2.1)}$$

with the constants $A_0 = 2.2718929$

$A_1 = -1.0108077.10^{-2}$

$A_2 = +1.0592509.10^{-2}$

$A_3 = +2.0816965.10^{-4}$

$A_4 = -7.6472538.10^{-6}$

$A_5 = +4.9240991.10^{-7}$

where $n_{G_{ph}}$ = refractive index of optical glass BK 7

λ = wavelength of carrier wave of EDM instrument (µm).

The dispersion formula (F.2.1) is accurate to $\pm$ 5 ppm in the spectral region between 365 nm and 1014 nm [62].

Because of the EDM ray being modulated, the group refractive index according to equation (2.40) has to be considered:

$$n_G = n_{G_{ph}} - \frac{dn_{G_{ph}}}{d\lambda} \lambda \qquad (F.2.2)$$

Differentiation of equation (F.2.1) provides the differential in equation (F.2.2). The group refractive index of BK 7 optical glass therefore yields:

$$n_G = n_{G_{ph}} - \frac{1}{n_{G_{ph}}} (A_1\lambda^2 - A_2\lambda^{-2} - 2A_3\lambda^{-4} - 3A_4\lambda^{-6} - 4A_5\lambda^{-8}) \qquad (F.2.3)$$

where n_G = group refractive index of BK 7 optical glass

$n_{G_{ph}}$ = phase refractive index of BK 7 optical glass

λ = wavelength of carrier wave of EDM instrument (µm)

A_i = constants of dispersion formula

In the table below the group refractive index n_G of BK 7 optical glass is listed for some important carrier waves.

λ (nm)	n_G (BK 7)	$n_{G_{ph}}$ (BK 7)
550	1.5460	1.5185
633	1.5365	1.5147
840	1.5252	1.5100
860	1.5246	1.5097
880	1.5240	1.5093
900	1.5235	1.5090
920	1.5230	1.5087

APPENDIX G

Parameters of the ICAO (International Civil Aviation Organization)

Standard Atmosphere [60]

Z = geometric altitude

T,t = atmospheric temperature

P = atmospheric pressure

Z, m	T, °K	t, °C	P, mb	P, mm Hg
-500	291.400	18.250	1074.78	806.151
-450	291.075	17.925	1068.49	801.436
-400	290.750	17.600	1062.24	796.743
-350	290.425	17.275	1056.01	792.073
-300	290.100	16.950	1049.81	787.425
-250	289.775	16.625	1043.65	782.799
-200	289.450	16.300	1037.51	778.195
-150	289.125	15.975	1031.40	773.614
-100	288.800	15.650	1025.32	769.054
-50	288.475	15.325	1019.27	764.516
0	288.150	15.000	1013.25	760.000
50	287.825	14.675	1007.26	755.505
100	287.500	14.350	1001.29	751.032
150	287.175	14.025	995.360	746.581
200	286.850	13.700	989.454	742.151
250	286.525	13.375	983.576	737.743
300	286.200	13.050	977.727	733.356
350	285.875	12.725	971.906	728.990
400	285.550	12.400	966.114	724.645
450	285.225	12.075	960.349	720.321
500	284.900	11.750	954.612	716.018
550	284.575	11.425	948.904	711.736
600	284.250	11.100	943.223	707.475
650	283.925	10.775	937.570	703.235
700	283.600	10.450	931.944	699.015
750	283.276	10.126	926.346	694.816
800	282.951	9.801	920.775	690.638
850	282.626	9.476	915.231	686.480
900	282.301	9.151	909.714	682.342
950	281.976	8.826	904.225	678.225
1000	281.651	8.501	898.762	674.127
1050	281.326	8.176	893.327	670.050
1100	281.001	7.851	887.918	665.993
1150	280.676	7.526	882.535	661.956
1200	280.351	7.201	877.180	657.939
1250	280.027	6.877	871.850	653.941
1300	279.702	6.552	866.547	649.964
1350	279.377	6.227	861.270	646.006
1400	279.052	5.902	856.020	642.068
1450	278.727	5.577	850.795	638.149
1500	278.402	5.252	845.596	634.249
1550	278.077	4.927	840.423	630.369
1600	277.753	4.603	835.276	626.509
1650	277.428	4.278	830.155	622.667
1700	277.103	3.953	825.059	618.845
1750	276.778	3.628	819.988	615.042
1800	276.453	3.303	814.943	611.258
1850	276.128	2.978	809.923	607.492
1900	275.804	2.654	804.928	603.746
1950	275.479	2.329	799.958	600.018
2000	275.154	2.004	795.014	596.309
2050	274.829	1.679	790.094	592.619
2100	274.505	1.355	785.199	588.947
2150	274.180	1.030	780.328	585.294
2200	273.855	0.705	775.482	581.659
2250	273.530	0.380	770.661	578.043
2300	273.205	0.055	765.863	574.445
2350	272.881	-0.269	761.091	570.865
2400	272.556	-0.594	756.342	567.303
2450	272.231	-0.919	751.618	563.760
2500	271.906	-1.244	746.917	560.234
2550	271.582	-1.568	742.240	556.726
2600	271.257	-1.893	737.588	553.236
2650	270.932	-2.218	732.958	549.764
2700	270.607	-2.543	728.353	546.310
2750	270.283	-2.867	723.771	542.873
2800	269.958	-3.192	719.213	539.454
2850	269.633	-3.517	714.677	536.052
2900	269.309	-3.841	710.166	532.668
2950	268.984	-4.166	705.677	529.301

APPENDIX H

RUEGERS DESIGN FORMULAE FOR EDM BASELINES

H.1 Length of Section Being Multiples of the Unit Length of the Instrument

The parameters are defined as follows:

U = unit length of EDM instrument (half of modulation wave length)

E = unit length of baseline (U or multiple of U)

A = shortest distance (E or multiple of E)

C_o = desired total length of baseline

C = final total length of baseline

B_o = design parameter (first estimate)

B = final design parameter (B_o rounded to nearest multiple of E)

Number of Stations	B_o
5	$\frac{1}{6}(C_o - 4A)$
6	$\frac{1}{10}(C_o - 5A)$
7	$\frac{1}{15}(C_o - 6A)$
8	$\frac{1}{21}(C_o - 7A)$

Section	Baseline with			
	5 Station	6 Station	7 Station	8 Station
1st	A + B	A + B	A + B	A + B
2nd	A + 3B	A + 3B	A + 3B	A + 3B
3rd	A + 2B	A + 4B	A + 5B	A + 5B
4th	A	A + 2B	A + 4B	A + 6B
5th	-	A	A + 2B	A + 4B
6th	-	-	A	A + 2B
7th	-	-	-	A
C =	4A + 6B	5A + 10B	6A + 15B	7A + 21B

Numerical examples may be found in references [49] and [64]. A mathematical form of the above tables has been published by PAULI [88] [89].

H.2 Baselines with Distances Spread Evenly Over Unit Length of Instrument

In addition to the parameters listed in section H.1, a second design parameter D is introduced.

Number of Stations	B_o	D
5	$\frac{1}{6}(C_o - 4A - U)$	$\frac{1}{16}U$
6	$\frac{1}{10}(C_o - 5A - U)$	$\frac{1}{25}U$
7	$\frac{1}{15}(C_o - 6A - U)$	$\frac{1}{36}U$
8	$\frac{1}{21}(C_o - 7A - U)$	$\frac{1}{49}U$

Section	Baseline with			
	5 Stations	6 Stations	7 Stations	8 Stations
1st	A + B + 3D	A + B + 3D	A + B + 3D	A + B + 3D
2nd	A + 3B + 7D	A + 3B + 7D	A + 3B + 7D	A + 3B + 7D
3rd	A + 2B + 5D	A + 4B + 9D	A + 5B + 11D	A + 5B + 11D
4th	A + D	A + 2B + 5D	A + 4B + 9D	A + 6B + 13D
5th	-	A + D	A + 2B + 5D	A + 4B + 9D
6th	-	-	A + D	A + 2B + 5D
7th	-	-	-	A + D
C =	4A + 6B + 16D	5A + 10B + 25D	6A + 15B + 36D	7A + 21B + 49D

A numerical example may be found in reference [67]. Some caution has to be employed whilst deriving instrument constants from data obtained on such baselines [50] [67] [70] [90].

BIBLIOGRAPHY

[1] WERNER, A.P.H. 1968. Lecture Notes on History of Surveying. *Australian Surveyor.* 24, June, 1968.

[2] INTERNATIONAL UNION OF GEODESY AND GEOPHYSICS. 1975. Resolutions, XVIth General Assembly, 1975, Grenoble, France. *Bulletin Geodesique,* No. 118, p.365.

[3] NATIONAL STANDARDS LABORATORY. 1972. *The Australian Standard for the Measurement of Physical Quantities.* C.S.I.R.O., Melbourne.

[4] SAASTAMOINEN, J.J. (ed.). 1969. *Surveyors Guide to Electromagnetic Distance Measurement.* Hilger, Bristol.

[5] AGA. 1969. *Geodimeter Model 6A Operational Manual.* Publication 571/071, AGA, Lindigö, 53pp.

[6] BURNSIDE, C.D. 1971. *Electromagnetic Distance Measurement.* Crosby Lockwood, London.

[7] LAURILA, S.M. 1976. *Electronic Surveying and Navigation.* John Wiley, New York, 545pp.

[8] BROWN, D.C. 1976. Doppler Surveying with the JMR-1 Receiver. *Bulletin Geodesique.* Vol. 50, No. 1, 1976.

[9] RADIO CORPORATION OF AMERICA. 1974. *Electro-Optics Handbook.* EOH-11. RCA, Commercial Engineering, Harrison NJ, 255pp.

[10] HÖPCKE, W. 1964. Ueber die Bahnkrümmung elektromagnetischer Wellen und ihren Einfluss auf die Streckenmessungen. *Zeitschrift für Vermessungswesen.* 89, 183-200.

[11] BRUNNER, F.K. 1975. Coefficients of Refraction on a Mountain Slope. *Unisurv G 22,* 81-96.

[12] NATIONAL MEASUREMENT LABORATORY. 1975. *Tests and Measurements.* C.S.I.R.O., Melbourne, 139pp.

[13] BOMFORD, G. 1975. *Geodesy.* Oxford University Press, 3rd edition, reprint, London.

[14] LIST, R.J. 1958. *Smithsonian Meteorological Tables.* 6th revised edition, Publication 4014, Smithsonian Miscellaneous Collection, 114, Washington.

[15] NATIONAL PHYSICAL LABORATORY. 1960. *The Refractive Index of Air for Radio Waves and Microwaves.* National Physical Laboratory, London.

[16] BRUNNER, F.K. & FRASER, C.S. 1977. An atmospheric turbulent Transfer Model for EDM Reduction. (In) *Proceedings, International Symposium on EDM and the Influence of Atmospheric Refraction,* Wageningen, 10pp.

[17] RINNER, K. & BENZ, F. 1966. *Die Entfernungsmessung mit Elektro-Magnetischen Wellen und Ihre Geodätische Anwendung.* Vol. 6 of JORDAN, EGGERT & KNEISSL. *Handbuch der Vermessungskunde.* 10th edition, Metzlersche Verlagsbuchhandlung, Stuttgart. (In German).

[18] SAASTAMOINEN, J. 1962. The Effect of Path Curvature of Light waves on the Refractive Index. *Canadian Surveyor.* 16, 90-100.

[19] SAASTAMOINEN, J. 1963. Some Experimental Results on the NASM-4B Geodimeter. *Canadian Surveyor.* 17, 47-52.

[20] SAVAGE, J.C. & PRESCOTT, W.H. 1973. Precision of Geodolite Distance Measurements for Determining Fault Movements. *Journal of Geophysical Research.* 78, 6001-6008.

[21] HUGGETT, G.R. & SLATER, L.E. 1975. Precision Electro-Magnetic Distance Measuring Instrument for Determining secular strain and fault movement. *Technophysics*. 29, 1-4.

[22] MURRAY, F.W. 1967. On the Computation of Saturation Vapour Pressure. *Journal of Applied Meteorology*. 6, p.203.

[23] BORN, M. & WOLF, E. 1970. *Principles of Optics. Electro-magnetic Theory of Propagation, Interference and Diffraction of Light.* Pergamon Press, London, 4th edition.

[24] BRUNNER, F.K. & ANGUS-LEPPAN, P.V. 1976. On the Significance of Meteorological Parameters for Terrestrial Refraction. *Unisurv G 25*, 95-108.

[25] MORITZ, H. 1967. Application of the Conformal Theory of Refraction. *Oesterreichische Zeitschrift für Vermessungswesen*. Sonderband 25, 323-334.

[26] WARREN, F.E. 1975. A Note on the Reduction of Measured Distances to the Ellipsoid. *Survey Review*. 23, 40-42.

[27] ESSEN, L. & FROOME, K.D. 1951. The Refractive Indices and Dielectric Constants of Air and its Principal Constituents at 24 000 Mc/s. *Proc. Phys. Soc.* (London), B-64, 862-875.

[28] SAASTAMOINEN, J. 1964. Curvature Correction in Electronic Distance Measurement. *Bulletin Geodesique*. 73, 265-269.

[29] NSW DEPT. OF LANDS. 1976. *Manual of the New South Wales Integrated Survey Grid.* NSW Department of Lands, Sydney, 166pp.

[30] BRUNNER, F.K. 1975. Trigonometric Levelling with Measured Slope Distances. (In) *Proceedings, 18th Australian Survey Congress*, Institution of Surveyors, Australia, Perth, 79-94.

[31] BRUNNER, F.K. 1973. The Effect of Deviation of Vertical in Trigonometric Levelling with Steep Sights. *Oesterreichische Zeitschrift für Vermessungswesen und Photogrammetrie.* 61, 126-134. (In German).

[32] BARRELL, H. & SEARS, J.E. 1939. The Refraction Dispersion of Air for the visible Spectrum. *Phil. Trans. Royal Society*. Series A, London, p.238.

[33] EDLEN, B. 1953. The Dispersion of Standard Air. *J. Opt. Soc. Amer.* 43, p.339.

[34] ELMIGER, A. 1977. Three-Dimensional Adjustment of terrestrial Geodetic Networks. (In) *Proceedings, XVth International Congress of Surveyors*, FIG, Stockholm. (In German).

[35] KAHMEN, H. 1977. *Electronic Methods of Measurement in Geodesy. Fundamentals and Applications*. H. Wichmann, Karlsruhe, 406pp. (In German).

[36] NÜNLIST, R. Correspondence, 1975-1977.

[37] MÜNCH, K.H. 1973. The Infrared Distance Meter Kern DM 1000. *Allgemeine Vermessungs-Nachrichten (AVN)*. 80, 201-207. (In German).

[38] MÜNCH, K.H. 1974. The Electronic Distance Meter Kern DM500: Part of a Modern Survey System. *Allgemeine Vermessungs-Nachrichten (AVN)*. 81, 48-54. (In German).

[39] GROSSMANN, W. 1975. *Surveying II. Angle and Distance Measuring Instruments, Traversing, Triangulation and Trilateration.* 2nd. ed., Sammlung Göschen Vol. 7469. de Gruyter, Berlin, 209pp. (In German).

[40] AGA PRODUCTS AUSTRALIA, 1975. *Newsletter*. 13.

[41] KEUFFEL & ESSER COMPANY. 1976. *Electronic Distance Measuring Equipment.* Catalog 10b, Morristown N.J.

[42] DABROWSKI, W. & MAIER, V. 1977. Determination of Horizontal Distance and Height Difference from Combined Applications of EDM Instruments and Theodolites. *Allgemeine Vermessungs-Nachrichten (AVN).* 84, 111-117. (In German).

[43] SPINDLER & HOYER CO. Fine Optical Construction Elements. List 31. Publication B4.576, Göttingen.

[44] PLESSEY AUSTRALIA PTY. LTD. 1975. *Nickel Cadmium Cells.* Plessey Components, product data PD 2098.

[45] GENERAL ELECTRIC. 1975. *Nickel-Cadmium Battery.* Application Engineering Handbook. General Electric Company, Publ. GET 3148A, 2nd ed., Gainesville, Florida.

[46] UNION CARBIDE. *Eveready Sealed Nickel-Cadmium Rechargable Batteries.* Sydney.

[47] KAHMEN, H. & ZETSCHE, H. 1974. Comparative Investigations into Electrooptical Short Range Distance Meters. *Zeitschrift für das Vermessungswesen (ZfV).* 99, 68-81. (In German).

[48] RÜEGER, J.M., SIEGERIST, C. & STÄHLI, W. 1975. Investigations into Electrooptical Short Range Distance Meters. *Vermessung-Photogrammetrie-Kulturtechnik (Mitteilungsblatt).* 73, 73-76, 93-100, 126-133, 270. (In German).

[49] RÜEGER, J.M. 1977. Design and Use of Base Lines for the Calibration of EDM Instruments. (In) *Proceedings, 20th Australian Survey Congress,* Institution of Surveyors, Australia, Darwin, 175-189.

[50] RÜEGER, J.M. 1976. Remarks on the joint Determination of Zero Error and Cyclic Error for EDM Instrument Calibration. *Australian Surveyor.* 28, 96-103.

[51] ELMIGER, A. & SIEGERIST, C. 1977. Practical Tests and Experiences with the Mekometer. (In) *Proceedings, 7th International Course for High Precision Engineering Surveys,* THD Schriftenreihe Wissenschaft und Technik, Darmstadt, Vol. 1, 203-219.

[52] KERN & CO. LTD. 1974. Test Line for Electrooptical Distance Measuring Instruments. *Kern Bulletin.* 20.

[53] COUCHMAN, H.D. 1974. A Method of Evaluating Cyclic Errors in EDM Equipment. *Australian Surveyor.* 26, 113-115.

[54] KÜPFER, H.P. 1968. Ground Reflections and Measurement Technique in Microwave Distance Measurement. *Schweizerische Zeitschrift für Vermessung, Photogrammetrie und Kulturtechnik.* 66, 290-309, 329-348. (In German).

[55] KÜPFER, H.P. & HOSSMANN, M. 1971. The Concept of the new Microwave Distance Meter Distomat DI 60. A Contribution to the Solution of the Reflection Problem. *Allgemeine Vermessungs-Nachrichten (AVN).* 78, 50-64. (In German).

[56] HEWLETT-PACKARD. 1973. Hewlett-Packard Prisms. *Insight.* 2, 1-2. Hewlett-Packard Civil Engineering Products, Loveland, Col.

[57] BRUNNER, F.K. 1975. *Lecture Notes on Electronic Distance Measurement.* (unpublished).

[58] ROBINSON, A.J. 1975. *Lecture Notes on Electronic Distance Measurement.* (unpublished).

[59] DALCHER, A. 1975. Simplified Theory of the Deformation of a Reflector due to Unequal Temperature. *Vermessung-Photogrammetrie-Kulturtechnik (Fachblatt).* 27, 237-239. (In German).

[60] ICAO. 1964. *Manual of the ICAO Standard Atmosphere extended to 32 kilometres (10500 feet).* International Civil Aviation Organization, Doc. 7488/2, 2nd Edition.

[61] MELLES GRIOT. 1975. *Optics Guide.* Melles Griot, 1770 Kettering Street, Irvine, Cal. 92714, U.S.A.

[62] SCHOTT. *Glass Catalogue.* Mainz, F.R.D.

[63] ZETSCHE, H. 1979. *Electronic Distance Measurement (EDM).* Konrad Wittwer, Stuttgart, 434pp. (In German).

[64] RUEGER, J.M. 1976. An Aid for the Design of Baselines for Electronic Distance Measuring Instruments. *Vermessung-PhotogrammetrieKulturtechnik (Mitteilungsblatt),* Vol. 74, 249-251. (In German).

[65] RUEGER, J.M. 1978. Computation of Cyclic Errors of EDM Instruments Using Pocket Calculators. *Australian Surveyor,* Vol. 29, 268-284.

[66] RUEGER, J.M. 1978. Misalignment of EDM Reflectors and its Effects. *Australian Surveyor,* Vol. 29, 28-36.

[67] RUEGER, J.M. 1978. Design of Baselines of the Schwendener Type for Electro-optical Distance Meters. *Vermessungswesen und Raumordnung, (VR),* Vol. 40, 315-324. (In German).

[68] RUEGER, J.M. 1978. Variation with Temperature of Frequencies of Short-Range EDM Instruments. *Unisurv G28,* School of Surveying, University of N.S.W., Sydney, 47-58.

[69] RUEGER, J.M. 1978. Frequency Calibration of Short-Range EDM Instruments. *Vermessung-Photogrammetrie-Kulturtechnik,* Vol. 76, 125-130. (In German).

[70] RUEGER, J.M. 1976. Problems in the Joint Determination of Cyclic Error and Additive Constant of Electro-optical Distance Meters. *Allgemeine Vermessungs-Nachrichten (AVN),* Vol. 83, 338-344. (In German).

[71] RUEGER, J.M. 1976. The Effect of Phaseinhomogeneities During the Use of Plane Mirrors for Electro-optical Distance Measurement. *Zeitschrift fur Vermessungswesen (ZfV),* Vol. 101, 391-392. (In German).

[72] RUEGER, J.M. 1980. Recent Developments in Electronic Distance Measurement. *Australian Surveyor.* (In press).

[73] RUEGER, J.M. 1980. Legal Requirements for the Calibration of EDM Instruments. (In) *Proceedings, 22nd Australian Survey Congress (Hobart),* Institution of Surveyors, Australia, Sydney.

[74] COVELL, P.C. 1979. Periodic and Non-Periodic Errors of Short-Range Distance Meters. *Aust.J.Geod.Photo.Surv.,* No.30, 79-101.

[75] FRASER, C.S. 1979. Identification of Optimum Meteorological Conditions for EDM via Potential Refractivity. *Canadian Surveyor,* Vol. 33, 27-38.

[76] BRUNNER, F.K. 1977. On the Refraction Coefficient of Microwaves. *Bulletin Geodesique,* Vol. 51, 257-264.

[77] BRUNNER, F.K. 1977. Experimental Determination of the Coefficients of Refraction from Heat Flux Measurements. (In) *Proceedings, International Symposium on EDM and the Influence of Atmospheric Refraction,* Wageningen, 11p.

[78] MENZIES, G.H. 1972. Eccentric Distance Measurement. *South African Survey Journal,* Vol. 13, 3-7.

[79] LE ROUX, Z.P. 1976. Reduction of Eccentric Distance Measurements. *South African Survey Journal,* Vol. 15, 62-63.

[80] BRUNNER, F.K. & FRASER, C.S. 1977. Application of the Atmospheric Turbulent Transfer Model (TTM) for the Reduction of Microwave EDM. *Unisurv G27,* School of Surveying, University of New South Wales, Sydney. 3-26.

[81] FRASER, C.S. The Empirical Determination of Sensible Heat Flux for Refraction Corrections. *Unisurv G27,* School of Surveying, University of New South Wales, Sydney, 42-51.

[82] FRASER, C.S. & BRUNNER, F.K. 1977. On the Analysis of Multiple Meteorological Measurements for Microwave EDM. *Unisurv G26,* School of Surveying, University of New South Wales, Sydney, 47-81.

[83] ANGUS-LEPPAN P.V. 1977. The Atmospheric Corrections on EDM Lines Over the Sea. *Unisurv G27,* School of Surveying, University of New South Wales, Sydney, 88-98.

[84] RICHTER, H. 1970. Visibility and Range of Electro-Optical Distance Meters. *Vermessungstechnik, (VT),* Vol. 18, 31-35. (In German).

[85] HUGGETT, G.R. 1979. Two-Colour Terrameter. *Symposium on Recent Crustal Movements, XVII General Assembly, IUGG, Canberra,* December 1979. 16p.

[86] BRUNNER, F.K. 1979. Vertical Refraction Angle Derived from the Variance of the Angle-of-Arrival Fluctuations, 227-238. (In) TENGSTROM, E., TELEKI, G. (ed.) *Refractional Influences in Astrometry and Geodesy,* Reidel Publishing Co., Holland.

[87] BRUNNER, F.K. 1979. Atmospheric Turbulence: The Limiting Factor to Geodetic Precision. *Aust.J.Geod.Photo.Surv.*, No. 31, 51-64.

[88] PAULI, W. 1977. Calibration of and Baselines for Electro-Optical Distance Meters. *Vermessungstechnik (VT),* Vol. 25, 265-267. (In German).

[89] PAULI, W. et al. 1979. Establishment of a Baseline of VEB Carl-Zeiss Jena for the Calibration of Electro-Optical Distance Meters. *Vermessungstechnik (VT),* Vol. 27, 135-137. (In German).

[90] SCHWENDENER, H.R. 1972. Electronic Distancers for Short-Ranges: Accuracy and Checking Procedures. *Survey Review,* Vol. 21, No. 164, 273-281.

[91] BRUNNER, F.K. & GROENHOUT, K.I. 1979. Microwave Distance Measurements During Rainfall. *Australian Surveyor*, Vol.29, 569-580.

INDEX

Publications from
THE SCHOOL OF SURVEYING, THE UNIVERSITY OF NEW SOUTH WALES.

All prices include postage by surface mail. Air mail rates on application. (Effective January 1988)

To order, write to Publications Officer, School of Surveying, The University of New South Wales, P.O. Box 1, Kensington N.S.W., 2032 AUSTRALIA

NOTE: ALL ORDERS MUST BE PREPAID

UNISURV REPORTS - G SERIES

Price (including postage): $3.50

The following issues are available - for details write to Publications Officer.

G14, G16 - G27 & G29

AUSTRALIAN JOURNAL OF GEODESY, PHOTOGRAMMETRY AND SURVEYING

Price (surface mail postage included)	Individuals	$7.00
	Institution	$10.00
Annual Subscriptions (2 issues):	Individuals	$14.00
	Institutions	$20.00

J32. Aust.J.Geod.Photo.Surv. No. 32, (June, 1980), 121 pp.
van Gysen, "Gravimetric deflections of the vertical",
Fraser, "Self calibration of non-metric camera",
Rizos, "Ocean circulation from SST studies",
Trinder, "Film granularity and visual performance".

J33. Aust.J.Geod.Photo.Surv.No. 33, (December, 1980), 85 pp.
Burford, "Controlling geodetic networks";
Masters & Stolz, "Crustal motion from LAGEOS";
Fraser, "Variance analysis of adjustments", and
Brunner et al., "Incremental strain near Palmdale".

J35. Aust.J.Geod.Photo.Surv. No. 35 (December, 1981), 106pp.:
Kahar, "Geoid in Indonesia";
Morgan, "Crustal motion in Papua New Guinea";
Stolz et al, "Baseline values from LAGEOS", and
Bishop, "Digital elevation models".

J36. Aust.J.Geod.Photo.Surv. No. 36 (June, 1982), 97pp.
Nakiboglu and Torenberg, "Earth's gravity and surface loading";
Nakiboglu, "Changes in sea level and gravity";
Villanueva, "Geodetic boundary value problem";
Stolz and Harvey, "Australian geodetic VLBI experiment";
Gilliland, "Free-air geoid for South Australia";
Allman, "Geoid for S.E. Asia and S.W. Pacific", and
Angus-Leppan, "Gravity measurements in levelling".

J37. Aust.J.Geod.Photo.Surv. No. 37 (December, 1982), 113pp.
Niemeier, Teskey, & Lyall, "Monitoring movement in open pit mines";
Banger, "Refraction in levelling";
Angus-Leppan,"GPS - prospects for geodesy", and
Zwart, "Costs of integrated surveys".

J38. Aust.J.Geod.Photo.Surv. No. 38 (June, 1983), 93pp.:
Forster, "Radiometric registration of LANDSAT images";
Fryer, "Photogrammetry through shallow water";
Harvey, Stolz, Jauncey, Niell, Morabito and Preston,
"Australian geodetic VLBI experiment";
Gilliland, "Geoid comparisons in South Australia", and
Kearsley, "30' mean gravity anomalies from altimetry".

J39. Aust.J.Geod.Photo.Surv. No. 39 (December, 1983), 85pp.:
Coleman & Lambeck, "Crustal motion in South Eastern Australia";
Salih, "The shape of the geoid in The Sudan";
Rueger, "The reduction of mekometer measurements", and
Angus-Leppan, "Preliminary study for a new levelling system".

J40. Aust.J.Geod.Photo.Surv. No. 40 (June, 1984), 112pp.:
Holstein & Williamson, "Converting land titles in N.S.W.";
Fryer, "Depths by through-water photogrammetry";
Stolz, Masters & Rizos, "GPS orbits in Australia";
Forster & Trinder, "Resampling of LANDSAT data";
Lambert, "World wide astro/geodetic datum"; and
The photogrammetry forum:- Contributions from Davies,
Urban, Kirkby, Cleaves and Trinder.

J41. Aust.J.Geod.Photo.Surv. No. 41 (December, 1984), 100pp:
Gee & Forster, "Investigation of Landsat Multispectral Data";
Faig, "Mining Subsidence determination";
Patterson, "Effect of an Estimated Variance Factor";
Rueger, "Temperature Models in EDM".

J42. Aust.J.Geod.Photo.Surv. No. 42 (June, 1985), 106pp:
Kubik, Weng & Frederiksen, "Oh, Grosserorors!";
Cruger Jorgensen, Frederiksen,Kubik &Weng,
"Ah, Robust Estimation";
Ali, "Accuracy of Satellite Radars";
Harvey & Stolz, "VLBI/SLR - Baseline Comparisons";
Kearsley, "High Precision Geoid Solutions".

J43. Aust.J.Geod.Photo.Surv. No. 43 (December, 1985), 100pp:
Patterson, "Outlier Detection";
Harvey, "VCV of VLBI";
Fryer & Kniest, "Through Water Photogrammetry";
Trinder & Burns, "35mm Lens Distortions";
Salih, "Doppler Methods in the Sudan".

J44. Aust.J.Geod.Photo.Surv., No. 44 (June 1986), 89 pp:
Argeseanu, "Network adjustment by collocation"
Clarke, "Gravimetric $\xi\ \eta$".
Fryer, "Zoom lens distortion"
Ali, "Monoplotting from SLR imagery"
Aziz, "LRIS and Education".

J45. Aust.J.Geod.Photo.Surv.,No.45 (December, 1986), 100 pp.
Morgan et al, "Testing GPS Surveys"
Bretreger,"Tidal Effects on Levelling"
Shortis, "Close Range Photogrammetry"
Ali, "Mapping from SAR Imagery".

UNISURV REPORTS - S SERIES

S8-S19	Price (including postage):	$7.50	
S20 onwards	Price (including postage):	Individuals	$18.00
		Institutions	$25.00

S8. A. Stolz, "Three-D Cartesian co-ordinates of part of the Australian geodetic network by the use of local astronomic vector systems", Unisurv Rep. S 8, 182 pp, 1972.

S9. H.L. Mitchell, "Relations between MSL & geodetic levelling in Australia", Unisurv Rep. S 9, 264 pp, 1973.

S10. A.J. Robinson, "Study of zero error & ground swing of the model MRA101 tellurometer", Unisurv Rep. S 10, 200 pp, 1973.

S12. G.J.F. Holden, "An evaluation of orthophotography in an integrated mapping system", Unisurv Rep. S 12, 232 pp, 1974.

S14. Edward G. Anderson, "The Effect of Topography on Solutions of Stokes` Problem", Unisurv Rep. S 14, 252 pp, 1976.

S15. A.H.W. Kearsley, "The Computation of Deflections of the Vertical from Gravity Anomalies", Unisurv Rep. S 15, 181 pp, 1976.

S16. K. Bretreger, "Earth Tide Effects on Geodetic Observations", Unisurv S 16, 173 pp, 1978.

S17. C. Rizos, "The role of the gravity field in sea surface topography studies", Unisurv S 17, 299 pp, 1980.

S18. B.C. Forster, "Some measures of urban residual quality from LANDSAT multi-spectral data", Unisurv S 18, 223 pp, 1981.

S19. Richard Coleman, "A Geodetic Basis for recovering Ocean Dynamic Information from Satellite Altimetry", Unisurv S 19,332 pp, 1981.

S20. Douglas R. Larden, "Monitoring the Earth's Rotation by Lunar Laser Ranging", Unisurv Report S 20, 280 pp, 1982.

S21. R.C. Patterson, "Approximation and Statistical Methods in Physical Geodesy", Unisurv Report S 21, 179 pp, 1982.

S22. J.M. Rueger, "Quartz Crystal Oscillators and their Effects on the Scale Stability and Standardization of Electronic Distance Meters", Unisurv Report S 22, 151 pp, 1982.

S25. Ewan G. Masters, "Applications of Satellite Geodesy to Geodynamics", Unisurv Report S25, 208 pp, 1984.

S26. Andrew Charles Jones, "An Investigation of the Accuracy and repeatability of Satellite Doppler relative positioning techniques", Unisurv Report S26, 222 pp, 1984.

S27. Bruce R. Harvey, "The Combination of VLBI and Ground Data for Geodesy and Geophysics", Unisurv Report S27, 239 pp, 1985.

S28. Rod Eckels, "Surveying with GPS in Australia", Unisurv Report S28, 220 pp, 1987.

S29. Gary S. Chisholm, "Intergration of GPS into Hydrographic Survey Operations", Unisurv Report S29, 190pp, 1987.

S30. Gary Alan Jeffress, "An Investigation of Doppler Satellite Positioning Multi-Station Software", Unisurv Report S30, 118pp, 1987.

PROCEEDINGS

Prices include postage by surface mail

P1. P.V. Angus-Leppan (Editor), "Proceedings of conference on refraction effects in geodesy & electronic distance measurement", 264 pp. Price: $6.50

P2. R.S. Mather & P.V. Angus-Leppan (Eds), "Australian Academy of Science/International Association of Geodesy Symposium on Earth's Gravitational Field & Secular Variations in Position", 740 pp. Price: $12.50

MONOGRAPHS

Prices include postage by surface mail

M1. R.S. Mather, "The theory and geodetic use of some common projections", (2nd edition), 125 pp. Price$9.00

M2. R.S. Mather, "The analysis of the earth's gravity field", 172 pp. Price $5.50

M3. G.G. Bennett, "Tables for prediction of daylight stars", 24 pp. Price $2.00

M4. G.G. Bennett, J.G. Freislich & M. Maughan, "Star prediction tables for the fixing of position", 200 pp. Price $5.00

M5. M. Maughan, "Survey computations", 98 pp. Price $8.00

M6. M. Maughan, "Adjustment of Observations by Least Squares", 61 pp. Price $7.00

M7. J.M. Rueger, "Introduction to Electronic Distance Measurement", (2nd Edition), 140 pp. Price $14.00

M8. A.H.W. Kearsley, "Geodetic Surveying". 77pp. Price $8.00

M9.** R.W. King, E.G. Masters, C. Rizos, A. Stolz and J. Collins, "Surveying with GPS", 128 pp.

M10. W. Faig, "Aerial Triangulation and Digital Mapping", 102. pp. Price $13.00

M11. W.F. Caspary, "Concepts of Network and Deformation Analysis", 183 pp. Price$22.00

** No longer for external sale from the School of Surveying. Now published by Ferd. Dümmlers Verlag, Kaiserstrasse 31-37, D-5300 Bonn 1, Federal Republic of Germany